UNIVERSITÀ DEGLI STUDI DI BRESCIA

UNIVERSITÀ
DEGLI STUDI
DI BRESCIA

DOTTORATO DI RICERCA IN INGEGNERIA MECCANICA E INDUSTRIALE D.M.45/2013

CHIM/07

CICLO XXXIII

MUNICIPAL SOLID WASTE COMBUSTION TOGETHER WITH SEWAGE SLUDGE: THE CHARACTERIZATION AND THE STABILIZATION OF THE ASHES PRODUCED

Dottorando:
AHMAD ASSI

Firma...

Relatore:
PROF.SSA ELZA BONTEMPI

Firma...

Coordinatore di Dottorato:
PROF.SSA LAURA ELEONORA DEPERO

Firma.....

RINGRAZIAMENTI

Ringrazio innanzitutto A2A per aver finanziato questa attività di ricerca, ed in particolare l'Ing. Nenci per la disponibilità dimostrata in questi 3 anni di attività.

Ringrazio la mia famiglia per il loro continuo supporto, durante gli anni di studio, e la loro fiducia in me.

Vorrei ringraziare tutti i miei colleghi del laboratorio di chimica per le tecnologie che mi hanno accompagnato e supportato moralmente e scientificamente nel mio percorso di Dottorato, in particolar modo la professoressa Bontempi per i suggerimenti e le conoscenze che mi ha tramandato, la professoressa Depero per il suo sostegno e supporto, ed infine, la professoressa Borgese per le numerose ore dedicate a me.

Vorrei ringraziare anche tutti i miei amici e compagni di Dottorato che mi sono stati vicini in questi anni, soprattutto Federico Ceresoli.

Grazie a te che mi hai riportato il sorriso.

INDEX

FIGURES INDEX

TABLES INDEX

Riassunto

Lo smaltimento dei rifiuti solidi urbani è uno dei maggiori problemi ambientali di enorme impatto che il mondo e in particolare l'Europa deve affrontare. Il conferimento in discarica dei rifiuti solidi urbani è ancora il principale metodo di trattamento, tuttavia le direttive europee richiedono un cambio di tendenza con la riduzione dei rifiuti, e quindi il riciclo e il recupero energetico di tutti i rifiuti prodotti.

Nel **primo capitolo** viene introdotta e spiegata la situazione del termovalorizzatore in Europa e soprattutto in Italia. Inoltre, viene riportata una spiegazione sui principali sottoprodotti e sullo stato dell'arte dello smaltimento delle ceneri leggere.

Il **secondo capitolo** introduce il progetto Rendering, la nuova tecnologia proposta e l'upgrade del processo di stabilizzazione.

Il **terzo capitolo** definisce e riporta la composizione di tutte le materie prime utilizzate in questo lavoro di tesi.

Il **quarto capitolo** riporta le diversi metodologie di preparazione ed analisi dei campioni.

Il **quinto capitolo** riporta i risultati ottenuti a seguito di una caratterizzazione approfondita dei campioni.

Il **sesto capitolo** riporta le metodologie, analisi effettuate ed i risultati ottenuti dalle prove di carbonatazione.

L'ultimo capitolo tratta infine il tema del riutilizzo: nel corso di questa tesi il materiale è stato testato come riempitivo all'interno di diverse matrici polimeriche.

Il conferimento in discarica, quindi, verrà sostituito dal termovalorizzatore e diventerà sempre più una valida alternativa. L'incenerimento dei rifiuti solidi urbani porta alcuni vantaggi indiscussi, come la riduzione del volume dei rifiuti e la generazione di energia derivata dalla combustione. Tuttavia non può essere considerata una tecnologia a impatto zero: il processo di incenerimento produce infatti ulteriori rifiuti pericolosi che devono essere opportunamente smaltiti.

Pertanto, in questo lavoro di tesi il problema verrà affrontato dapprima con la presentazione di una metodologia proposta dall'Università degli Studi di Brescia, che prevede l'inertizzazione delle ceneri leggere prodotti durante il processo di termovalorizzazione. Il metodo è stato sviluppato all'interno di un progetto RENDERING e ha portato alla produzione di un materiale inerte partendo da ceneri pericolose utilizzando alcuni

sottoprodotti e al suo riutilizzo come riempitivo in matrici polimeriche. Il processo avviene a temperatura ambiente e prevede principalmente l'utilizzo di materiali di scarto: il suo impatto ambientale ed economico è quindi molto contenuto, rispetto alle tecnologie attualmente utilizzate per trattare questi rifiuti.

L'applicazione industriale di questo metodo non solo può portare alla stabilizzazione di un rifiuto pericoloso, ma può anche consentire di ottenere un materiale inerte riutilizzabile come materia prima secondaria, che consente di ridurre l'utilizzo di altre materie prime creando un valore oltre e dal punto di vista ambientale ed economico.

Il progetto RENDERING punta a sostituire l'utilizzo delle ceneri pesanti come fonte di alto contenuto di silice amorfa al fine di rendere il processo sostenibile dal punto di vista economico; questo nuovo metodo ha quindi permesso di ottenere un materiale inerte con minori costi di produzione e con un impatto ambientale ancora inferiore.

Il processo presenta alcune variabili che non sono prive di criticità: l'utilizzo delle ceneri pesanti necessario per la reazione di inertizzazione ha una fase di pretrattamento che prevede basse energie. Tuttavia, la stabilizzazione richiede circa un mese per verificarsi, quindi è necessario un luogo adatto per conservare le ceneri durante questo periodo.

Introduction

Municipal solid waste (MSW) disposal is one of the major environmental problems of a huge impact that the world and specially Europe has to deal with. MSW landfilling is still the main method of treating, however the European directives require a change in trend with the reduction of waste, and therefore the recycling and energy recovery of all waste products.

The **first chapter** introduce and explain the situation of the waste-to-energy plant in Europe e specially in Italy. Also, report an explanation about the main by-products and the state of art of fly ash (FA) disposal.

The **second chapter** introduce the Rendering project, the new technology proposed and the scale up of this process.

The **third chapter** defines and reports the composition of all the raw materials used in this thesis work.

The **fourth chapter** shows the different methods of preparation and analysis of the samples.

The **fifth chapter** reports the results obtained following an in-depth characterization of the samples.

The **sixth chapter** reports the methodologies, analyzes carried out and the results obtained from the carbonation tests.

The **last chapter** finally deal with the theme of reuse: during the course of this thesis, the material was tested as a filler within different polymeric matrixes.

Therefore, landfilling will be substituted by the waste-to-energy plant and it will increasingly become a valid alternative. Municipal solid waste incineration (MSWI) brings some undisputed advantages, such as the reduction of the volume of waste and the generation of energy derived from combustion. Nonetheless, it cannot to be considered a zero-impact technology: the incineration process in fact produces additional hazardous waste which must be properly disposed of.

Therefore, in this thesis work the problem will be dealt with at first with the presentation of a method proposed by the University of Brescia, which provides for the inertization of the FA produced during the waste-to-energy process. The method was developed within a RENDERING project and led to the production of an inert material starting from hazardous ashes using some by-products and its reuse as a filler in polymeric matrixes. The process takes place at room temperature and mainly involves the use of waste materials: its

environmental and economic impact are therefore very low, compared to the technologies currently used to treat this waste.

The industrial application of this method can not only lead to the stabilization of a hazardous waste, but it can also make it possible to obtain a reusable inert material as a secondary raw material, which allows to reduce the use of other raw materials creating an added value beyond and from an environmental and economic point of view.

The RENDERING project point to replace to use bottom ash (BA) as a source of high content of amorphous silica in order to make the process sustainable from an economic point of view; this new method has therefore made it possible to obtain an inert material with lower production costs and with an even lower environmental impact.

The process has some variables that are not without criticalities: the use of the BA necessary for the inertization reaction has a pretreatment phase that involves low energy. However, the stabilization requires about one month to occur, then need suitable location to store ashes during this time.

1 Waste-to-energy in Europe

The management and disposal of urban solid waste produced in Europe is one of the most important and serious problem of our generation. The aim of the EU is to use new methods for the management of MSW to reduce their environmental and health impacts and to reduce the EU's resource efficiency. Reducing waste disposal (for example landfilling) and focusing on waste prevention, reuse, recycling and recovery in order to generate greater economic returns at lower costs to the environment. Incineration is considered as waste disposal. However, incineration has some by-products (like: BA and FA) and some gas emissions. This has an impact on the environment due to ashes toxicity, however it must have considered that this method allows to recover energy, that can be in form of steam, electricity or hot water with a significant mass and volume reduction, by approximately 90% through waste-to-energy plants can limit the consumption of raw sources to produce energy [1]. In 2016 the European Union, have indicate that about (53.2%) of the waste was treated in recovery operations: recycling, backfilling or recovery or disposed of otherwise. This can be slightly different between some Member States concerning the use they made of these various treatment methods[2].

According to [3] all the modern Waste-to-Energy plants meets the strictest emission limit values.

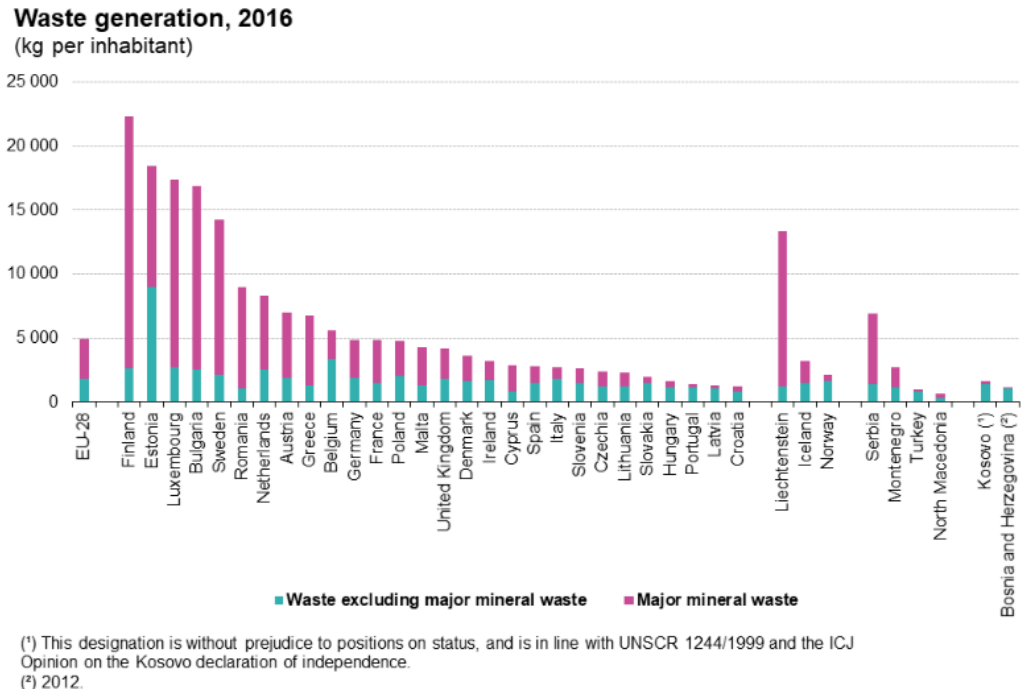

Figure 1 Waste generation, 2016 (kg per inhabitant) Source: Eurostat (env_wasgen)

Figure 1 shows a high quantity of waste generated per inhabitant in 2016 for some smaller EU Member States like Finland, where on average 22.4 tons of waste per inhabitant, more than four times the 5.0 tones per inhabitant average across the EU-28.

During the period 2004-2016 the quantity of waste recovered or incinerated with energy recovery grew by 28.2% as shown in Figure 2.

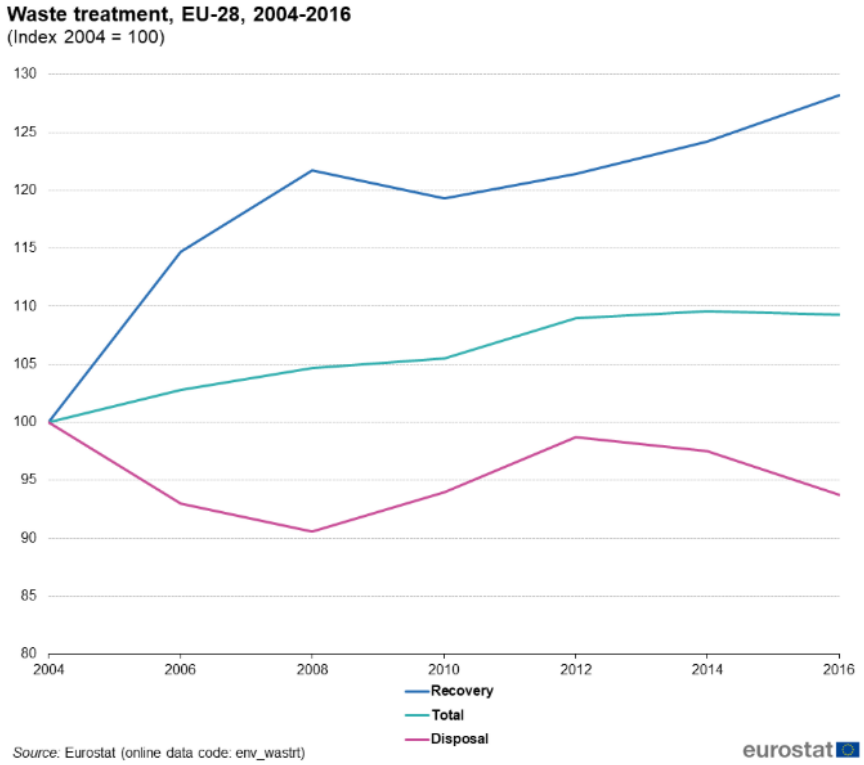

Figure 2 Waste treatment, EU-28, 2004-2016 (Index 2004 = 100) Source: Eurostat (env_wastrt)

1.1 Municipal solid waste

MSW as defined by the European Environment Agency "Municipal waste is mainly produced by households, though similar wastes from sources such as commerce, offices and public institutions are included. The amount of municipal waste generated consists of waste collected by or on behalf of municipal authorities and disposed of through the waste management system". The classified non-hazard waste is the domestic, commercial and daily street activities waste, partly organic (such as food and paper) and inorganic (for example plastic and glass). It is evident that the characteristics and the composition of MSW that strongly influenced by economic factors have changed over time according to the changing needs of the consumer society, due to social behavior, regional and cultural aspects. On the other hand, the increase amount of MSW generated depends on the population and urbanization growth as reported by [2]. Figure 3 shows the comparison of MSW generation by country between 2005 and 2018 expressed in kilograms per capita. The variations of the

total amount of MSW generated depend also, on how MSW is collected and managed, as well as recycling. For example, in Italia the MSW generation vary considerably, ranging from 546 kg per capita during 2005 to 499 kg per capita during 2018.

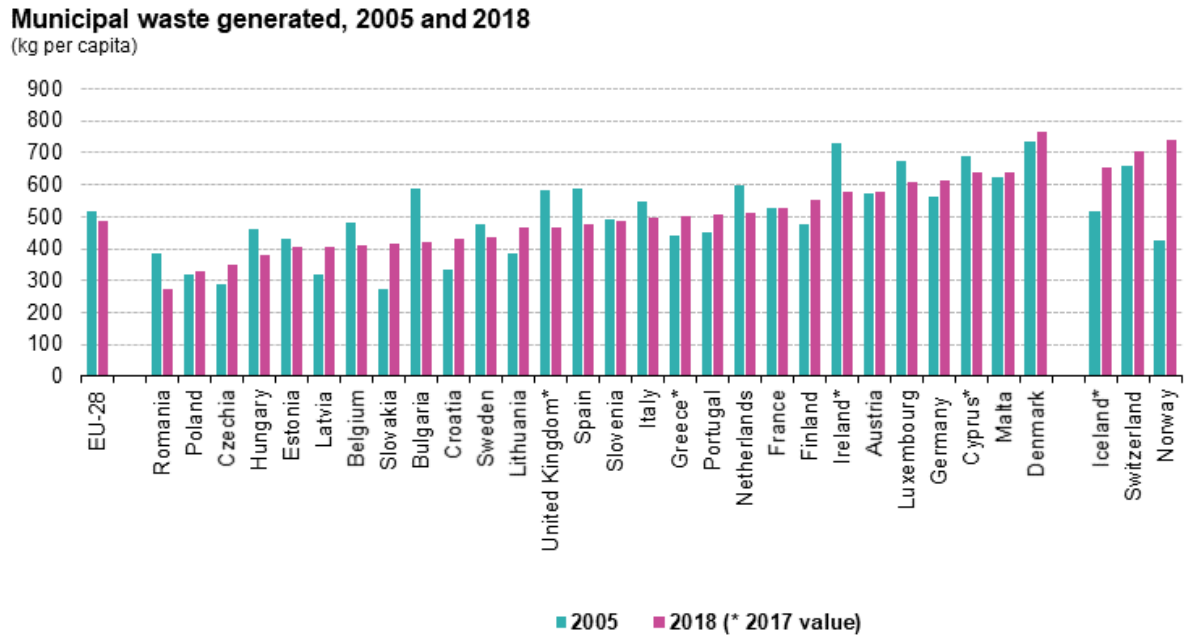

Figure 3 MSW generation in Europe

The MSW divided into two main types, domestic waste and packaging, each type can be divided into seven product categories: paper and cartons, textiles and wood, plastic materials, metal materials, inert materials, organic fraction and screening material. The screening material is essentially composed of non-combustible minute material and organic matter. It can observed that in recent years the waste has become drier: the organic fraction decreases in parallel with the increase in combustible components such as plastic and cellulose; metallic and inert materials, on the other hand, are present in more or less constant quantities.

The Directive 2008/98/CE provides for a target of 50% to be achieved by 2020 for the preparation for the reuse and recycling of municipal waste. With the issue of Directive 2018/851/ EU, further objectives have been introduced, to be achieved by 2025 (55%), 2030 (60%) and 2035 (65%). The three new objectives do not consider specific product fractions but will have to be applied to the entire amount of municipal waste. In 2018, the percentage of preparation for reuse and recycling, considering the organic fraction, paper and cardboard, glass, metals, wood and plastic, attests to 50.8% and therefore above the target set, and to 45.2% considering all types of municipal waste [4].

1.2 Municipal urban waste management

Municipal waste sent to intermediate mechanical-biological forms of treatment before a final destination for recovery or disposal represents, in 2018, was about 35% of the municipal waste produced. Not accounting for this waste, therefore, it would not allow to close the cycle of municipal waste management. These treatments, in fact, are widely used before disposal in landfills or incineration with the aim, on the one hand, to improve the biological stability of the waste, reducing its humidity and volume, on the other hand to increase their calorific value to make the combustion process more efficient [4].

In 2018, 94% of municipal waste disposed of in landfills and 49% of incinerated waste were treated prior to disposal. It is necessary to note that art. 7 of Legislative Decree no. 36/2003 transposing directive 99/31 / CE on waste landfills, establishes that waste can be placed in landfills only after treatment [4].

In many cases, the mechanical biological treatment plants are located in the same site where there are also landfills or incinerators constituting real treatment platforms. In addition, in several cases both the mechanical biological treatment plant and that of the organic fraction of separate collection are present in the same platform.

About 646 urban waste management plants were operational in 2018. Of these, 339 are dedicated to the treatment of the organic fraction of separate collection (SC) (281 composting plants, 35 plants for integrated aerobic/anaerobic treatment and 23 anaerobic digestion plants), 131 are plants for mechanical or mechanical biological intermediate treatment of waste, 127 are landfill plants in addition to 38 incineration plants and 11 industrial plants which carry out the co-incineration of municipal waste [4].

In order to avoid duplication of data, in the accounting of the quantities of waste subjected to mechanical biological treatment and subsequently sent to other management operations, in Figure 4, which represents the percentage breakdown of the various forms of management in the year 2018, this percentage is not reported [4].

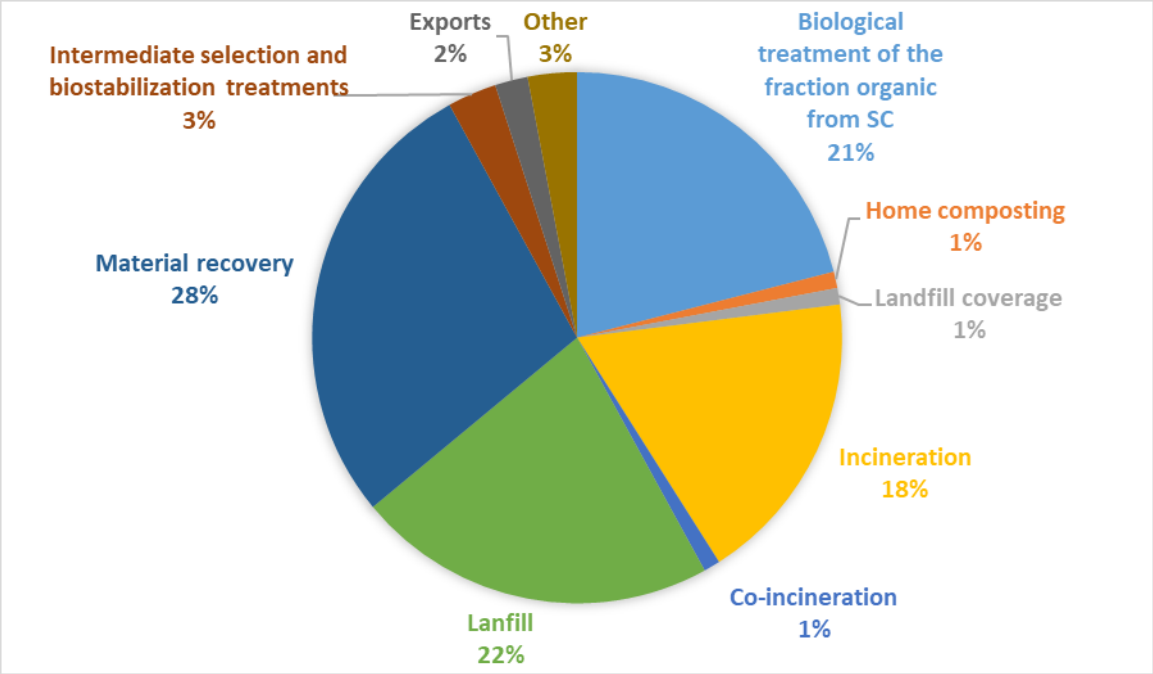

Figure 4 Various forms of waste management in the year 2018

1.3 MSW incineration: The Italian situation

Waste-to-Energy plants on the Italian territory are 39 plants (80 lines) with a total nominal capacity of 903.81 t/h for mainly urban solid waste. The thermal load is estimate to be about 2987.98 MW, while the installed electrical power is 832.98 MW [4].

About 68% of the infrastructures is located in the northern regions (26 plants); in Lombardia and Emilia Romagna there are 13 and 8 plants respectively. Both the Center and the South have 6 operational insertion plants. Figure 5 shows the trend of the quantities of waste from the urban circuit incinerated in the period 2008-2018. The per capita incineration of municipal waste shows an increase from 87.1 kg/inhabitant in 2017 to 92.3 kg/inhabitant in 2018 [4].

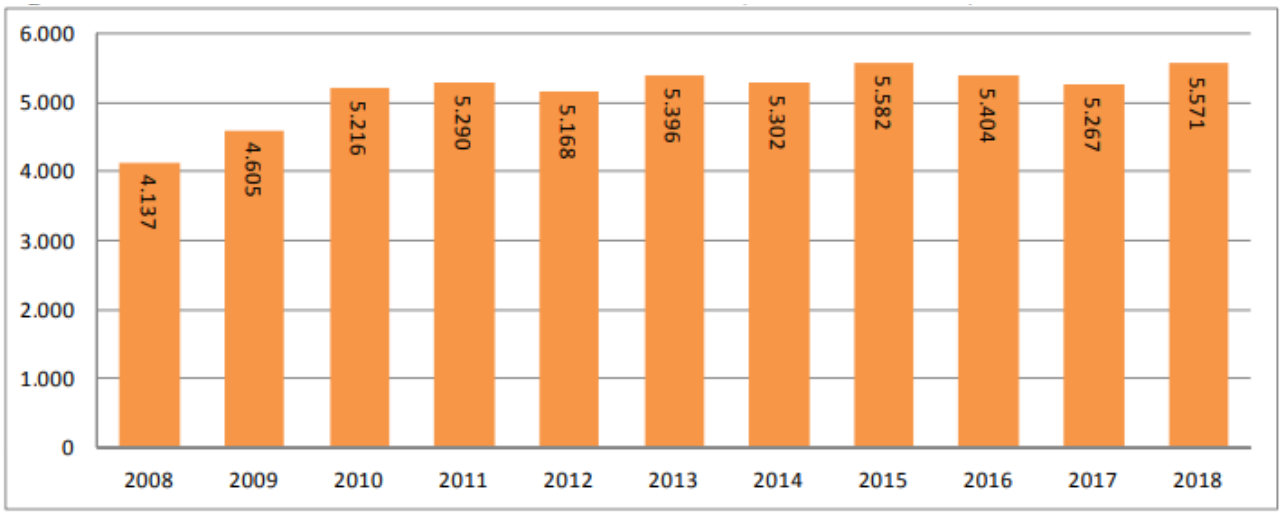

*Figure 5 Municipal waste incineration in Italy (1,000 * tons), 2008-2018*

The most used equipment in the heat treatment plants are the following types: grid combustors, fluidized bed and rotating drum. They can be classified by their incidence of 86.7%, 11.4% and 1.9% for grid combustor, fluidized bed and rotating drum respectively. In addition, the grid combustor is adopted on 67 lines (83.8%), followed by the fluidized bed on 8 lines (10.0%) and the rotary drum combustor on 5 lines (6.3%).

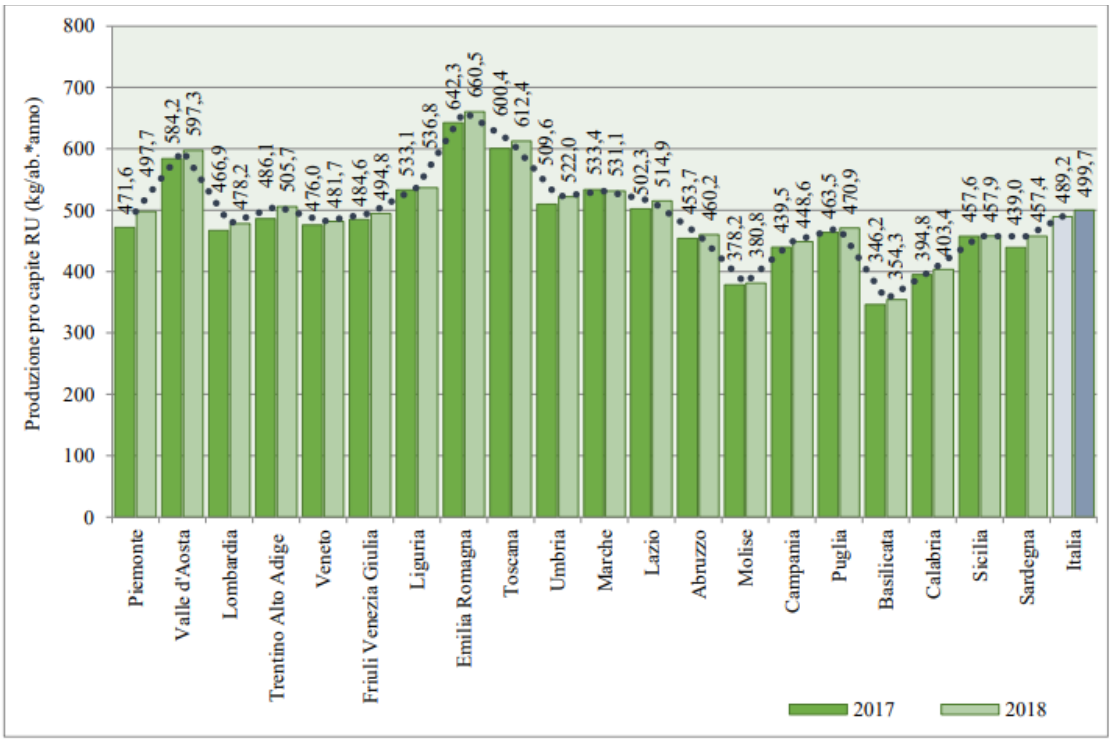

Figure 6 Per capita production of municipal waste by region, years 2017-2018

As shown in Figure 6, the production per capita of urban solid waste expressed in kilograms per inhabitant. The growth percentage of 2.2% between 2017 and 2018 of solid waste production.

Data relating to energy recovery show that, in 2018, all plants on the national territory produced energy; 26 plants treated 3.9 million tons of waste and only carried out the electrical energy recovery of 2.8 million MWh. The remaining 12 plants, on the other hand, are equipped with cogeneration cycles and incinerated over 2.4 million tons of waste with a recovery of 2 million MWh of thermal energy and 1.6 million MWh of electricity. It should be noted that the recovery of electrical/thermal energy is attributable to the total waste treated by the individual plants, since it is not possible to distinguish the portion relating to the incineration of municipal waste only Figure 7.

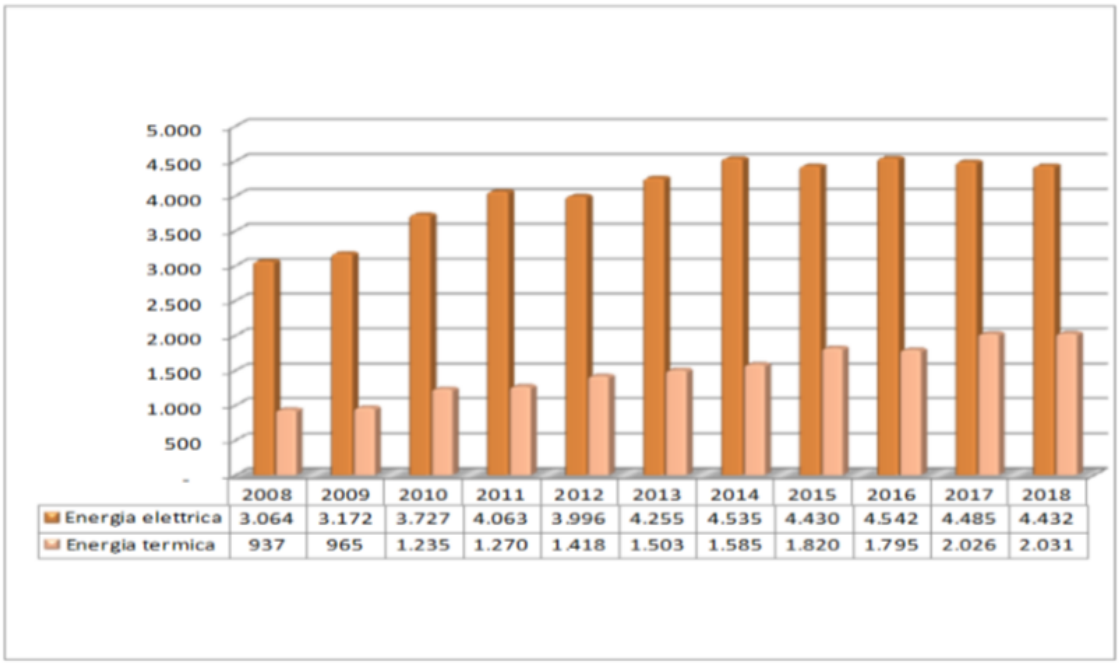

	2008	2009	2010	2011	2012	2013	2014	2015	2016	2017	2018
Energia elettrica	3.064	3.172	3.727	4.063	3.996	4.255	4.535	4.430	4.542	4.485	4.432
Energia termica	937	965	1.235	1.270	1.418	1.503	1.585	1.820	1.795	2.026	2.031

*Figure 7 Energy recovery in incineration plants (1.000*MWh), years 2008-2018*

1.4 By-products deriving from the incineration of municipal solid waste

To date, most of the waste produced at home and by small companies is destined for landfilling; a small percentage is managed in different way through recycling or incineration. MSW incineration is recognized to be a fundamental step for sustainable waste management [5] when recycling is not possible. The advantages of incineration are the reduction of the volume of waste, reduction of landfills and therefore the soil used for landfilling, reduction of pollution due to landfills and the reduction of the environmental impact of the use of fossil fuels for energy production by the recovery of energy through their combustion. This method has seen growth in the past decade. However, the incineration of MSW involves the

production of other by-products that are difficult to manage and of a certain danger in addition to the emissions due to incineration. Different types of ashes are produced due to the incineration: the BA which is the majority of ash produced about 25-30% of the total amount of the incinerated waste is collected at the bottom of the combustion chamber grid, generally consisting of large and small particles. BA residues from incineration are generally considered a byproduct mainly contains heavy metals with low volatilization, which are present as carbonates that is already used, for examples, during the substitution of quartz sand in cement production. The FA that corresponds to the 1-3% of the total amount of incinerated waste and is managed as a toxic waste and destined for landfilling, which are generated in MSW incineration plants and contain more heavy volatile metals in comparison with to BA (such as Zn, Ni, Cu, As, Hg, Cr, and Cd) in a generally leachable form.

BA recycle is a common practice in several EU (Spain, Italy, Germany, Denmark, Netherland, Belgium, etc.) and non-EU countries, such as China, USA, and Taiwan [6]. This is possible thanks to BA chemical composition; this by-product is mainly composed by oxide aggregates, silicates and metals [7], with the latter ones present as large pieces of scrap metals. Then, the main BA recycle applications concern to the building industry, metal secondary source and by substitution of aggregate and filler in the case of concrete construction [8]. Indeed, even if limited, some full scale applications for reuse this by-product as cement kiln feed are available, mainly in Asian countries. Nevertheless, BA have been already used to synthesize adsorbents [9], mesoporous silica [10], zeolites [11], ceramics [12], and other building materials [13]. Indeed, despite that BA contains a high amount of chloride and metals like Fe and Cu [14,15], it is considered as non-hazardous waste [16], requiring minimal treatments before its reuse.

According to European regulation, BA can be reused (for example in construction field, or other materials) if the quantities of salts and toxic elements, which can leach into ground water, are below a certain threshold [17].

In contrast, FA is managed as a toxic waste and destined for landfilling. It is evident that FA disposal turns out to be an irreversible material loss, which is in contrast with circular economy principals. Moreover, several other disadvantages make the avoidance of landfilling among the main environmental priorities in Europe. Currently, legislative development revealed an increase in landfill costs and a decrease of available landfill sites [18]. Additionally, long-term consequences on the environment may be caused by FA landfilling, due to the presence of leachable contaminants. Finally, it has an impact on climate change due to generated greenhouse gas emissions.

Therefore, the adequate treatment of ashes and their reutilization is preferred rather than landfilling. To promote FA reuse, it is fundamental to decrease the leaching toxicity of potentially heavy metals present in water soluble phases. The stabilization of FA ash is proposed by employing several methods, such as using chelating reagents, washing, cement solidification, calcination, melting, and chemical agent extraction [19] and promoting its reuse.

However, several of the proposed stabilization technologies have shortcomings [20]. For example, melting requires high costs. Reagents consumption and the higher mass of treated residues are the main drawbacks of chemical reagent stabilization. Even though some FA treatment technologies were defined as zero-waste treatments [21], they often require FA pre-treatments, which are not suitable for treatment at the incineration plants due to the use of some additional processes and raw materials.

The proposed stabilization technology in this work has a goal to reduce the toxicity of the FA by valorizing and recovery of other by-products.

1.5 State of the art and fly ash disposal

MSWI FA is managed as a toxic waste and destined for landfilling generally. Many different methods of FA treatment have been discussed recently, some are related to the stabilization of FA, their use in the construction civil sector and other are related to their disposal in special landfills the method more used so far.

Several alternative methods to landfilling have been studied but none have yet proven competitive.

- Vitrification process: It consists by reporting the waste to very high temperatures (around 1300 ° C) and to cool it abruptly in order to obtain an inert amorphous mass. In this way the metals and the dangerous substances present remain trapped in the glass matrix. Unfortunately, this method has some disadvantage: firstly, a lot of energy is requested to bring the waste to high temperature; secondly, reaching such high temperatures volatile compounds will form which risk being released into the environment if not properly filtered. It has been estimated that cadmium copper and lead are almost totally volatilized at temperatures above 1000 ° C, depending on the oxidizing or reducing conditions of the process, up to 50% of zinc is lost. Using this method, the slag meets the requirement for leaching as reported by [22]. [23] reports

that except in the HCl solution, the treated samples present a good leachability characteristics and chemical durability.

- Separation process: Various separation process technologies are available in order to increase the FA utilization value by concentrating finer particles, such as unburned carbon, magnetite, glassy cenosphere, etc [24]. Another method usually used for FA separation is by washing or leaching process. Some soluble compound can be obtained like; NaCl and KCl. On the other hand, soluble metals leachability depends on the pH conditions of the solution. Therefore, the treatment condition must be controlled depending on the type of recovered metal. Furthermore, it is possible to add compounds that can favor the removal of metals such as EDTA.
- Solidification or stabilization processes: Through the use of organic or inorganic reagents it is possible to solidify and stabilize FA. An example is the cementing treatment, by treating the waste with cement it is possible to block the release of some metals but the problem of soluble salts still remains, the carbonation that occurs during the maturation process of the cement allows to decrease the leaching of Cu, Pb and Zn but in turn increases the release of Cr [25,26]. However, the solidification and stabilization methods involve a considerable increase in volume, with consequent problems of disposal.

[27] discuss the possibility to reduce the heavy metals leachability by washing FA with water pre-treatment and then reduce the pH values of the solution to 6.5-7.5 by precipitation of aluminium hydroxide ad adsorption of cadmium, lead and zinc ions onto floc particles of $Al(OH)_3$. A good result was obtained by [28,29] by the immobilization of FA using the cement/portland cement by reducing the surface leaching rate. Moreover, [29] have investigated the possibility the potential to use FA as solidification binder to treat industrial waste sludge, this solution has two advantages by immobilizing the industrial waste sludge and to stabilize FA at the same time. Other studies [30] reports the possibility of producing cement clinker from different MSWI FA by the addition of silica and iron oxide. Chemical stabilization was also studied to reduce the leaching of heavy metals from the FA as reported by [31].

2 The RENDERING project

The new technology has recently been proposed by the project "RENDERING" = Recupero Energetico dei fanghi di Depurazione e loro Riutilizzo, IN alternativa ad alcune risorse naturali, per la produzione di composti Green (Energy recovery of sewage sludge (SS) and its reuse, as an alternative to some naturale resources, for the production of green compounds) this project (supported by the Ministry of the Environment and the Protection of the Territory and the Sea) supervised by the laboratory of chemistry for technology.

The biological wastewater treatment process generates significant volumes of semi-liquid sludge, the excess part of which requires treatment and final disposal or recovery. The sludge deriving from the treatment of civil and industrial wastewater, are classified as special waste (Legislative Decree 152/06 Art. 127), and therefore are subject to the regulation of waste. In recent years the problem of the treatment and disposal of these sludge has become increasingly important both nationally and internationally [32]. ISPRA data show that in 2017 the sludge from urban wastewater treatment produced on the national territory amounted to over 3 million and 183 thousand tons Figure 8.

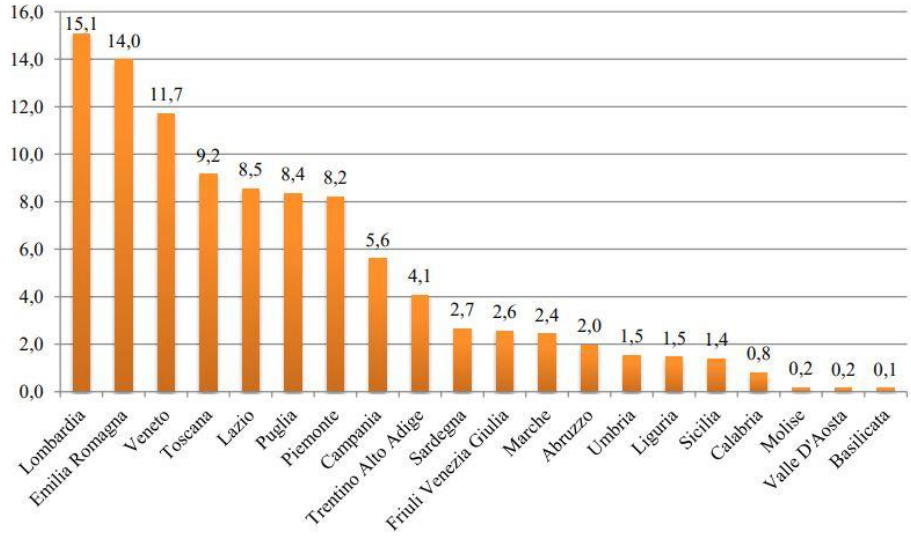

Figure 8 Percentage of sludge produced by urban wastewater treatment by region (EER Code 190805), year 2017.

This high quantity of special waste produced is comparable (equal to about one fifth) with the quantity of waste that is recovered annually (through recycling) in Italy. This data accounts for the size of these special wastes, to which must be added the quantities (data not available for Italy and for many other European countries) of the SS produced by industrial plants and

companies (for example food and livestock). It is evident that in Italy most of this sludge is destined for landfills. If we then consider the actual quantity of sludge (more than 450 thousand tons annually) that is disposed of in this way it is noted that Italy is the tail light of Europe in terms of transferring this waste to landfill Figure 9 [2].

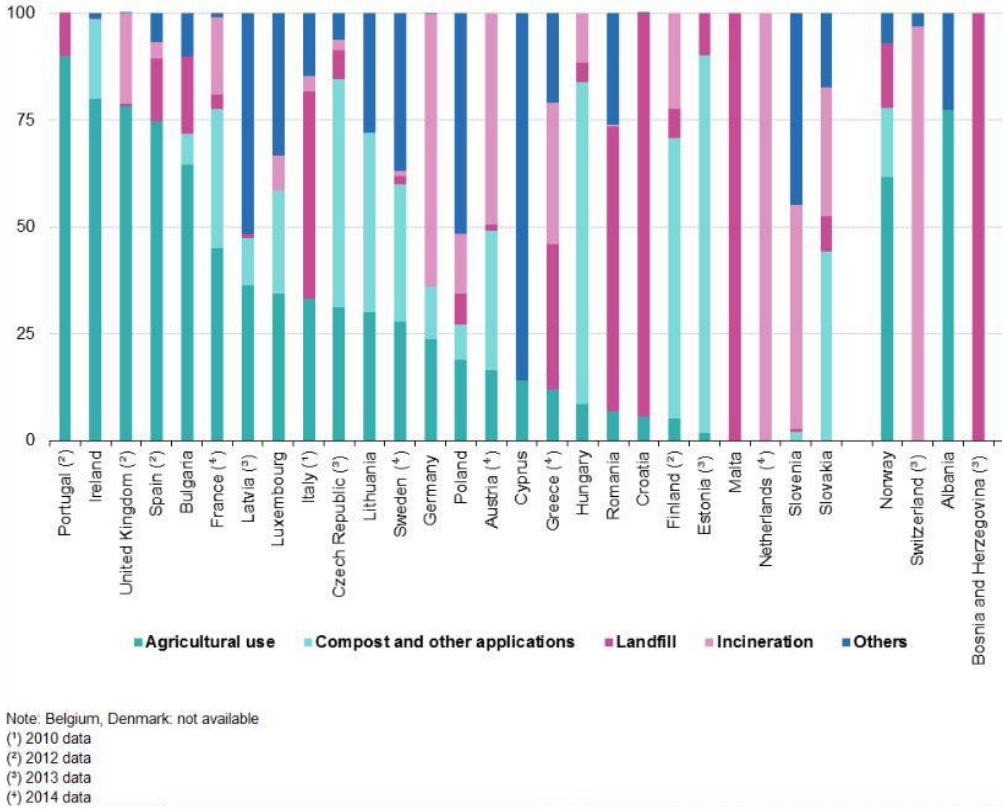

Figure 9 Sewage sludge disposal from urban wastewater treatment in Europe, by type of treatment, 2015 (% of total mass).

The progressive implementation of Directive 91/271/CEE, implemented at national level by Legislative Decree 152/99 and then by Legislative Decree 152/06, which has led to an increase in the purification level present in urban agglomerations, together with the an increasing number of sewage treatment plants and the more restrictive regulations on the disposal of recoverable organic waste in landfills (Legislative Decree 36/2003), have forced us to consider the possibilities of reuse of sludge with increasing attention [33]. In reality, despite the possible reuse in agriculture, after verifying the feasibility in terms of safety, of the sludge, no other sustainable recovery methods of this waste have been proposed. The reuse of sludge, although with very different relevance and criticality from region to region and from province to province, can be considered a cross-cutting theme that affects the entire north-south axis of Italy. There are many incentive campaigns for the reuse of sludge in agriculture. However, also following the Proposal for a CE Directive on soil protection (COM 2006/232 final proposal for a CE Directive establishing a framework for soil

protection), and the recent events that have come to the attention of the sludge reuse report toxic in agriculture (especially in Lombardy), a certain concern has arisen about the common practice of distributing sludge in agricultural land. In fact, unfortunately, in some cases, in the absence and non-fulfilment of the control activities, and in the presence of gaps in the definition of the criteria for carrying them out, unpleasant situations have occurred, with contamination and degradation of resources and in particular of the soil, due to the presence of polluting substances in sludge. It is evident that, although the recovery of these materials in agriculture must be encouraged, very often it is not possible to allocate all of this waste to this destination, so other technologies must be proposed for the reuse of the sludge now destined for the landfill. Recent economic evaluations regarding the treatment of these wastes have shown how combustion processes (for energy recovery) of SS will be necessary in the near future [33]. In fact, the cost of landfilling (including transport) reached a value of around 180 €/ton, while the cost of waste-to-energy was estimated at values of around the half [33]. Energy recovery therefore arises as the only real alternative to reuse in agriculture, when this type of recovery cannot be achieved. While to encourage the reuse of SS in agriculture, clearer and more effective rules and control systems are needed, the possible use of sludge in waste-to-energy processes, which is necessary mostly to be able to remedy disposal in a landfill (and support re-use of the ashes produced, as this project proposes), requires the development of a project aimed at demonstrating and optimizing a new technology.

The waste-to-energy treatment of SS is already widespread in Europe: the fraction of incinerated sludge, compared to the total, has reached values of over 50% in Switzerland, Denmark, Sweden and Belgium [34]. In the USA and Japan this fraction took on a value of 25% and 55% respectively. In Italy the fraction of incinerated sludge, compared to the total, is 2% [33]. This technology can be used for energy enhancement and material recovery. For example, in Germany, sludge waste-to-energy is used as a disposal technology and for the recovery of phosphorus (P). It is important to highlight, however, that the combustion of SS alone is not yet convenient, due to the fact that the dedicated waste-to-energy plants is very expensive. Furthermore, the sludge (which is humid) does not have a good calorific value, so it is necessary to use other fuels to obtain an advantageous combustion [35]. Finally, the problem of heavy metals presents in the ashes (such as Pb, Zn. Hg, As, Cd) has not yet been solved with adequate technology. For example, the European project Susyphos has shown that waste-to-energy is an efficient technology for the recovery of P, which is concentrated in the ashes, but it required the creation of ad hoc plants, with the combustion of chlorine sources (for example plastics such as PVC), to decrease the solubility of heavy metals. The

LCA analysis of possible sludge treatment technologies, aimed at the recovery of P, carried out within the European P-REX project (and confirmed by the ROUTES project), highlighted the potential for using the energy component of these wastes, underlining how co-incineration can increase the sustainability of the process, also significantly mitigating the production of greenhouse gases, compared to the combustion of sludge alone.

For this reason, the RENDERING project proposes co-combustion, that is, the waste-to-energy treatment of these sludges, in conjunction with the combustion of other waste, and, in particular, solid urban waste, on large plants. While the combustion (or co-combustion) of biomass is a technology already widely used, the co-combustion of SS is a technology that can be considered new, especially if we consider large plants [36]. In fact, some measures to manage the impact must be introduced in this case (such as the pumping method of the sludge and the control of their humidity).

The advantages that can be obtained, however, are many. First of all, many chlorides (specifically used in single combustion lines to reduce the solubility of heavy metals) are already present in MSW (and are found in FA produced as waste). Recent studies have shown that the combustion of SS can produce some atmospheric pollutants, if it does not occur in suitable conditions. In particular, high concentrations of sulfur oxide are produced [37]. On the contrary, co-incineration, with a quantity of sludge limited to about 10-15% of the incinerated waste, does not lead to an increase in the pollutants present in FA [38]. It has also been verified that the addition of some calcium-based compounds (such as CaO) allows to reduce the polycyclic aromatic hydrocarbons (PAH) and sulfur oxides, produced in the combustion of only sludge. These materials are already used to reduce the pollutants present in the fumes of the waste-to-energy plants, therefore the pollutant abatement systems, already active on the waste-to-energy plants of solid urban waste, also lend themselves to improving the quality of the fumes and light ash obtained from the co-combustion. Lastly, the RENDERING project aims to reuse the FA obtained in these co-combustion processes. In fact, while BA is reused, FA is classified as toxic and must therefore be treated. To obtain a reusable material, it is necessary to stabilize the light ashes coming out of the waste-to-energy plant, since, being considered hazardous waste, they are generally disposed of in salt mines in Germany.

For this purpose, the RENDERING project aims to begin from recent technologies, and implemented thanks to the support of the European Commission, in the COSMOS and COSMOS-RICE projects. These technologies will be adapted in comparison with the basic formulation. The proposed new technology is based on the first promising results obtained in

the laboratory (already patented). During the RENDERING project, tests of the new technology it were carried out on a pilot plant, to obtain validation (as described in paragraph 2.4).

The project can be considered an initiative aimed primarily at promoting the prevention and reduction of the production and harmfulness of waste, in particular by:

a) The development of a new sustainable technology, which will allow a more rational use and a greater saving of natural resources;

b) The development (and subsequent placing on the market) of materials designed to reduce, with their manufacture, the environmental impact of the composites that contain them, without increasing the quantity or harmfulness of the waste and the risks of pollution; indeed in some cases, these materials, proposed to replace some brominated flame retardants, will help reduce the release of pollutants into the environment;

c) The development of a new technology for the elimination (pathogens and organic pollutants) and the entrapment (heavy metals) of dangerous substances contained in the waste SS and in the FA produced by the waste-to-energy treatment, in order to favor its recovery;

d) The adoption of a method of assessing the sustainability of the new materials produced, aimed at the recovery of waste by recycling, intended to obtain secondary raw materials, as well as the use of waste as an energy source;

e) The development of regional guidelines for the reuse (disincentive of the landfill) of SS.

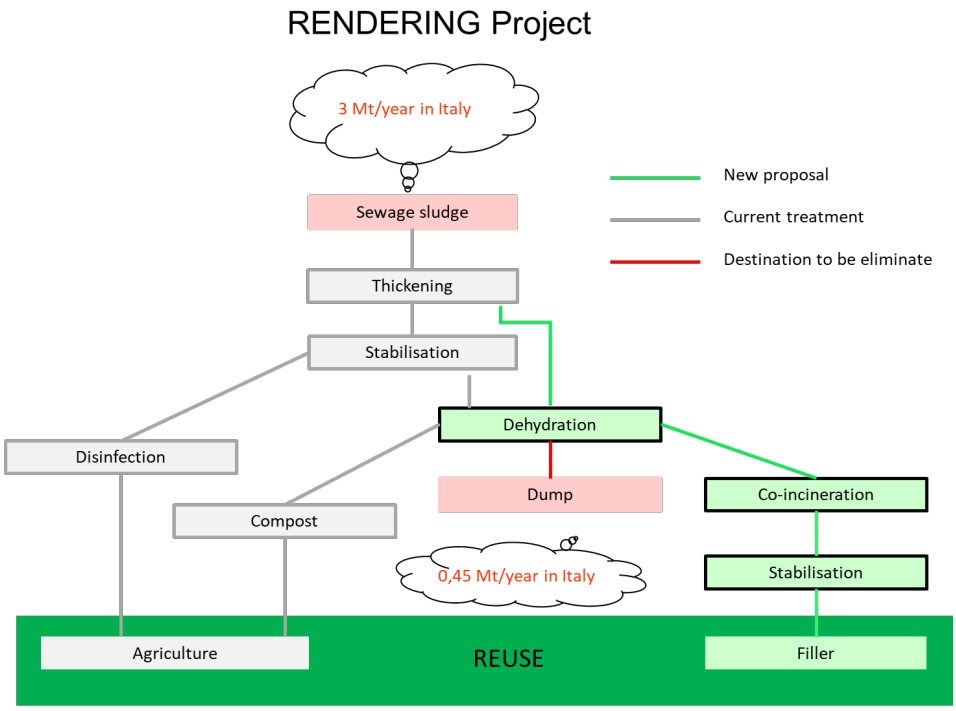

Figure 10 New technology proposed by Rendering project to manage SS.

The new project aims not only to reuse the SS as reported in Figure 10, destined for the landfill, but also to simplify the already consolidated stabilization technique (COSMOS technology) due to the particular chemical-physical characteristics of the ash obtained by co-combustion. The basic idea of the new technology is the use of only one waste ash (and in particular the flue gas desulphurization ash), for the stabilization of the FA produced by the co-combustion, since the main component used so far for the stabilization (the amorphous silica) is already contained in the sludge ashes. The aim is to obtain a powder (from the resulting FA as co-combustion waste), containing inorganic P, suitable for use as a filler for new composites. The presence of P should benefit the flame retardant characteristics of the obtained filler, increasing its performance, compared to the results already obtained with the COSMOS filler. This technology will have the advantage not only of recovering special and dangerous waste (sludge and FA), but also of proposing the reuse of stabilized ash, instead of some natural resources currently used as fillers (e.g. calcite and talc). In addition, the use of recycled flame retardant materials will allow to reduce or completely eliminate the use of current flame retardants, based on brominated, toxic and persistent compounds in the environment.

The RENDERING project therefore foresees the development of the stabilization technology of the FA obtained from the combustion of the SS together with the urban solid waste. The first tests carried out in the laboratory show how promising this new technology is. Therefore, the new technology it has been implemented on ad industrial scale using the pilot plant, situated at the waste to energy plant of Brescia, designed and implemented in the context of other projects already completed (COSMOS and COSMOS RICE).

After the stabilization and characterization of the new filler, it has been used to produce different composites. These composites they have been tested for fire resistance tests.

2.1 Stabilization processes developed by University of Brescia

The MSWI FA is managed as a toxic waste and destined for landfilling in special landfills due to their high heavy metal content. Further treatment process of FA is useful in order to prevent more pollution. Long-term consequences on the Soil and groundwater may be caused MSWI FA landfilling, due to the presence of leachable contaminants if are not properly disposed in landfill for hazardous waste. As well as, it is evident that MSWI FA disposal turns out to be an irreversible material loss, which is in contrast with circular economy

principles. Moreover, several other disadvantages make the avoidance of landfilling among the main environmental priorities in Europe. In addition, due to generated greenhouse gas emissions it has an impact on climate change.

Therefore, the adequate treatment like stabilization of ashes and their reutilization is preferred fairly than landfilling. Before MSWI FA reuse, it is fundamental to decrease the leaching toxicity of potentially heavy metals that can be present in water-soluble phases.

The stabilization of MSWI FA is proposed by employing several methods. The traditional stabilization processes developed at the University of Brescia, propose the mixing of MSWI FA, flue gas desulfurization (FGD), coal fly ash (CFA) and commercial colloidal silica at room temperature to obtain a material called COSMOS. The inert material obtained called COSMOS may be reused as a raw material for some applications (construction purpose, composite material filler, etc.). This method requires FA pre-treatments and the use of colloidal silica (a commercial man-made material), which are not suitable for treatment at the incineration plants due to the use of some additional processes and raw materials. Therefore, it has been developed a new another process called COSMOS-RICE that replace the use of colloidal silica by rice husk ash (RHA). RHA contain a high content of silica (60-90%), so may be considered as a precursor for silica production. In fact, by alkaline solubilization process and further acid washing of RHA, amorphous silica gel can be easily obtained. RHA was directly used for stabilize FA (without silica extraction) as a second step, in order to reach a method with higher sustainability. Nevertheless, this kind of process in comparison to COSMOS and COSMOS-RICE with silica gel requires more time to reach a complete stabilization of heavy metals [39,40]. Finally, COSMOS Fume produced using SF as stabilizing agent as reported by [41,42] has many advantages: the high reactivity allows to obtain an inertization results comparable to those of commercial silica in a short time, less than the time needed with COSMOS Rice technology. Also, in this case the materials used for the realization of COSMOS Fume are all by-products of other industrial processes.

2.2 Rendering stabilization process

The new method with zero-waste approach propose the use of all waste materials, to stabilize FA. This new stabilization process requires the mixing of the following four ash typologies including FGD, CFA, MSWI FA and MSWI BA.

In particular, BA is used as a stabilizing agent which is considered as a new urban mining source due to its pozzolanic characteristics (chapter 3). It is known that BA has a complex inorganic composition. As reported in literature BA contains several silicate phases with different compositions. However, the glass phases represent the main incineration products of BA, accounting for 50% of its composition [43]. As reported by [44] the characterization of the melt glass phase composition collected in various incineration facilities suggests the main representative components as the following elements: silicon, calcium, aluminium, and some alkaline and alkaline-earth metals. A high amounts of melt glass phases and different compounds (silicate-mineral and nonsilicate-mineral phases, such as spinels and metallic inclusions) and calcium-rich mineral phases (calcite and ettringite) account to a considerable proportion of the BA [43,45].

MSWI BA is proposed to be used as heavy metal stabilizer for FA. In particular, the presence of amorphous unstable phases and the consequent reactivity of BA, were used as the characteristics to determine the choice of this waste. In fact, it is expected that dissolved amorphous silica and alumina (derived from BA) in presence of calcium ions (and in a highly alkaline environment) promote a pozzolanic reaction with FA, leading to the formation of cementitious compounds such C-S-H and calcium aluminate hydrates C-A-H [46]. As reported by [47] the leaching of heavy metals can be reduced due to pozzolanic reaction. In similar processes, involving the FA stabilization, it was demonstrated that also carbonation process can occur due to the calcium hydroxide presence in the used wastes [48], producing pH reduction, with consequent heavy metals mobilization. A recent paper about BA characterization [45] shows that the finest fraction of BA (less than 200 Micron) contains a large amount of leachable heavy metals. In order to promote a safer reuse of BA, the new stabilization process suggest separating this fraction, from the rest of the BA. In addition, coarse particles appropriate for building applications, generally contain crystalline silica oxides, which are non-reactive [45].

The new proposed technology is in agreement with the EU policy approved and implemented for a circular economy that recommends closing the material use loop by utilizing waste for suitable and sustainable applications [49].

2.3 Comparison between COSMOS and RENDERING technologies

In this study we can distinguish between two macro-areas of different inertization processes reported in chapter 2:

- Inertization process using only by-products:
- Inertization process using by-products and chemical substances.

In the first type of inertization process using only by-products we have: COSMOS Rice, COSMOS fume and the new technology are present. Instead, in the second type we have just the COSMOS technology that depends on the use of chemical substances to inertize the FA.
The COSMOS Fume technology use the SF to stabilize the FA. As reported by [42,104] this technology involves also the employ of FGD and CFA to stabilize heavy metals, as a consequence, only waste (or by-product) materials are employed in the process. The new technology reported by Rendering project propose the use of BA produced by the co-incineration of SS and MSW due to its content of amorphous phases. CFA and FGD residues were also used. The simplicity of the proposed technology, which requires only the mixing of ashes from the same origin, makes it truly suitable to be applied directly to thermal treatment plants. Consequently, the new proposed strategy for MSWI waste management can be actually considered a zero-waste approach due to production of inert materials. Energy and materials recovery from waste-to-energy plants provides environmental advantage as it saves virgin materials, returns waste materials to the economic cycle and approximately 2630 t CO_2-eq/day. The versatility of this process, which occurs at room temperature and requires the use of wastes produced at the same location, has the following benefits: (1) avoids landfilling of MSWI FA (and some BA residues); (2) avoids the transport of waste to another area for stabilization; (3) saves non renewable resources and, consequently, safeguards them; (4) saves CO_2 emission and sequestrates carbon dioxide due to carbonation reactions with good actions on climate change; (5) produces materials that may be reused as a filler and (6) opens new perspective markets and business models.
The samples preparation can be divided into two different categories: the first one contains the comparison between stabilization process of using SF and the stabilization process using BA; and the second one contain the comparison between the stabilization method using SF and the stabilization method using different granulometric size of BA.

2.4 Scale up of the process by using pilot plant

As mentioned before the pilot plant adopted by the new technology to produce the stabilized ash, it has been projected and implemented firstly during the first COSMOS project. The pilot plant was built at the A2A (is an Italian multi-utility, operating in the environment, energy, heat, grids and technologies for smart cities sectors) in order to verify the real industrial applicability of the production process. The plant basically consists of four distinct units described below:

1) Storage and handling unit for powders and liquids;
2) Mixing unit;
3) Dosing unit for powders and liquids / Control panel;
4) Sludge washing unit.

2.4.1 Storage and handling unit for powders and liquids

Up to 6 distinct components are used in order to obtain the inert material adopting the new technology developed by the University of Brescia, as reported and explained more in detail in chapter 4:

1) FA from co-incineration of MSW and SS incineration (CER 190105* - Filtration residues produced by the treatment of fumes produced from the incineration process);
2) CFA (CER 100102 - CFA, used as a substitute for other additives and in limited quantities compared to FA) from the Lamarmora thermoelectric plant of A2A Energia S.p.A., in via Malta, 25 in Brescia;
3) Flue Gas Desulphurization residues (CER 100105 - Solid waste produced by calcium-based reactions in the processes of fumes desulphurization, used as a substitute for other additives and in limited quantities compared to FA) also from the Lamarmora thermoelectric power station;
4) BA from co-incineration of MSW and SS incineration (CER 190111*-recovered from the bottom camber combustion);
5) SF, produced by the metal industry;
6) Tap water.

The component 4 and 5 are interchangeable as sources of amorphous silica, which can be used in adequate quantities as will be shown in the chapter relating to the comparison of the

inerting powder of the various sources of amorphous silica that can be used. The SF, or alternatively the BA, can be mixed with component 2 (coal ash) or replace it entirely. The following diagram reported in Figure 11 describes the process in its individual steps:

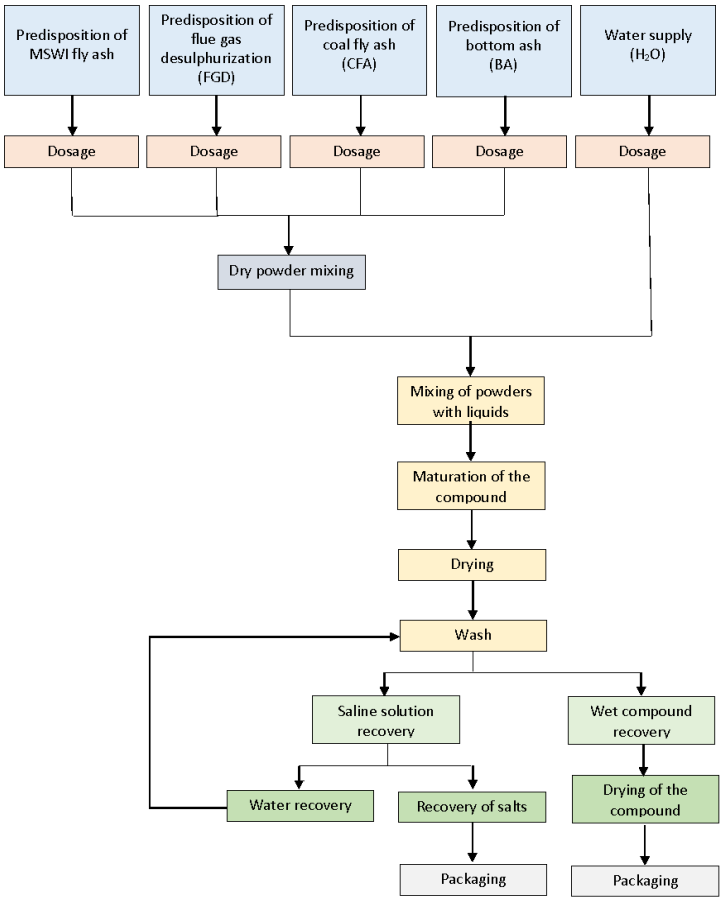

Figure 11 New inertization process steps

The necessary powders are stored in 1 m^3 bags equipped with a discharge valve on the bottom. These big bags arrive already packaged and filled at the plant, ready to be loaded inside a hopper with a capacity of about 200 kg Figure 12.

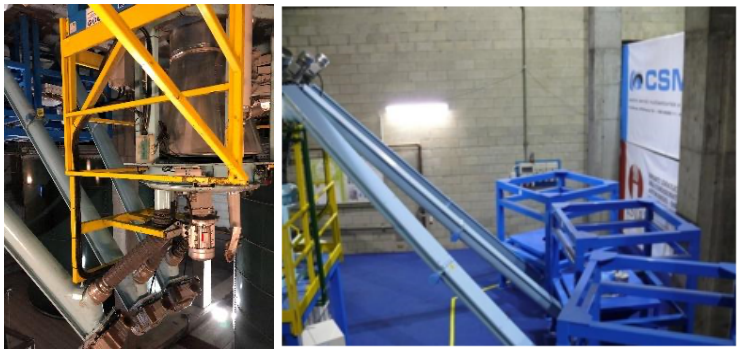

Figure 12 Big-bag holder structures on hopper and powder feeding screw.

The big-bag is connected to the hopper and, using a sleeve it is possible to open the discharge valve which allows the bag to be emptied, to avoid direct contact of the operator with the

ashes. The liquid components are loaded with the help of self-priming centrifugal Jet pumps with cast iron body (1x220-240 V; Power supply 50Hz P1 max kW 0.85 P2 nominal 0.6 kW 0.8 hp In A 3.8 Capacitor 12.5Uf 450 Vc).

2.4.2 Mixing unit

The mixer consists of a truncated-cone-shaped steel container (AISI 304) with a capacity of approximately 200 litters Figure 13.

Figure 13 Mixer container.

Inside the vertical axis mixer there are the homogenizing blades of the components, which are driven by a 1.5 kW motor equipped with a gear-motor (35/1 rpm output) controlled by an inverter. The mixer is sealed with a lid which, if necessary, can be opened to inspect the mixer itself. On the cover there are three couplings for powders and two couplings for liquids Figure 14. Finally, there is the last quick connection to allow the system's washing water to be connected.

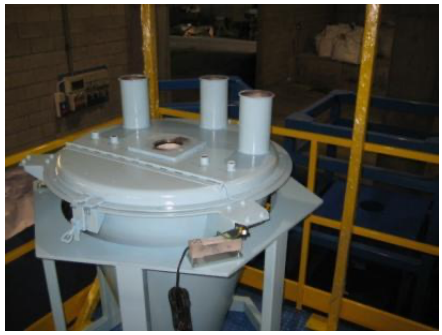

Figure 14 Powders and water connections.

The lid is equipped with safety systems, if opened during the mixing phase the rotation of the blades is immediately interrupted. The mixer rests on calibrated load cells to check in real time the quantities added through the augers. It is mounted on a steel structure which can be accessed through a special ladder, below the mixer a 1 m^3 tank is placed to collect the washing water of the mixer itself Figure 15.

Figure 15 Washing water collection tank and the supporting structure.

It should be considered that the plant is in his experimental phase and therefore it is possible to treat between 50 and 100 kg of product at a time. On the bottom of the mixer there is a guillotine valve with the function of regulating the discharge of the mixed material. At the end of the mixing cycle, the compound obtained is discharged into trays of about 5kg which are left to mature in a special structure Figure 16.

Figure 16 Trays supporting structure.

2.4.3 Control unit for dosing the powders and liquids

The control panel is located near to the structure, this allows the operator to activate the augers and appropriately dose the different ingredients to be inserted in the mixer. The controller also allows to adjust the mixing times and speeds, and to store pre-set programs.

Figure 17 Control panel unit.

3 Raw materials used

The materials used in this study and the raw waste material are described in this chapter. All the by-products are provided by the thermal-valorization and the electrical power plants of A2A located at Brescia for waste and coal combustion respectively, to produce thermal and electric energy.
The initial waste material divided into two categories, provided from different sources:

- MSW;
- SS.

The by-products of the thermal-valorization:

- Co-incineration MSWI FA;
- Co-incineration MSWI BA.

The by-products of the electrical power plant:

- FGD;
- CFA.

The by-product of the industrial melting processes of iron-silicon alloys and metal silicon:

- SF.

3.1 Sewage sludge

During the sewage treatment of industrial and municipal wastewater, the residual semi-solid material produced is defined SS. The last functional phase of a purification treatment is the treatment of sludge, the aim of this procedure is to improve the quality of the final waste, in order to decide the final destination either properly dispose of it or reuse it [50]. The sludge of a purification plant, when it is no longer reusable internally, follows a series of operations called sludge treatment. In this phase the sludge that contains almost all the residual Biochemical Oxygen Demand (BOD_5) and which, due to the presence of significant quantities of bacterial material, are highly putrescible, are stabilized so as to make them suitable for subsequent drying and disposal [50]. The final goal of the sludge treatment is to improve the characteristics of the sludge so that it can be properly disposed of as waste or

(only if it meets certain requirements) reused in agriculture. It should be noted that the treatments commonly used can belong to either one of the two categories (for example, as described below, the conditioning treatment) or to both simultaneously (for example the incineration treatment).

The main sequential sludge treatment operations are listed below [50]:

- Thickening or concentration (this phase serves to increase the dry matter content of the mud in order to reduce the volumes necessary for its treatment);
- Biological stabilization (it has the function of mineralizing part of the putrescible organic substances and eliminating pathogenic bacteria and parasites normally present in the mud);
- Conditioning (has the function of weakening the bonds of water with solid particles to facilitate its escape);
- Dehydration and drying (it is used to eliminate a good part of the water present in the stabilized sludge);
- Incineration or compaction (they constitute the phase preceding the final disposal).

Incineration is generally carried out on sludges that contain dangerous substances that put at risk the possibility of reuse or transfer to landfills. It is carried out in incinerators (preferably waste-to-energy plants) where the mud is burned. Since the combustion of the mud is self-sustaining when the humidity is less than 70%, only the sludge dehydrated with the filter presses does not need any fuel (methane, diesel, coal, etc.) while the sludge dehydrated with the other systems it therefore entails higher incineration costs. It is evident that in incineration particular care must be dedicated to the purification of the fumes before they are released into the atmosphere.

As reported in chapter 2, the aim of RENDERING is to valorise SS by its co-incineration with MSW recovering the energy produced and their reuse as an alternative to some natural resources.

3.1.1 Type of sludges

The sludge generated by a traditional purification plant treatment are as follows:

- Primary sludge: these are the sludge deriving from the primary sedimentation process, made up of fresh organic matter which separates from the raw sewage without having undergone any treatment (granulated sludge) and contain a

quantity of solids equal to 4% (96% humidity). These sludges degrade more quickly anaerobically than other types of sludge and produce more biogas;

- Secondary, biological or active sludge: these are the sludge deriving from the biological oxidation processes (percolating filters or excess sludge from activated sludge plants). They are flocked sludge and have a lower percentage of solids than that of primary sludge, with a typical value of 1% (99% humidity), but they are richer in nitrogen and phosphorus;
- Chemical sludge: it is the sludge deriving from clariflocculation processes.

As a rule, however, combined sludges arrive at the sludge line, i.e. primary and secondary sludges which have a high humidity, equal to 96-99%. This moisture must be removed from the mud to allow for its final disposal, minimizing environmental damage and at the lowest possible cost.

3.1.2 Chemical composition of sewage sludge

The characteristics of the SS depend strongly on the quality of the incoming wastewater, both for industrial waste and for urban waste [51]. Many pollutants, including metals and fat-soluble organic compounds, condense in the sludge resulting in high concentrations in the solid phase. The wastewater treatment typology, the addition of chemicals, biological activity, etc. also have a significant influence on the quality of the sludge. Some parameters characterize the SS (such as the solids at 105 °C and at 600 °C) are specifically linked to the ways in which they are produced (for example, they are characteristics influenced by the presence of primary sludge or by the age of the biological sludge) or, however, strongly influenced by the treatments they undergo (aerobic digestion, anaerobic digestion, chemical stabilization).

The chemical composition of the SS destined to incineration of different producer supplied to the waste-to-energy plant of Brescia are reported in Table 1. The SS supplied by the fourth supplier and the seventh are dehydrated and biological sludge respectively.

Table 1 Characterization of SS from different producers

		Producer											
Parameter	**Unit**	**1**	**2**	**3**	**4**	**5**	**6**	**7**	**8**	**9**	**10**	**11**	**12**
Residual at 105 °	%	17	24	16	16	27	29	20	22	30	17	18	25
Residual at 600 °	%	3	4	6	4	11	10	6	9	5	6	6	9
Lower calorific value	kJ/Kg	669	4017	<100	-	1501	6822	<500	227	2589	<100	175	<100
Total chlorine	%	0	1	0	-	0	0	0	0	1	0	0	0
Sulfur	%	<0.1	0	<0.1	-	0	0	0	<0.1	0	<0.1	0	<0.1
Lead	mg/Kg	12	16	8	19	117	83	132	103	87	10	5	29
Copper	mg/Kg	51	359	40	200	690	547	276	703	383	62	37	137
Manganese	mg/Kg	17	55	95	-	504	150	175	803	115	98	56	50
Cadmium	mg/Kg	0	0	0	<1	1	2	1	3	2	0	0	0
Arsenic	mg/Kg	<1	4	1	11	12	5	7	22	6	1	<1	1
Mercury	mg/Kg	<0.1	1	<0.1	0	1	3	<1	1	1	0	<0.1	0
Chrome	mg/Kg	16	252	48	65	136	140	1	455	201	7	63	44
Nickel	mg/Kg	7	34	18	-	118	44	33	209	61	6	17	57
Zinc	mg/Kg	188	334	108	244	1186	2000	654	1248	2038	132	66	263
Vanadium	mg/Kg	3	7	3	-	18	17	8	25	18	3	2	3
Cobalt	mg/Kg	<1	7	12	-	8	7	9	23	6	<1	6	1
Antimony	mg/Kg	1	66	0	-	1	6	4	4	8	0	0	1
Potassium	mg/Kg	1294	4225	647	3100	3100	nd	3	2668	1414	419	479	432
Thallium	mg/Kg	<1	<0.1	<1	-	<0.1	nd	<5	0	0	<1	<1	<1

The maximum concentration values of heavy metals in the SS intended for incineration not exceed those allowed by Legislative Decree 99/1992 for sludge intended for use in agriculture as reported in Table 2 [4].

Table 2 Limit values of heavy metals

Parameter	Limit value [mg/kg]
Cadmium	20
Mercury	10
Nickel	300
Lead	750
Copper	1000
Zinc	2500

3.2 Raw ashes

3.2.1 Fly ash from co-incineration

Co-incineration of SS and MSW generate huge volumes of flue gas that carry residues from incomplete combustion and a wide range of toxic pollutants. The flue gases always carry ash, heavy metals, and a variety of organic and inorganic compounds. The pollutants are present as particles (dust) and gases such as hydrochloric acid (HCl), hydrogen fluoride (HF), and sulfur dioxide (SO_2). Common composition of flue gases follows:

- Particulate pollutants: FA, including the heavy metals of antimony (Sb), arsenic (As), cadmium (Cd), chromium (Cr), cobalt (Co), copper (Cu), lead (Pb), manganese (Mn), mercury (Hg), nickel (Ni), thallium (TI), and vanadium (V);
- Gaseous pollutants: HCl mainly from the combustion of polyvinyl chloride, SO_2 from combustion of sulfurous compounds, HF from combustion of fluorine compounds, and nitrogen oxides (NO_x) from part of the nitrogen in the waste and N_2 in the air.

Some harmful compounds such as mercury, dioxins, and NO_x can be fully removed only through advanced and costly chemical treatment technologies. Primary and secondary measures can help reduce emission of pollutants. Primary measures, which are initiatives that actually hinder the formation of pollutants. Secondary measures consist of the Air Pollution Control (APC) system that precipitates, adsorbs, absorbs, or transforms the pollutants. An APC system is comprised of electrostatic precipitators (ESPs); baghouse filters; dry, semi-dry, semi-wet, and wet acid gas removal systems; catalysts.

For example, waste-to-energy plant of Brescia use the baghouse filters as a secondary measure of the APC system. Bag filters ensure very efficient collection of dust, while at the same time they further absorb the acidic residue. For the attainment of this further absorption, it is important that a layer of dust be maintained on the fabric as it collects particles with diameters smaller than micrometers. In this way, heavy metals and dioxins, usually smaller particles are removed efficiently.

The automatic system of controlling and cleaning the filters (activated by a detected pressure difference of filters) ensures the presence of a continuous dust layer on the bags/filters. The cleaning process is programmed to take place when these are in operation (it is not necessary

to isolate the filter part being cleaned) and not influence the process of cleaning. Gases flow through bag filters from the outside of the bag toward the inside, and dust is collected on the outside. Gases reach the bag filters through a pipe and are distributed via openings to various filter sections.

FA is captured on the dust layer formed on the bags and the filter itself. Clean gases flow through the upper openings of the compartment outlet damper and via the outlet pipe through the induced draft fan. They then reach the chimney and finally the atmosphere.

The dust layer increases the bag filter efficiency while remaining quantities of lime react with acidic compounds. Dioxins and the rest of VOCs are absorbed by the activated carbon, and the PAC particles are captured by the dust layer. When pressure of the filter is increased up to a certain point, this means that the dust layer has become too thick and the cleaning process should be activated.

The FA that stays at the outer surface of the filter bags is periodically removed by an air pulse and blown into the bag from the inner side. This cleaning releases the particles, which fall into the discharge hopper.

3.2.2 Bottom ash from co-incineration

The noncombustible fraction of the MSW charged to the furnace forms a residue (ash) remaining on the bottom of the grate at the completion of the combustion cycle. This material is generally referred to as BA (BA) but is also called grate ash, slag, or clinkers. BA is the most significant by-product, generated at a rate of approximately 20-25% by weight of the input combusted materials, but only 5-10% by volume, accounting about 80% of the residual wastes remaining after combustion [52]. BA must be taken out of the furnace in such a way that maintains control over the combustion process. A seal on the furnace is normally provided by a column of water. The water bath also serves to extinguish any remaining combustibles and cool the ash. Furthermore, large pieces of clinker fracture when quenched, reducing their size. The BA leaves the furnace wet, thereby minimizing fugitive dust emissions.

This by-product is similar in appearance to a porous, greyish, silty sand with gravel and contains small amounts of unburned organic material and chunks of metal. The BA stream consists primarily of glass, ceramics, ferrous and nonferrous metals, and minerals [7].

According to European regulation, BA can be reused (for example in construction field, or other materials) if the quantities of salts and toxic elements, which can leach into ground

water, are below a certain threshold [17]. However, there is no harmonized test methods and EU countries have developed their own rules to regulate BA reuse in the construction sector [53]. For example, recent works have shown that BA chemical characteristic may, sometimes, not comply with some local existing limit values for its unlimited reuse as, for instance, in clinker production and in road construction [54]. For this reason, BA treatment becomes necessary before its recycle. In particular, a standard pre-treatment of BA, which involves a screening stage to remove the oversized metals fractions (fractions larger than 1 cm) [55], is generally performed. Separating the various size fractions of BA is also proposed [56], which leads to an increase recovery of the valuable materials. Finally, BA grinding is a suggested procedure to reduce the average particle size and make it more suitable for uses as building materials in construction field.

Depending on its final destination, the BA particle size can be subjected to adjustment such as sieving for use as fine building aggregate or grinding for further uses as a cement component [57,58].

The above-mentioned procedures are considered simple and cost-effective pre-treatment strategies, which can also be implemented at a plant scale. In this context, it is evident that the different BA size fractions must be studied in detail, to better address their recycle strategy. For recovery purposes, BA fraction below 4 mm is usually separated because it contains leachable heavy metals, such as Cu, Cr and some other metals like: Mo, Pb, Zn and Sb [59] and inorganic salts (such as chlorides and sulfates) [60].

Several works about BA characterization are available in literature (see for a global literature view the reference [61]. The recently publishes studies [45,62–64] demonstrate the high scientific interest to investigate different possibilities to recover this waste, by particles size selection.

However, despite that several works discuss the BA composition and detailed phases amount, often the amorphous content is not considered. Amorphous is formed due to a rapid waste combustion, cooling, and quenching, in conditions that are far from equilibrium. As a consequence, BA can contain large amount of amorphous phase that make it generally metastable under environmental conditions [61] This can severely affect a reliable BA characterization, because it is highly susceptible to chemical and mineralogical alteration over time.

The characteristics of the BA produced from co-incineration of MSW and SS must be investigated, because they can differ from that of BA produced from MSW incineration only.

In my PhD study, BA derived from co-combustion processes involving MSW and SS is characterized in detail. This is the first study dealing with this topic, offering a basis work, also with the aim to propose BA recycle.

A deep characterization of BA based on various size fractions was performed. The BA reactivity is investigated on the basis of a recent proposed technology used to stabilize FA [65]. This research highlights an advantage of the BA recycle.

3.2.3 Flue gas desulfurization residues

FGD is a by-product resulting from current coal combustion processes. The use of dry processes, based on lime or sodium reagents, is widespread for sulfur dioxide (SO_2) emission removal in the coal thermal power plant. The FGD material produced from these processes in generally landfilled together with BA and FA materials. In the frame of waste management technologies, the physical and chemical characterization of FGD enables a more detailed assessment of beneficial and safe end-use options. Moreover, it provides a greater level of understanding relative to proper landfill management or the operational considerations for their correct reuse.

The composition of FGD residues is very variable. The residues derived from forced oxidation processes are mainly characterized by 80% of gypsum mixed with FA, although many residues contain less gypsum (20-50% of the bulk material). FGD residues are very stable in atmospheric conditions at room temperature [66].

The FGD residues contain two main components: a silico-aluminous FA part and calcic FGD phases. The FGD XRD pattern identified portlandite ($Ca(OH)_2$) as the main mineral phase present in this material, followed by calcium sulphite hemihydrate (hannebachite, $CaSO_3 \cdot 0.5H_2O$) and gypsum ($CaSO_4 \cdot 2H_2O$) [67]. In the literature, the XRD spectrum of FGD residues also revealed the presence of SiO_2, mullite, and hematite, which derived from the presence of FA in the sample. On the other hand, the semi-dry FGD ash showed the existence of some amorphous vitreous material and unburned carbon [68].

The elemental chemical analysis of leachate FGD pointed out S and Ca as the major constituents [42,69,70]. Other than S and Ca, FGD ashes are dominated by the presence of Al, Fe, and Si [71].

The leaching solution of FGD enhances the lack of large amounts of soluble heavy metals. A low Zn amount was found in the FGD leaching solution, while Pb was lower than the

detection limit. A quantitative analysis revealed that Cr, Mn, Fe, and Cu were found in trace concentrations [67].

The changes in the elemental content of FGD were mainly due to the addition of gypsum granules in the desulfurization tower and the SO_2 removal by $CaO/CaCO_3$. The increase of S and Ca in FGD residues could be related to the entrainment of dissolution and gypsum slurry, where S and Ca in gypsum and limestone were the main elements [72].

The morphology of FGD particles before and after desulfurization by SEM was performed. Before desulfurization, the particles were fairly dispersed with an irregular spherical shape, while the agglomerates increased after desulfurization, forming an irregular and dense structures. As further study focused on the comparison of the morphology of FGD residues deriving from a plant and steel factory revealed noticeable differences [68]. The FGD particles from steel factories were characterized by irregular shapes, smooth surfaces, and loose constructions, while semi-dry FGD ash from the thermal power plant included some FA, had a rough surface, and a micro-porous structure. Particle size was another difference between two types of FGD. The FGD particles deriving from the power station are usually bigger in size than those of the steel factory – around 1-50 μm and 0.5-25 μm, respectively.

3.2.4 Coal fly ash

CFA is a by-product generated during the pulverized coal combustion process in thermal power plants. The characterization of CFA by means of XRD revealed quartz (SiO_2) and mullite ($Al_{4.75}Si_{1.26}O_{9.63}$) as the major non-magnetic fractions present in the crystalline phase, confirming the data reported by Bosio et al. (2014), since CFA powders have the same origin [73]. Other studies report that the magnetic phase present in CFA is magnetite, also report the presence of hematite [74,75]. According to the American Society for Testing and Materials (ASTM) [76], CFA can be categorized as class F FA or C FA on the basis of the silica, alumina, and iron amount. In particular, the percentage weight of $SiO_2 + Al_2O_3 + Fe_2O_3$ in higher than 70% or between 50% and 70% for CFA class F and C, respectively [77].

On the contrary of SF, the elemental composition of CFA varied, owing to coal heterogeneity. This variation was confirmed by an elemental chemical analysis of leachates performed by the total reflection X-ray fluorescence (TXRF) [67,78]. The obtained results revealed that CFA was mostly aluminosilicate material and the major constituent elements were the following: Al, Ca, Fe, K, and Si [79]. The literature results also confirm the

presence of unburned carbon and other elements in trace amount, some of which could become toxic elements due to their ability to accumulate over time [76]. Particle size was the major factor in determining the CFA toxicity. The smaller the size of the particle, the greater its surface area to volume ratio, and the higher its chemical and biological reactivity [80]. A SEM analysis was employed to investigate the morphological characteristics of CFA. The parameters that influence the CFA morphology are combustion temperature, cooling rate, and also the chemical composition of CFA particles [81]. The SEM images, demonstrated the presence of irregular, rough surfaces to smooth, spherical shapes with sizes ranging from 0.2-25 μm. Furthermore, the aggregation of the microspheres with small particle sizes connected to surfaces was identified.

As reported by Zanoletti [82], the EDX analysis revealed that the predominant elements in CFA are generally C, O, Si, Al, S, K, Ca, and Fe in various proportions. Sometimes, some residual amounts of other elements can be detected [83].

The TEM analysis confirmed the spherical shape of CFA particles and the presence of agglomerates. Moreover, EDX maps allow the elemental distribution of the sample to be investigated. The EDX chemical analysis showed a non-homogenous elemental distribution. Indeed, Al is found in the proximity of Si and often co-localized, reflecting the presence of alumina-silicate compounds and also the mullite phase, corroborating the results of the XRD patterns and SEM analysis [84]. On the contrary, Fe and Ca demonstrate a homogenous distribution on the agglomerate surface. Our TEM data agreed with the finding of Chen [85], who reports the presence of alumina-silicate phases.

3.2.5 Silica fume

Also called silica smoke, it is a by-product of the industrial melting processes of iron-silicon alloys and metal silicon. These alloys are produced through the use of electric arc furnaces, in which very high temperatures close to 2000°C is reached. During the process some silicon micro particles are formed which are entrained by the fumes, which coming into contact with the oxygen present in the colder parts at the exit of the oven leads to the re-oxidation of the silicon which condenses in the form of very fine particles. These are then suitably separated from the emission gas flow thanks to a filtering apparatus. Sudden cooling leads to the formation of amorphous micro silica spheres which aggregate in clusters with a maximum size of a few tens of microns. A simple mechanical stirring can separate these clusters,

transforming the silica smoke into a very fine material with particle sizes ranging from 0.01 to 0.50 μm [86]. The composition of the material in this case also depends strictly on the production process and the raw materials used.

Before the eighties, SF was considered only a waste and as such stored in special landfills. Subsequently, thanks to its pozzolanic characteristics, it was used as a filler in the building field. The physical and chemical properties of this material make it suitable for the packaging of cements and concretes. It allows to reduce porosity by increasing the mechanical properties of the composite obtained; in addition, the following are also better: resistance to chemical attacks, resistance to freeze-thaw cycles and adherence to the reinforcement bars. This is due to the pozzolanic action brought by the amorphous silica and the very fine grain size of the material. Normally the excess water, used to work the cement mix, evaporates tending to leave gaps and spaces within which salts or corrosive agents can deposit. SF allows to reduce this effect by increasing the quality of the final material.

The characterization of SF shows that its particles had a diameter ranging from 20 to 500 nm [87,88], with a specific surface area of 220 m^2/g, bulk density of 200-350 kg/m^3, and porosity of 0.84. The TEM analysis revealed the presence of spherical particles assembled in agglomerates, which are formed during collection and cooling processes. Table 3 reports the elemental analysis of SF that contain a high percentage of silicon and oxygen, as confirmed by the literature [89,90].

Table 3 EDX analysis in TEM mode [91,92]

Element (w %)	O	Mg	Si	K
SF	29.79	0.86	65.16	4.19

The X-ray diffraction (XRD) pattern revealed the presence of an amorphous phase, a broadened peak at around $2\theta = 22^{o}$, and cristobalite, which describes the small presence of crystalline SiO_2 formed during the production process.

4 Sample Preparation and Methodology

Sample preparation is highly important to perform analytical procedures. Errors caused by sample preparation may be greater than those by analysis, depending on objectives and subjects of analysis. Therefore, sample preparation has to be done very carefully.

4.1 Sample preparation, analysis and data processing

Different samples were prepared by mixing as reported in Figure 18 20 g of SF with 200 g of [FA + CFA+ FGD] as described by [42] or 20 g of BA with 200 g of [FA + CFA + FGD]. The samples exhibit a relative weight percentage as follow: 65% FA, 20% FGD and 15% CFA. Then, approximately 200 mL of milliQ water, was added and the mixture mixed manually at room temperature for 20 min. Samples were aged for 2 months at room temperature. Then, each prepared sample was divided, one half was placed in the oven for 4 h at 120 °C (sample A), while the other half was dried at room temperature (sample B). At defined time of aging, a sample was removed from the container and analyzed.

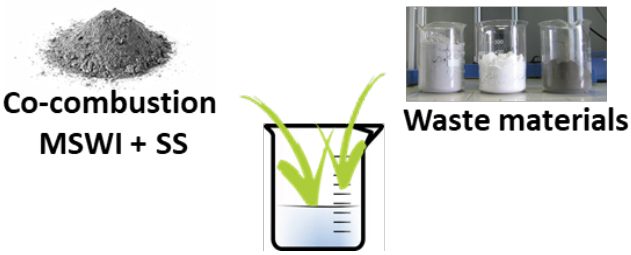

Figure 18 Mixing process

In the Table 4, the different receipts for the Experimental plan are reported. The COSMOS Fume technology was introduced in order to have a reference to compare the results obtained by the new technology using BA as stabilizing agent sample 3.

Table 4 Different receipts for the experimental plan

	Powder mass (g)						V (mL)
Samples	**FA**	**CFA**	**FGD**	**Borax**	**BA**	**SiO^2**	**H_2O**
1	130	30	42.4	-	-	20	220
2	130.1	30.7	40	20.3	-	-	200
3	130.2	33.6	40.3	-	20.2	-	200
4	130.2	32.3	42.2	-	-	-	200
5	130.6	60.2	10.4	-	-	-	200
6	130.1	10.4	60.3	-	-	-	200

The input factors of this experimental plan were the SF and the BA. Indeed, all the other factors were being fixed in order to obtain a comparable result. For example, the mixing time, drying temperature and the aging time were being fixed for both receipts.

As output factors P, S, Cl, K, Ca, Cr, Mn, Fe, Cu, Zn, Br, Rb, Sr, Ba, Pb and pH were considered.

4.2 Leaching Test

Leaching test was performed to raw ashes (MSW-FA, BA, CAR and FGD) according to the CEN normative (CEN EN 12457-2) [91] and optimized procedure [70,92]. For leaching tests, 20 g of sample was mixed with 200 mL of milliQ water (1:10) and mixed at room temperature for 2 h by a magnetic stirrer. After that, samples were filtered through 0.45 μm pore membranes and the pH of the filtrates was checked by pH-meter (Metrohm, model 827 Lab, Origgio, Italy).

The elemental chemical analysis of the leachate solutions was investigated by a S2 Picofox system from Bruker (Bruker AXS Microanalysis GMBH, Berlin, Germany) equipped with Mo tube operating at 50 kV and 750 μA and a Silicon Drift Detector (SDD) following the protocol previously described in [65]. A stock solution of 1 g/L Ga in nitric acid (Ga-ICP Standard Solution, Fluka, Sigma Aldrich, Saint Louis, MO, USA) was used as an internal standard in order to calculate the concentration of interested analysts present in the sample.

Samples were prepared by weight. Approximately 0.0105 of 100 mg/L of Ga solution was added to the prepared solutions to obtain a final concentration of 1 mg/L Ga. Solutions were homogenized using a vortex shaker for 1 min at 2500 rpm. A 10 μL drop of sample was deposited in the center of a plexiglass reflector. Afterwards, the reflectors were dried on a hot plate at 50 °C under a laminar hood and the residues were measured by irradiation for 600 s of live time. Three spectra were analyzed with the instrumental software using routine deconvolution based on mono-element profiles to evaluate the peak areas. Under the present experimental conditions, low Z elements such as P, S, and Cl are underestimated. For this reason, the quantification of these elements was corrected using the calculated relative sensitivities for P and S obtained by the calibration curves [93].

4.2.1 Sample digestion

Approximately, 0.25 g of each powder tested was placed in a Teflon vessel and a mixture of 6 mL of HNO_3 (≥65%), 2 mL of HCl (37%) and 2 mL of HF (48%) was added. The vessels were capped, and a CEM SP-D microwave system was employed to perform the mineralization process. The complete digestion was obtained using an automatic procedure through the following five steps: 3 min at 160 °C, 5 min at 180 °C, 3 min at 200 °C, and 10 min at 210 °C. Finally, the digested mixtures were transferred to 50 mL flasks and MilliQ water was added to adjust the volumes.

4.3 Assessment of the stabilization with different size grains of bottom ash

BA with dimensions higher than 2 cm was manually separated. Due to high sample moisture, BA was dried at 100 °C for about 2 h. Then, a series of six sieves with diameter from 1400 μm to less than 300 μm were employed to obtain various fractions of BA. In particular, metals that are separated from BA can be subsequently used as a secondary raw material in metal industry. The particle size distribution of BA was evaluated by the weight of each individual fraction retained within each sieve. Thus, the percentage of the total initial weight for every single grain size class to which it belongs was evaluated. A sample (named BA Mix) contains all the investigated size fractions is also considered. For XRD and EDXS characterization (see in the following), each fraction and BA Mix were grounded till to reach

a particles dimension of about 100 μm to obtain homogenous and fine particles. This also allows to avoid preferred orientation effects in XRD data collection.

4.3.1 Sample preparation, analysis and data processing

To verify the BA reactivity in metals immobilization, a method already tested [66] was carried out involving also MSW co-incinerated FA provided by the same plant. The stabilization technology consists in the use of CFA, FGD residues, and SF as reported by [42]. As better described in the available literature about the proposed method as reported by [78], the materials selection for FA stabilization was made with the proposition to use wastes and/or by-products as stabilizing agents. In particular, FGD residues were selected because they contain calcium hydroxide. SF is made by amorphous silica and CFA contain aluminosilicate glass [94]. Detailed characterization of these materials was very recently published [66].

Four samples were prepared (see Table 5) by mixing 20 g of SF with 200 g of [FA + CFA +FGD] [42] or 20 g of three BA fractions (1400 μm; <300 μm; and BA Mix) with 200 g of [FA + CFA + FGD]. The samples exhibit a relative weight percentage as follow: 65% FA, 20% FGD and 15% CFA. Then, approximately 200 mL of MilliQ, was added and the mixture mixed for 20 min. Samples were aged for 2 months at room temperature.

Table 5 Different receipts to stabilize FA, mono-combustion FA (MIFA), co-combustion BA (COBA)

	Powder mass (g)				
Samples					
	MIFA	**CFA**	**FGD**	**SiO_2**	**BA**
1	130	30	40	20	-
					1400 μm
2	130	30	40	-	20
					COBA Mix
3	130	30	40	-	20
					< 300 μm
4	130	30	40	-	20

After separation of the larger particles size (larger than 2 mm), the resulting BA were fractionated as reported previously. Cumulative particle size distribution of BA is shown in Figure 19. Generally, the retained amount of COBA decreases with the reduction of sieve opening. On the contrary, the amount of material size fractions below or equal to 300 μm is about 25%. This result may be related to the combustion chamber of MSWI injecting urea to decompose NO_x and many of these fine particles stich to the surface of the bigger particles as reported in literature [95,96].

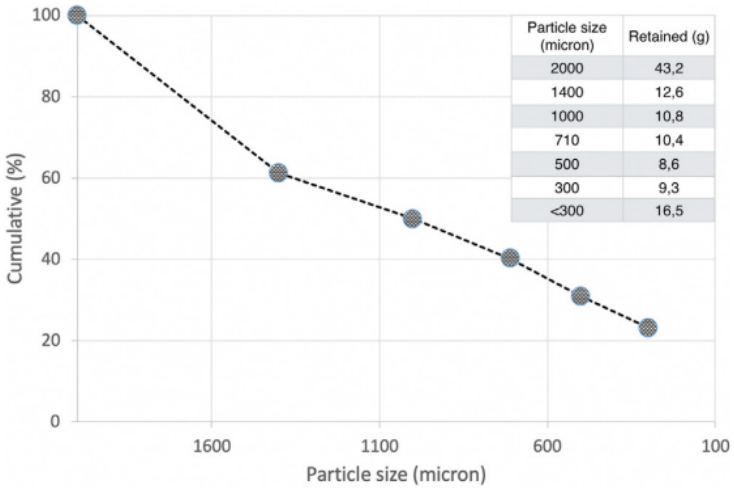

Figure 19 Cumulative particle size distribution of BA

4.3.1.1 XRD and Rietveld analysis

XRD was employed for phase identification of different BA size fractions. To quantify the amount of the individual components of the crystalline and amorphous phases, quantitative XRD analyses were performed, by using Rietveld's method as it was already reported by [65]. This is a full-pattern analysis that is based on the principle of minimization the difference between experimental and calculated XRD spectra by a least-squares procedure [99]. The approach is based on the use of the diffraction pattern of each mineral to evaluate the quantity of detected phases, rather than relying upon several peaks for the phases determination. The phases scaling factors, optimized during the refinement procedure, are used to evaluate the proportion of detected crystalline phases. The method is combined with the internal procedure [100] to account the amorphous contribution. For this aim, high purity of Al_2O_3 corundum was used as an internal standard for Rietveld analysis since it was not present in the interested samples. All powder samples were mixed with Al_2O_3 corundum

(50% in weight). For this study, data refinement was made by PROFEX software packages [101].

4.4 SEM and TEM analysis

The morphology of the raw powders was characterized by a SEM. A very thin layer of gold was deposited on the specimen surface in order to ensure the electrical charge. To characterize the composites, the morphology of samples was scanned under backscatter mode.

Although XRF has been widely employed for elements analysis, recently studies have demonstrated that EDX large area mapping can be successfully applied to characterize amorphous and crystalline BA (produced from mono-combustion of MSW) phases [62]. Generally, datasets obtained from two techniques are in good agreement [62]. Nevertheless, EDXS is preferred since light elements (such as phosphorus) are usually underestimated by XRF [102,103]. P is an interesting element that may derive from SS. For this reason, EDXS large area mapping is employed to evaluate the elemental concentrations. SEM-EDXS analyses were also performed in all BA fractions. The obtained morphological images are very similar, then only images collected on one fraction are reported in Figure 20. For all samples an area of about 2.5 mm^2 was selected for the EDXS analysis.

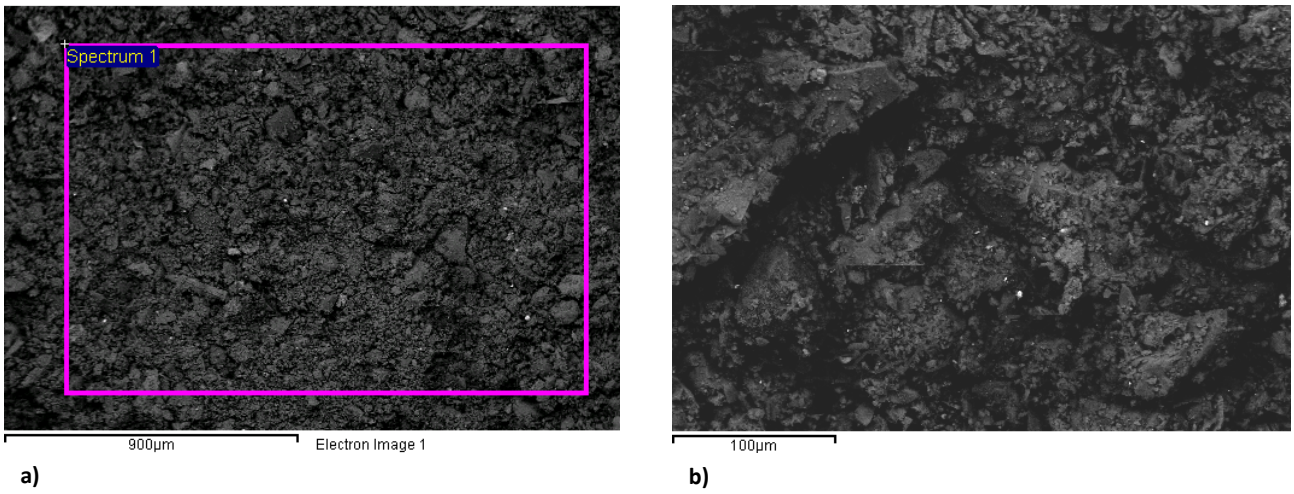

Figure 20 SEM images of the BA 1400 µm surface. Images were collected in backscatter mode, at the following magnifications: 40x (a) and 450x (b). Rectangular highlighted area was analysed by EDX

5 Results

In this chapter the results of all tests and analysis will be reported.

5.1 Leaching test and TXRF analysis

All starting raw ashes were analyzed, the amount of metals found in the ashes and leaching solutions used were assessed through elemental chemical analysis using TXRF. Before analysis, the samples were prepared as reported in the previous section. TXRF results of leachate solutions and digested samples of raw ashes are reported in Table 6, with good agreement with previous studies [105–107]. These data highlight the composition of the starting ashes and their soluble elements. The essential constituents MSWI BA are Ca, and Fe. The literature reports that amorphous silica, which in more than 50 wt.%, is the main phase present in MSWI BA [108]. Other elements, such as Zn, K, and S, are found in relevant quantities. Generally, the presence of glass in the waste is responsible for the higher ratio of silicon in BA than in FA [107]. Indeed, Al and Fe silicates, which have higher boiling points, can generally be found in BA [107]. In contrast, the calcium content is comparable in FA and BA, but in FA, its presence is due to the addition of $Ca(OH)_2$, which is used to adsorb acid gases (such as SO_2 and HCl), derived from the waste incineration process. MSWI FA also contains high quantities of S, which is ascribed to the lower boiling points and higher volatility of the sulphate phases [107]. In comparison with metals, non-volatile elements such as Fe, Cu, and Cr are present in the BA. Zn and Pb, which are classified as moderately volatile metals, show significant differences between FA and BA according to data reported in the literature [107,109].

The data reported in Table 6 show that S, K, Ca, and Fe are the major elements in CFA (Si was not quantified, but it is reported that CFA is extremely rich in Si according to the literature [79], while FGD residues are characterized by the presence of high amounts of S and Ca (due to their origin), which is in good agreement with previous results [42,70]. Leaching tests enhanced the lack of large amounts of soluble heavy metals: quantitative analysis of the leaching solutions of both CFA and FGD residues revealed that Cr, Mn, Fe and Cu, if present, are in trace concentrations. Low Zn amounts are found in the leaching solutions of these ashes, while Pb was not detected.

In contrast, a leaching test performed on MSWI FA (Table 6) showed different results.

The major elements in leachable FA are Cl, Ca and Br. Ca is also identified as the essential constituent of BA but its higher presence in FA is expected due to the addition of $Ca(OH)_2$ to adsorb acid gases (like SO_2 and HCl), produced during the incineration process. S is another element found in higher amount in FA in comparison with BA due to the lower boiling points and higher volatility of the sulphate phase [67]. K, P are also found in relevant amounts. Other elements are found in trace amounts in all raw ashes. Zn and Pb show significant differences between FA and BA, in agreement with reported literature [78]. These two metals are almost one order of magnitude higher in FA compared to BA and lower in CFA and FGD. The high concentration of Zn and Pb in FA is likely related to the high pH (about 12) with consequent high Zn and Pb solubility. As reported in Table 6 these ashes contain mostly Ca and S [70], while other elements are in low concentrations. Literature reports extremely high concentration of Si in CFA [79] but under this experiment conditions, Si could not be quantified.

Table 6 TXRF results of leachate solutions and digested samples of raw ashes

Elements	MSWI-FA		MSWI-BA		CFA		FGD		Si Fume	
	Digested (mg/kg)	Leaching (mg/L)	Digested (mg/kg)	Leaching (mg/L)	Digested (mg/kg)	Leaching (mg/L)	Digested (mg/kg)	Leaching (mg/L)	Digested (mg/kg)	Leaching (mg/L)
pH	1.53	12.38	1.1	12.15	2.3	12.01	2.33	12.68		
P*	1995 ± 95	30 ± 5	3962 ± 457	5 ± 1	687 ± 225	5.71 ± 2.47	1003 ± 429	9.4 ± 1.8	1743 ± 929	5.5 ± 1.0
S*	13097 ± 926	57 ± 14	1589 ± 212	40 ± 7	5175 ± 1163	173 ± 10	54432 ± 9942	315 ± 49	41238 ± 15677	111 ± 9
Cl*	1502 ± 436	10331 ± 829	3700 ± 660	673 ± 82	897 ± 187	1.74 ± 1.06	75 ± 6	402 ± 53	1407635 ± 235788	7405 ± 1404
K	24614 ± 1684	1621 ± 147	8518 ± 308	107 ± 4	6357 ± 1118	30.6 ± 2.3	2042 ± 273	10 ± 2	130026 ± 49468	617 ± 263
Ca	69179 ± 3140	6852 ± 275	79111 ± 7393	273 ± 11	4181 ± 916	449 ± 28	38311 ± 3379	1736 ± 225	517821 ± 60301	2477 ± 547
Cr	212 ± 6	0.22 ± 0.07	320 ± 18	0.42 ± 0.12	64 ± 39	0.21 ± 0.03	<LOD	<LOD	0.56	0.31
Mn	267 ± 13	0.38 ± 0.06	703 ± 83	0.16 ± 0.07	281 ± 16	<LOD	19 ± 9	<LOD	19 ± 3	0.06
Fe	3749 ± 170	0.26 ± 0.16	29815 ± 9315	0.68 ± 0.06	21473 ± 693	0.27 ± 0.01	156 ± 29	0.12 ± 0.04	14 ± 11	0.10 ± 0.05
Cu	707 ± 17	1.41 ± 0.16	2422 ± 83	1.65 ± 0.06	710 ± 32	<LOD	2045 ± 115	0.83 ± 0.28	1741 ± 40	0.54 ± 0.02
Zn	8795 ± 201	4.98 ± 0.11	4274 ± 122	0.11 ± 0.02	2439 ± 130	0.21 ± 0.14	2918 ± 245	0.10 ± 0.04	6 ± 2	0.08 ± 0.02
Br	<LOD	210 ± 10	<LOD	3.19 ± 0.20	11 ± 6	0.20 ± 0.03	7.50 ± 0.14	1.7 ± 0.2	20983.94 ± 6906.95	76.6 ± 3.8
Rb	44 ± 3	5.0 ± 0.4	<LOD	<LOD	<LOD	<LOD	<LOD	<LOD	2.878.888.224	2.472.843.373
Sr	204 ± 4	14.3 ± 0.3	207 ± 18	2.24 ± 0.13	58 ± 13	3.43 ± 0.18	24 ± 4	2.84 ± 0.34	2354 ± 296	10.61 ± 0.28
Ba	<LOD	<LOD	<LOD	1.57 ± 0.38	2826 ± 280	0.76 ± 0.40	2023 ± 208	<LOD	120 ± 86	0.55
Pb	1034 ± 48	81 ± 2	3738 ± 195	1.10 ± 0.16	<LOD	<LOD	<LOD	<LOD	<LOD	<LOD

Figure 21 shows the TXRF spectra of digested (black) and leaching solution (grey) from MSWI FA. Qualitative analysis identified the following elements in both spectra: Al, P, K, Ca, Cl, Ba, Fe, Cr, Cu, Mn, Zn, Pb, Br, Sr, and Rb. While Ti and Ni were detected only in the digested samples. By comparing the peak intensities, Figure 21 highlights the high concentrations of Fe, Mn, Cu and Zn in the digested samples, while Cl, Pb and Br amounts are significantly higher in the leaching solutions (see also the data reported in Table 6). The most important data for the FA toxicity regard heavy metals leachability. Table 6 shows that

Pb and Zn concentrations, which are generally the metals of major concern in waste leaching solutions, are approximately 80 and 5 mg/L, respectively.

The high Cl contents in FA may be due to the incineration of plastics such as PVC [110]. Paint materials, electronic devices, batteries and crystal glass are identified as the main sources of Pb and its associated compounds in waste [111]. Furthermore, it is reported that high Cl in MSWI FA affects the leachability of Pb, due to water-soluble salt ($PbCl_2$) formation.

In contrast, the MSWI BA sample leaching test showed that Cl, Zn, and Pb concentrations are lower in comparison with MSWI FA. For this waste, even though the amount of heavy metals is relatively high (see the data about digested samples reported in Table 6), the concentrations of all leachable metals are generally much less than those in MSWI FA. It is reported that metals in MSWI BA usually exist as different chemical combinations, even with additional non-metal elements, principally concentrated in non-silicate minerals (like spinels and metallic inclusions) [111]. This was observed for Zn^{2+}, Mn^{2+}, and Cr^{3+}. Because Pb has a large ionic radius, it cannot be easily incorporated into mineral species [112]. However, PbO

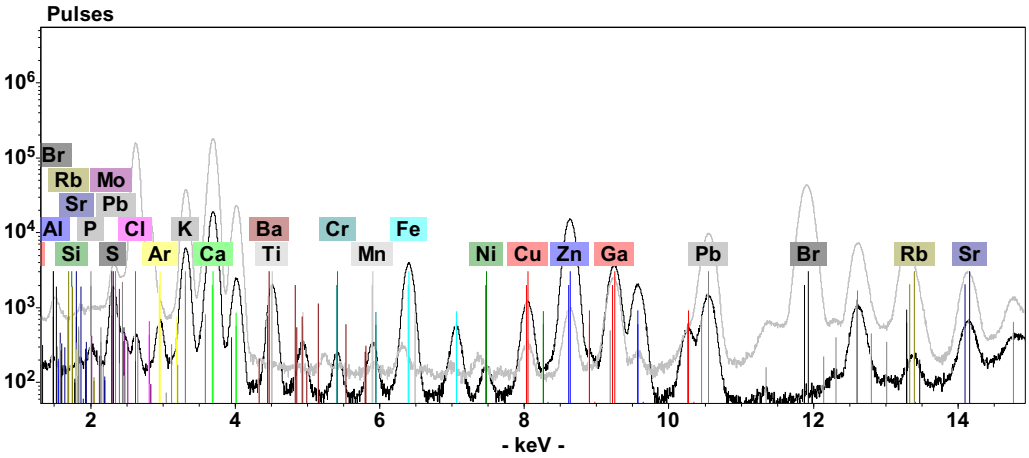

Figure 21 TXRF spectra of digested (black) and leaching solution (grey) from MSWI FA

was found to be incorporated in spinel crystals [111].

To understand the technological advantages of the proposed processes, all samples of the obtained stabilized materials with different receipts were analyzed. Leaching tests, pH measurement, and XRD analyses were done immediately after sample preparation, in order to avoid results alteration.

The eluate of leaching tests were analyzed with the TXRF technique. For each sample, 3 measurements were performed and the mean value and the standard deviation were calculated.

Stabilized samples revealed a significant decrease in heavy metals leaching, independent of the treatment at high temperature, while Pb concentration is lower than LOD by TXRF spectrometry (see Table 7 and 8), which is 0.002g/L. The data reported in Table 7 and 8 show that Zn concentration is almost one order of magnitude lower than in FA powder Table 6. In contrast, the S concentration in stabilized samples is higher compared with MSWI-FA Table 6 because of the addition of FGD residues. The results obtained after the first and second month of the stabilization process did not show any significant difference in the elemental concentrations, suggesting that the stabilized materials are stable over time. The results of the heavy metals leachability allow us to conclude that Pb and Zn are reduced by at least 2 order of magnitude, in stabilized samples (see data collected on samples 2M-Table 7) in comparison with the starting MSWI FA Table 6. The lower solubility of these metals must be attributed to a stabilization effect by only considering the MSWI FA dilution (that represents more than 50% of mass of all used ashes), the expected concentration of these two metals in solution should be approximately one half in comparison with the original value.

It is fundamental to consider the pH of all starting powders and final stabilized mixtures to determine the mechanism of heavy metal stabilization. Indeed, pH is a key factor that affects heavy metals leaching behaviors. It is extremely interesting to note that all ashes have a starting pH higher than 12. In contrast, stabilized samples have a pH lower than 11 (see Table 7 and 8). Two months after stabilization, samples A has a pH lower than 10.

This stabilization effect and the pH reduction were attributed to carbonation reactions. As reported in Table 7 and 8 the two different receipts for the stabilizing of FA using SF and BA gave the same results. In fact, an appreciated reduction of metals leachability has been noticed.

Table 7 TXRF analysis of leachate elements after one month of the samples A and B for different receipts

Stabilized samples-1 month-A (mg/L)																								
Elements	1			2			3			4			5			6								
pH	**9.82**			**11.51**			**10.66**			**10.88**			**10.86**			**11.4**								
P	13	±	7	22	±	7	20	±	10	20	±	9	23	±	18	15.5	±	29.4						
S	218	±	43	29	±	12	120	±	20	120	±	24	77	±	23	156	±	25						
Cl	7281	±	885	10040	±	1001	8600	±	2600	9477	±	1250	10317	±	1989	8732	±	2896						
K	776	±	99	998	±	171	760	±	360	948	±	193	850	±	296	712	±	455						
Ca	2750	±	372	3578	±	384	3120	±	1130	3459	±	417	3561	±	809	3181	±	1325						
Cr	0.58	±	0.08	0.14	±	0.03	0.25	±	0.07	0.29	±	0.13	0.46	±	0.12	0.24	±	0.004						
Mn	0.10	±	0.03	0.32	±	0.13	0.12	±	0.08	0.21	±	0.08	0.18	±	0.07	0.11	±	0.05						
Fe	2.25		1.32	0.14	±	0.01	1.70	±	1.56	0.12	±	0.08	0.18	±	0.08	0.07	±	0.03						
Zn	0.120	±	0.070	0.61	±	0.14	0.28	±	0.08	0.17	±	0.09	0.13	±	0.06	0.127	±	0.033						
Br	69	±	6	88	±	6	113	±	33	97	±	7	119	±	17	111	±	4						
Rb	2.89	±	0.31	2.8	±	1.2	3.3	±	0.3	3.40	±	0.10	4.1	±	0.6	3.8	±	0.5						
Sr	13.6	±	1.5	7.7	±	0.3	11	±	1	13.0	±	1.0	17.3	±	2.1	13.2	±	0.6						
Ba	1.34	±	0.31	2.3	±	0.3	1.70	±	0.50	1.43	±	0.65	2.51	±	0.16	1.35	±	0.47						
Pb	<LOD			1.4	±	0.1	<LOD			<LOD			<LOD			<LOD								

Stabilized samples-1 month-B (mg/L)																								
Elements	1			2			3			4			5			6								
pH	**11.05**			**11.51**			**10.77**			**11.47**			**10.49**			**11.89**								
P	19	±	10	26	±	7	10	±	6	12	±	1	23	±	8	24	±	3						
S	73	±	47	44	±	12	40	±	16	39	±	14	35	±	14	53	±	17						
Cl	8276	±	2557	9851	±	468	8900	±	2000	9337	±	2303	10320	±	716	11751	±	2811						
K	656	±	360	1008	±	57	740	±	360	790	±	365	952	±	111	1189	±	429						
Ca	2570	±	1115	3734	±	112	2750	±	960	2942	±	1053	3220	±	408	4020	±	990						
Cr	0.33	±	0.09	0.22		0.12	0.19	±	0.10	0.27	±	0.11	0.48	±	0.18	0.26	±	0.12						
Mn	0.16	±	0.080	0.20	±	0.09	0.18	±	0.07	0.18	±	0.08	0.18	±	0.04	0.54	±	0.24						
Fe	0.33	±	0.18	0.32	±	0.12	0.39	±	0.03	3.4	±	1.6	0.31	±	0.1	1.1	±	0.4						
Zn	0.18	±	0.07	0.44	±	0.03	0.12	±	0.07	0.14	±	0.08	0.29	±	0.13	0.41	±	0.22						
Br	92	±	3	97	±	9	90	±	4	96	±	5	97	±	6	96	±	14						
Rb	3.1	±	0.2	3.1	±	0.3	2.9	±	0.2	3.10	±	0.40	3.3	±	0.4	3.1	±	0.5						
Sr	12.7	±	0.5	4.9	±	0.3	12	±	1	12.0	±	1.0	15	±	1	11	±	2						
Ba	1.6	±	0.6	1.1	±	0.0	1.5	±	0.9	0.92	±	0.06	1.79	±	0.32	1.6	±	0.1						
Pb	<LOD			0.87	±	0.18	<LOD			<LOD			<LOD			0.48	±	0.12						

Table 8 TXRF analysis of leachate elements after two months of the samples A and B for different receipts

Stabilized samples-2 month-A (mg/L)												
Elements	1	2	3	4	5	6
pH	**9.3**	**9.67**	**9.73**	**9.4**	**9.3**	**9.84**
P	4.8 ± 0.1	18 ± 8	9 ± 5	11 ± 7	18 ± 4	11 ± 6
S	270 ± 78	27 ± 9	210 ± 80	179 ± 12	109 ± 74	136 ± 21
Cl	8290 ± 4653	10312 ± 1491	7200 ± 1200	9029 ± 1895	8525 ± 2888	7369 ± 1480
K	670 ± 78	1026 ± 185	660 ± 250	762 ± 194	868 ± 55	657 ± 283
Ca	3038 ± 1746	3083 ± 383	2600 ± 300	3014 ± 566	2812 ± 1065	2554 ± 702
Cr	0.63 ± 0.15	0.20 0.06	0.56 ± 0.06	0.74 ± 0.04	0.49 ± 0.16	0.71 ± 0.26
Mn	0.06 ± 0.03	0.26 ± 0.08	0.10 ± 0.01	0.14 ± 0.06	0.14 ± 0.02	0.1 ± 0.01
Fe	0.21 ± 0.07	0.01 ± 0.00	0.07 ± 0.06	0.25 ± 0.12	0.12 ± 0.04	0.015 ± 0.001
Zn	0.080 ± 0.020	0.04 ± 0.01	0.02 ± 0.01	0.05 ± 0.04	0.07 ± 0.03	0.12 ± 0.07
Br	93 ± 20	99 ± 7	110 ± 40	103 ± 5	104 ± 5	93 ± 11
Rb	3.1 ± 0.6	3.4 ± 0.3	2.9 ± 0.2	3.40 ± 0.10	3.3 ± 0.4	3.1 ± 0.6
Sr	13.0 ± 4.0	8.2 ± 0.5	12 ± 2	14.0 ± 1.0	16 ± 1	12 ± 2
Ba	0.8 ± 0.1	1.4 ± 0.5	0.61 ± 0.44	0.92 ± 0.42	1.12 ± 0.52	0.78 ± 0.08
Pb	<LOD	<LOD	<LOD	<LOD	<LOD	<LOD

Stabilized samples-2 month-B (mg/L)												
Elements	1	2	3	4	5	6
pH	**9.77**	**10.1**	**10.14**	**9.81**	**9.75**	**10.22**
P	13 ± 4	22 ± 9	6 ± 1	14 ± 6	4.4 ± 0.9	12 ± 5
S	73 ± 7	110 ± 46	110 ± 10	57 ± 17	85 ± 28	87 ± 12
Cl	8625 ± 1709	10234 ± 793	7400 ± 1400	8726 ± 2043	8211 ± 2694	7287 ± 2145
K	844 ± 227	1011 ± 96	620 ± 260	743 ± 331	660 ± 410	525 ± 324
Ca	2785 ± 653	3570 ± 250	2500 ± 500	2749 ± 681	2657 ± 1212	2338 ± 560
Cr	0.56 ± 0.06	0.21 0.02	0.31 ± 0.17	0.44 0.03	0.46 ± 0.13	0.52 0.2
Mn	0.14 ± 0.06	0.17 ± 0.04	0.06 ± 0.01	0.16 ± 0.09	0.068 ± 0.03	0.03 ± 0.003
Fe	0.09 0.02	0.71 ± 0.25	0.10 0.05	0.19 0.1	0.09 0.02	0.0322 ± 0.0369
Zn	0.050 ± 0.020	0.08 ± 0.03	0.08 ± 0.02	0.08 ± 0.00	0.061 ± 0.03	0.021 ± 0.006
Br	88 ± 3	124 ± 3	80 ± 4	94 ± 15	92 ± 7	89 ± 8
Rb	2.9 ± 0.1	3.1 ± 0.2	2.5 ± 0.3	3.10 ± 0.90	2.8 ± 0.12	2.8 ± 0.3
Sr	12.0 ± 1.0	5.3 ± 0.2	10.6 ± 0.3	12.4 ± 0.9	14 ± 1	12 ± 1
Ba	1.2 ± 0.1	0.6 ± 0.1	0.6 ± 0.3	0.78 ± 0.28	1.3 ± 0.1	0.92 ± 0.37
Pb	<LOD	<LOD	<LOD	<LOD	<LOD	<LOD

5.1.1 Leaching test and TXRF analysis of different size grains of bottom ash

Leachates were prepared from the selected size fractions of BA without prior washing. A leaching test was carried out of powders and stabilized samples, according to optimized procedure [66,70]. Finally, leaching solutions were analyzed on one month (1 M) and two

months (2 M) after the stabilization in order to investigate the efficacy of the process. During this time samples were naturally aged in laboratory at room temperature.

The results of leaching tests performed for seven various BA (see Table 9) show that despite the heavy metals concentration is lower than that reported in other works [97] an increase of Cl, Zn, Cu, Ba, and Pb concentration by decreasing the BA particle size fractions is found in the leachate solutions, in accord with some already reported in finest BA fraction (< 300 μm), compared to the other fractions, was explained by the highest quantity of amorphous, which is generally found, in the BA (produced from mono-combustion of MSW) with the fine particle size [64]. In recent literature [98], it was observed that amorphous silica is responsible of heavy metals adsorption, in SS co-combustion with plants used to remove heavy metals from soil. In the present case, the situation is different: the highest amount of amorphous is detected on largest fraction size (1400 μm). As a consequence, this consideration strongly suggests that amorphous is not rich in silica.

Chemical analysis of BA (reported in chapter 3) shows that the concentration of most abundant elements (as for example Ca, Fe, K, Ti) is in accord with data reported in literature for BA (produced from mono-combustion of MSW) [61]. Also heavy metals concentration (Pb, Zn, Cr) results in the literature ranges for BA (produced from mono-combustion of MSW) [61]. Data about BA chemical composition of different fractions (reported in Table 9) show that the total contents of Si and Fe decrease with reducing the particle sizes. This behavior is in agreement with the results already reported in literature [45,64] The decrease of Fe amount may be attributed to the residue of stainless-steel wastes, which is generally present as large fractions. Indeed, it is easily removed during BA pre-treatment, involving separation of large dimension wastes. While the contents of other elements in various BA size fractions did not show significant differences.

*Table 9 TXRF results of leachate solutions of different BA size fractions. Data are reported as the average ± standard deviation of three TXRF measurements. * calculated values based on a calibration curve.*

Elements	Elemental concentration of COBA (mg/L)						
	1400 μm	1000 μm	710 μm	500 μm	300 μm	<300 μm	COBA Mix
P*	12.8 ± 4.4	21.7 ± 9.0	18.7 ± 0.5	28.4 ± 11.9	24.2 ± 9.8	15.6 ± 1.5	17.3 ± 0.9
S*	127 ± 39	199 ± 38	136 ± 51	190 ± 23	158 ± 46	107.9 ± 3.3	91.1 ± 3.7
Cl	572 ± 115	1203 ± 53	1173 ± 403	1252 ± 76	1557 ± 335	932 ± 78	969 ± 28
K	121 ± 3	231 ± 15	232 ± 86	225 ± 7	270 ± 41	151 ± 13	176 ± 7
Ca	358 ± 91	556 ± 94	535 ± 168	671 ± 281	710 ± 198	817 ± 29	869 ± 19
Mn	<LOD	<LOD	<LOD	<LOD	<LOD	<LOD	<LOD
Fe	0.15 ± 0.10	0.21 ± 0.11	0.15 ± 0.11	0.92 ± 0.71	0.63 ± 0.37	0.15 ± 0.12	0.3 ± 0.03
Ni	0.09 ± 0.03	0.19 ± 0.07	0.19 ± 0.11	0.27 ± 0.16	0.25 ± 0.04	0.14 ± 0.04	0.18 ± 0.03
Cu	7 ± 2	11 ± 3	11 ± 4	12 ± 2	13 ± 4	7 ± 1	8.6 ± 0.3
Zn	0.07 ± 0.01	0.19 ± 0.1	0.09 ± 0.06	0.13 ± 0.07	0.14 ± 0.07	0.38 ± 0.06	0.37 ± 0.11
Br	2.6 ± 0.3	4.9 ± 0.3	5.7 ± 1.6	5.2 ± 0.4	6.9 ± 0.9	4.1 ± 0.5	4.7 ± 0.2
Sr	2.7 ± 0.5	4.7 ± 1.1	5.1 ± 2.7	4.7 ± 0.3	6.1 ± 1.4	4.7 ± 0.4	5.7 ± 0.2
Ba	0.91 ± 0.53	0.99 ± 0.05	0.93 ± 0.30	0.90 ± 0.30	1.1 ± 0.03	1.01 ± 0.78	2.07 ± 0.33
Pb	0.42 ± 0.03	0.08 ± 0.04	0.26 ± 0.19	0.21 ± 0.06	0.21 ± 0.13	0.94 ± 0.07	0.72 ± 0.02

5.2 XRD and Rietveld analysis

Hereinafter it has been considered only the third receipts (sample 3). Stabilized samples A and B of the third receipts (1M and 2M) showed similar XRD patterns (see Figure 22). For all samples, the main calcite peak results in the most intense peak in all the patterns. This is in agreement with $CaCO_3$ formation that is due to the carbonation reaction. The XRD patterns of all the stabilized samples also show the presence of NaCl, quartz (SiO_2), calcium sulphite hemihydrate ($CaSO_3*0.5H_2O$), and calcium sulphate ($CaSO_4$).

The XRD patterns of the stabilized materials (see Figure 22) also appear to show a large peak at approximately 28° (in 2Theta) that can be attributed to calcium silicate hydrate (C-S-H) and is due to a pozzolanic reaction; this can also be obtained by mixing amorphous silica and calcium hydroxide. These compounds cannot be completely crystallized, which makes it difficult to detect pozzolanic reaction. However, calcium hydroxide and calcium chloride hydroxide phases (present in the initial powders) were not found in the stabilized samples, suggesting that the phases have reacted such as with the silica and/or alumina contained in the MSWI BA.

The main differences in the XRD patterns reported in Figure 22 can be found at the beginning. In particular, two peaks at approximately 9.7 and 10.3° are observed. These peaks have different intensity ratios compared to the two spectra reported in Figure 22. Thus, it is reasonable to assume that they derived from two phases. The peak at approximately 9.7° (in 2Theta) can be attribute to stilbite ($Al_{9.34}Na_{5.968}Si_{26.14}O_{72}$) an aluminosilicate that is already found in fly and BA [113,114]. The peak at approximately 10.3° can be attributed to kozulite ($Na_3[Mn_4(Fe)]Si_8O_{22}(OH)_2$) a Na-Mn-Fe silicate. From the XRD data, it is possible to conclude that sample A contains a Na-Mn-Fe- silicate, that does not appear to have changed over time (comparing XRD patterns A 1 M and A 2 M collected 2 months after stabilization). In contrast, sample B contains stilbite, with a contribution of kozulite, that appears to be lower compared to sample A. However, the main kozulite peak increased in the pattern collected two months after stabilization (B 2 M), probably due to the lower reaction kinetics in comparison with sample A (that was thermally treated). These silicates may be formed as a consequence of retreated. These silicates may be formed as a consequence of reactions occurring in the amorphous matrix. Changes that occurred in the amorphous phases due to the stabilizing reactions, but did not involve crystalline phases, cannot be excluded [115]. Another difference in the XRD patterns of the stabilized samples is the presence of gypsum

($CaSO_4$*$2H_2O$) in sample B (1 M and 2 M). This phase was not detected in sample A (1 M and 2 M), probably due to the thermal annealing.

Because it was already reported that pozzolanic reactions can stabilize metals cations and reduce the leaching of heavy metals [47], it is reasonable to suppose that the addition of BA can benefit in FA stabilization. Additionally, sample A 2 M has a lower pH compared to sample B 2 M, supporting the hypothesis of sample carbonation and, in particular, suggesting an accelerated carbonation reaction for this sample. Carbonation is probably also responsible (with the pozzolanic reactions) for the absence of calcium hydroxide and calcium chloride hydroxide phases in the stabilized samples [67,70].

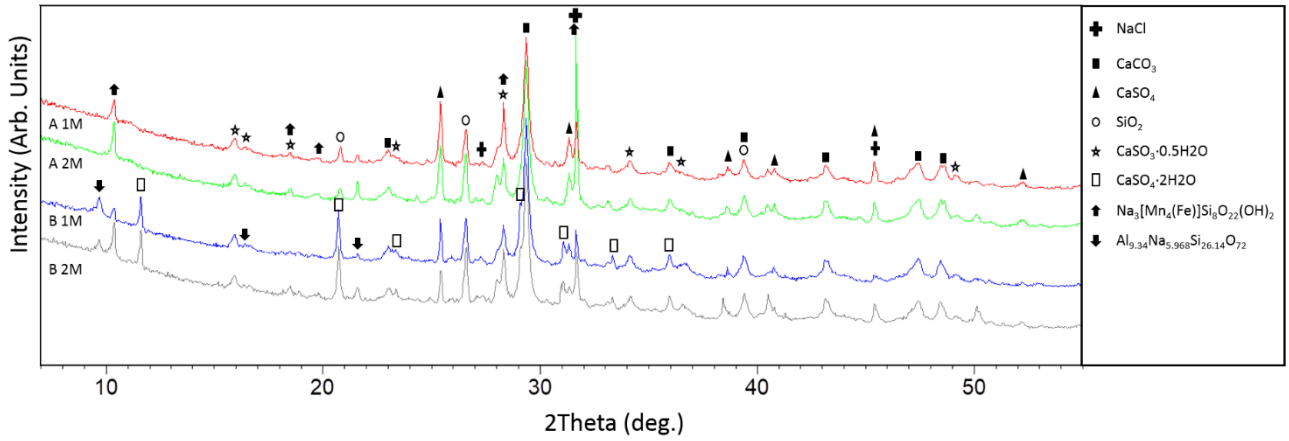

Figure 22 XRD pattern of stabilized samples after one and two months

5.2.1 XRD analysis of different size grains of bottom ash

Results of XRD analysis and quantification of crystalline phases performed by Rietveld's method of various BA fractions are reported in Table 10. The detected crystalline phases are the following: calcite, quartz, anhydrite, cristobalite, hydrocalumite, hydroxylapatite, hematite, magnesite, sodium chloride, portlandite, and albite.

Table 10 Results of Rietveld analysis for various BA fractions

Phases	COBA fractions size (μm)					
	1400 (%)	1000 (%)	710 (%)	500 (%)	300 (%)	<300 (%)
Amorphous	73	70	69	67	64	60
Calcite ($CaCO_3$)	6	6	8	8	9	13
Anhydrite ($CaSO_4$)	<1	<1	<1	<1	1	<1
Cristobalite (SiO_2)	2	1	<1	<1	<1	<1
Quartz (SiO_2)	5	5	3	5	3	4
Hydrocalumite ($Ca_4Al_2O_6Cl_2{\cdot}10H_2O$)	2	7	8	6	7	8
Hydroxylapatite ($Ca_5(PO_4)_3(OH)$)	5	5	6	7	8	7
Hematite (Fe_2O_3)	1	1	1	1	1	1
Magnesite ($MgCO_3$)	1	2	2	2	2	2
Sodium Chloride (NaCl)	1	1	<1	<1	1	1
Portlandite ($Ca(OH)_2$)	<1	1	1	1	1	2
Albite ($NaAlSi_3O_8$)	2	2	2	2	2	1

Data reported in Table 10 reveal that the most abundant crystalline phase in all samples, independently of size fractions, is calcite, that can have both natural and industrial origin [62]. As calcite, also crystalline silicon oxides (quartz and cristobalite) can derive from natural (known as common mineral on the earth's surface) or anthropogenic sources (providing from uses in building materials) [62]. Due to their crystalline structure, quartz and cristobalite are inert in comparison with amorphous silica. In addition, they are characterized by high mechanical resistence. As expected, they are more abundant in coarse BA fractions in accordance with other studies where the crystalline silicon oxides are generally found in relatively coarse particles [62]. Albite, a plagioclase is identified in BA samples. Data show that it is present in low quantities (few percent), confirming results already reported for BA (produced from mono-combustion of MSW) [63].

One of the most interesting result of the Rietveld refinement concerns the amorphous: its content in these samples is almost more than one order of magnitude higher (>60%) compared to each single crystalline phase. The high amount of the amorphous indicates that BA is mainly produced by an off-equilibrium thermal process [63]. This result suggests a potentially high reactivity of BA [116]. Several papers have already shown that the composition of different size fractions of MIBA (produced from mono-combustion of MSW) can differ significantly [63]. In the present case, apart the difference in the amount of amorphous, BA fractions with the smallest particle size (>300 μm) are particularly rich in calcite and portlandite. In addition, the phases analysis reveals further differences in the BA composition compared to those reported in literature for BA (produced from mono-combustion of MSW) [64]. For instance, gypsum and ettringite cannot be detected in BA fractions (see Table 10) because they are generally weathering products [62]. In addition, the amount of amorphous is extremely high compare to the few data available in literature for BA (produced from mono-combustion of MSW) [117]. As a consequence, the amounts of evaluated crystalline silica phases are lower (ranging from about 4% to about 8%), compared to data found for BA (produced from mono-combustion of MSW), where quartz is reported to prevalent phase in all the ash fractions [45].

Hydrocalumite is another crystalline phase identified in all BA fractions. This phase commonly derives from the reaction of calcium hydroxide and aluminates in pH range of 10-11 in fresh BA [118]. Hydrocalumite is unstable and is converted to more stable phases by natural weathering [118].

5.3 SEM and TEM analysis

SEM images collected in backscattering mode on stabilized sample B (magnification of 8000x) and the map of elements identified by EDX-SEM analysis are reported in Figure 23. The presence of spherical particles, containing Si (possibly silicates, or quartz) with diameters ranging from 5 to 13 μm was observed. Qualitative EDX-SEM analysis identified the following elements: C, O, Na, Mg, Si, P, S, Cl, K, Ca, Ti, Fe and Zn. Pb identification by EDX-SEM was not possible in either the starting MSWI FA or the stabilized sample due to the low amount of this metal compared with the total sample mass. It is worth noting that EDX-SEM maps show the co-location of Al with Si, while Fe and Zn appear to have an independent distribution.

It is already known that C-S-H does not have a uniform distribution and appears in different morphologies, such as fibers, flakes, honeycombs and tightly assembled grains [64]. In particular, the calcium/silicon ratio was found to be a significant factor affecting C-S-H morphologies at the nanoscale, showing that with increasing calcium/silicon ratios, C-S-H changes from a loose fibril-like morphology when this ratio is lower than approximately 1, to dense granular-like particles when this ratio is higher than approximately 1.5 [119].

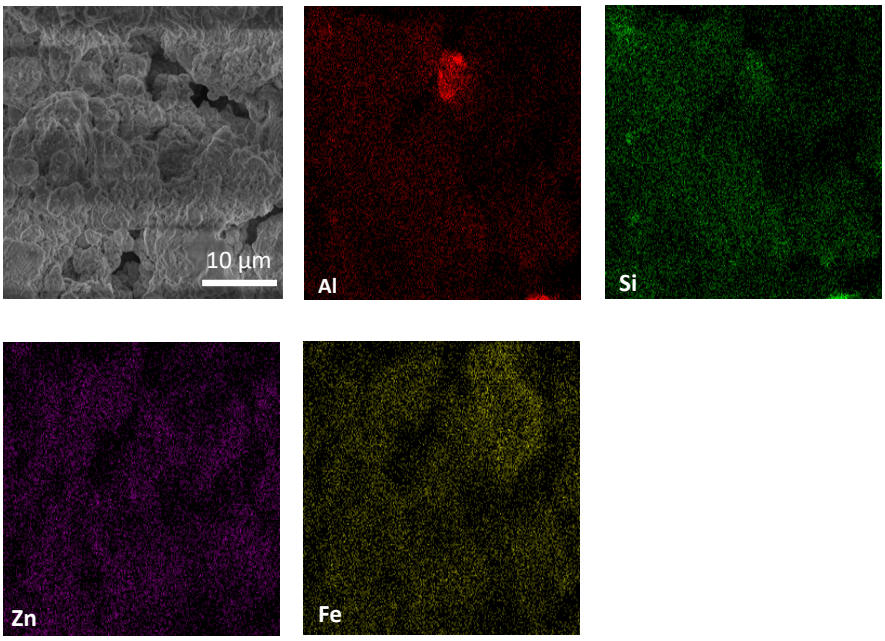

Figure 23 SEM images collected in backscattering mode on stabilized sample B (8000x)

TEM observations, coupled with chemical analysis of the obtained images (see Figure 24) performed at high magnification in comparison with SEM analysis, made it possible to analyze low samples amounts. Figure 24 reveals that stabilized sample B contained solid

spherical particles (Figure 24a, b, c) ranging from approximately 0.1 to 0.5 μm in diameter. Some of these particles are similar to agglomerates in an amorphous matrix (Figure 24a). In the present case, the sample morphology appears to include some fibrils (more evident in Figure 24b and c), which may be due to C-S-H with a Ca/Si ratio lower than 1.5 [119].

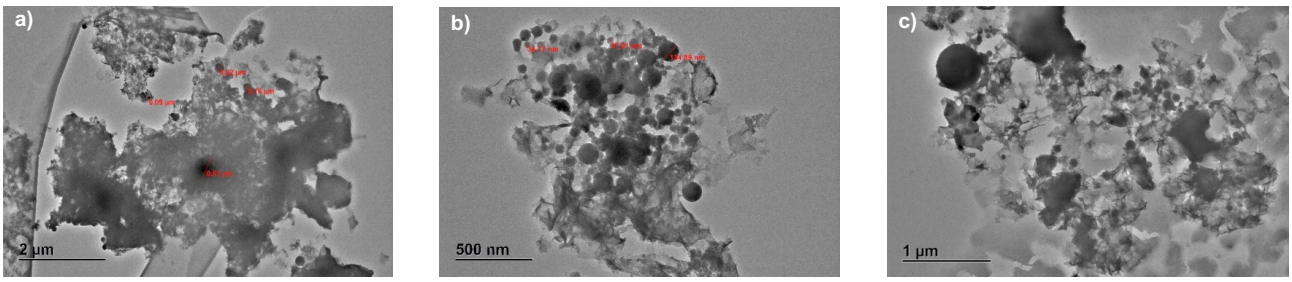

Figure 24 Map of elements identified by TEM analysis

TEM-EDX maps, which are reported in Figure 25(a-e), are collected from a single particle found in a small portion of B stabilized sample. This area was chosen because an EDX Pb signal was detected (Pb was not detectable by EDX-SEM). Table 11 reports the results as the normalized mass (%) of the chemical analysis performed in the area highlighted in Figure 25a. The elements present at higher concentrations are Si, Ca and Zn. This localized analysis revealed the presence of Pb and highlighted its spatial distribution (Figure 25e). The chemical map shows that Pb is mostly co-localized in proximity to silicon (Figure 25b) and Zn (Figure 25c), while Ca appears to be highly co-localized on the bottom part of the particle (Figure 25d). The composition of the identified particles (Figure 25a) is in good agreement with the C-S-H phase formation. This result strongly suggests the idea that Pb and Zn stabilization, which can be due to carbonation effects (with pH reduction), is supported by pozzolanic reeactions during C-S-H formation.

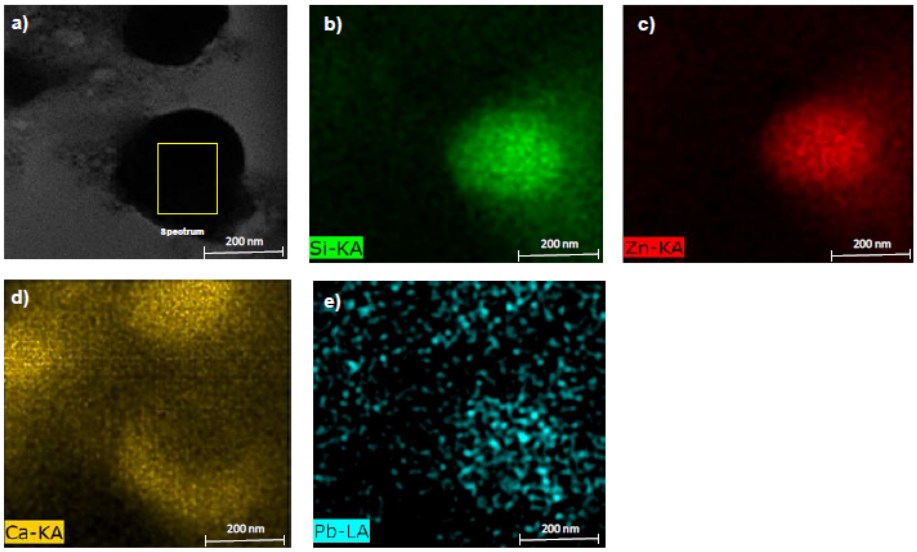

Figure 25 TEM-EDX maps

Table 11 Normalized mass (%) of the chemical analysis performed in the area highlighted

Spectrum	Elemental Concentration (%)												
	O	Na	Mg	Si	P	S	Cl	K	Ca	Fe	Zn	Br	Pb
Sample B	1,27	0,67	0,32	16,48	0,43	1,39	6,29	6,24	34,59	1,64	30,35	0,03	0,31

Based on the data presented in Table 11 it is also possible to evaluate probable atoms associations in the compounds detected in the XRD patterns, in the selected area. For example, Cl, K and Na can be justified considering that they can form from KCl and NaCl (originating from MSWI FA). However, Na may also be incorporated in the silicates.

Because Ca is also present, it is possible to evaluate the Ca/Si atomic ratio, resulting in approximately 1.47. This value corresponds to changes in the structural morphology of C-S-H from fibril-like to granular-like particles [119]. Due to its composition, it obviously is not possible to exclude that these particles may be a silicate phase (composition similar to kozulite, found in the XRD pattern); however, the presence of Ca (and the corresponding Ca/Si atomic ratio according to the particle morphology) supports the hypothesis that it may correspond to C-S-H.

In summary, the idea to take advantage of the reactivity of amorphous phases present in BA originate from its pozzolanic properties. Owing to the high amounts of silica (and probably alumina), BA can have pozzolanic or cementitious properties, but, similar to cement, it must be finely ground to increase the specific surface area and consequently the reactivity [13]. The addition of FGD residues to stabilize the samples allows to add calcium hydroxide to promote the pozzolanic reactions. Then, in addition to the newly formed calcium carbonate, we can suppose that the glass-derived products also influence the immobilization of heavy metals.

5.4 SEM and TEM analysis of different size grains of bottom ash

For all samples an area of about 2.5 mm^2 was selected for the EDXS analysis. Figure 20 shows the SEM images collected from surface of BA 1400 µm. BA surface is made up of a large number of agglomerated or sintered fine particles. Several spherical particles with different sizes, agglomeration of cubic-like, elongated and irregular shapes can be observed in the same picture. This is probably due to the different nature of MSW burn in the incineration system [117,120].

Table 12 presents the mean of three measurements of EDXS analysis performed on the selected area for all analyzed size fractions. For all samples, this analysis was performed on three different areas, with the same dimensions. The data show that O, Si, and Ca are in concentrations higher than other elements. Other elements found in BA fractions were Na, Mg, S, Cl, K, Ti, which is in accordance with literature data about BA (produced from mono-combustion of MSW) [45,121], except for P, that generally is not reported/found.

Data series obtained by XRD and Rietveld refinement (Table 10) and EDXS (Table 11) can be coupled to extract valuable information about the composition of amorphous, which is commonly not evaluated in literature. The amount of each element is determined by EDXS, while Rietveld analysis only accounts for elements that are in crystalline phases. Figure 26 shows the comparison of elements concentrations evaluated by EDXS and XRD. Obviously, because EDXS is not sensitive to the crystalline phases, the elements amount must be always higher (or comparable), compared to the corresponding values quantified by XRD. Then, the difference among the reported data can be attributed to the amount of the elements that may be in the amorphous. Figure 26 reports the data concerning elements with a resulting difference higher than 2% considering EDXS and XRD (except of P). The results about oxygen are not reported. It is interesting to notice that P content evaluated by EDXS corresponds to the expected amount of this element in the hydroxylapatite, i.e. in the crystalline state for BA size fractions lower than 500 μm. Coarse particle size fractions (till to 1400 μm) have higher amount of P, compared to that found in the crystalline part (also if this difference is not high), showing that P is probably contained also in the amorphous phase. The presence of P in the BA may derive from co-combustion of SS in the incineration plant [122].

Table 12 Results of energy dispersive X-ray spectroscopy (EDXS) performed on different BA fractions. Three different selected area with the same dimension were considered and the mean value (with corresponding standard deviation) for each element is reported.

Elements	Elemental Concentration (%) in COBA samples						
	1400 μm	1000 μm	710 μm	500 μm	300 μm	<300 μm	COBA Mix
O	52 ± 1	57 ± 1	54 ± 1	58 ± 1	56.7 ± 0.1	58 ± 1	56 ± 1
Na	1.92 ± 0.13	1.79 ± 0.26	1.56 ± 0.08	1.80 ± 0.31	1.81 ± 0.08	1.89 ± 0.29	1.94 ± 0.27
Mg	2.19 ± 0.12	1.66 ± 0.28	1.33 ± 0.24	1.43 ± 0.16	1.65 ± 0.09	1.62 ± 0.18	1.74 ± 0.22
Al	4.12 ± 0.10	3.60 ± 0.32	3.24 ± 0.20	3.56 ± 0.14	3.25 ± 0.15	2.84 ± 0.26	3.39 ± 0.33
Si	12.7 ± 0.4	7.51 ± 0.39	5.54 ± 0.44	6.37 ± 0.19	5.70 ± 0.27	4.91 ± 0.10	7.07 ± 0.22
P	1.35 ± 0.26	2.08 ± 0.10	1.55 ± 0.18	1.79 ± 0.05	1.45 ± 0.25	1.09 ± 0.18	1.39 ± 0.26
S	1.18 ± 0.87	1.16 ± 0.05	1.29 ± 0.10	1.34 ± 0.22	1.44 ± 0.13	1.38 ± 0.27	1.58 ± 0.15
Cl	1.85 ± 0.21	2.20 ± 0.12	2.32 ± 0.24	2.48 ± 0.13	2.89 ± 0.25	3.07 ± 0.12	2.41 ± 0.22
K	1.27 ± 0.03	0.94 ± 0.14	0.67 ± 0.12	0.76 ± 0.07	0.67 ± 0.07	0.73 ± 0.12	0.76 ± 0.12
Ca	18.5 ± 0.6	18.1 ± 0.4	17.7 ± 0.3	19.8 ± 1.1	21.1 ± 0.2	21.5 ± 0.5	20.4 ± 0.8
Ti	0.78 ± 0.12	0.66 ± 0.11	0.60 ± 0.16	0.85 ± 0.09	0.94 ± 0.07	0.73 ± 0.08	0.77 ± 0.26
Fe	3.66 ± 0.75	3.04 ± 0.51	2.24 ± 0.24	2.32 ± 0.18	2.07 ± 0.02	1.85 ± 0.24	2.65 ± 0.23

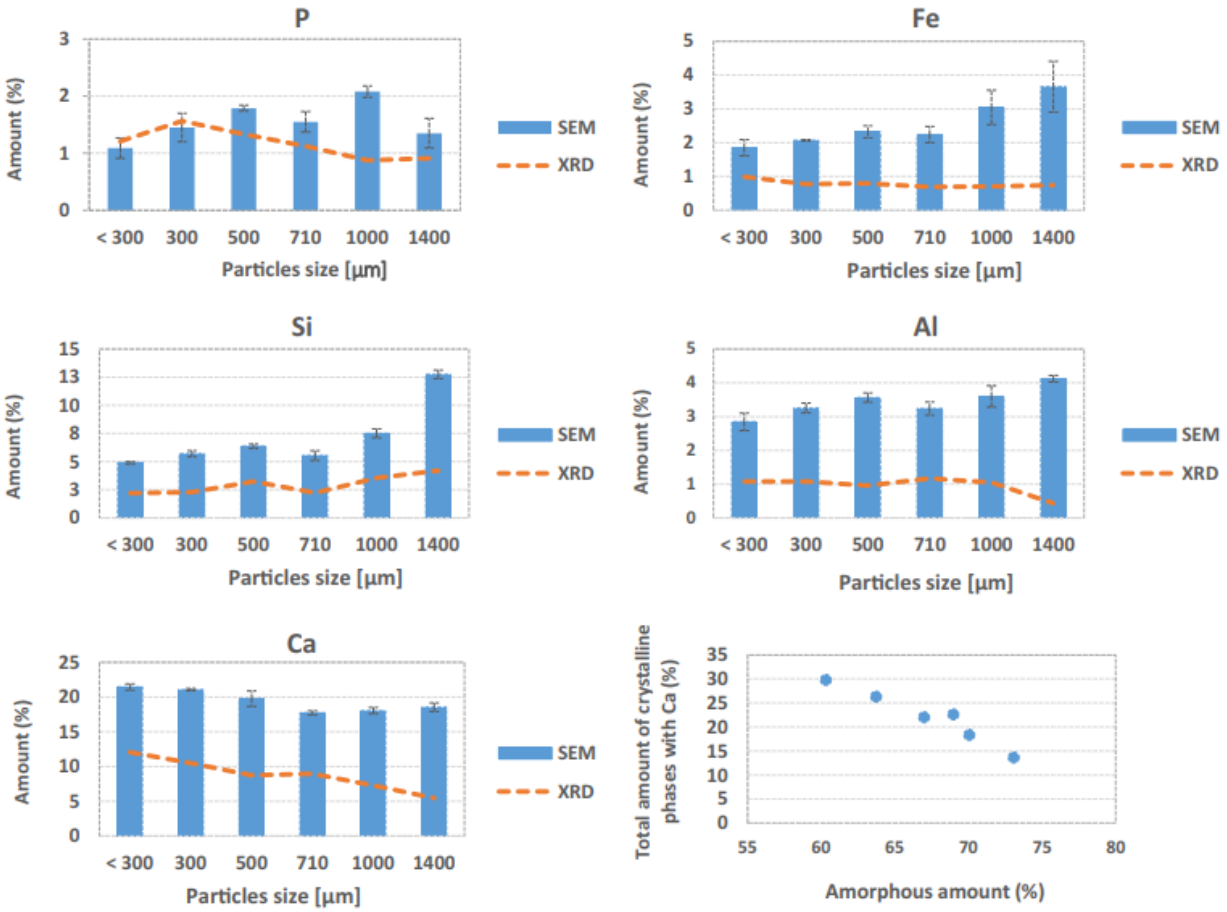

Figure 26 Amount of P, Fe, Si, Al, Ca (%) and the total amount of crystalline phases containing Ca (%) compared to the amorphous amount (%).

Based on these considerations it is possible to expect a pozzolanic behavior for BA [116]. Moreover, Figure 26 highlights that coarse grain sizes (1000-1400 µm) show a composition with increased SiO_2 + Al_2O_3 species. This is extremely interesting because Si and Al are the promoters of networking in glasses [123], with the possibility to develop silicate crystals or ceramic glass structures (by using thermal energy). Literature suggests the possibility to reuse also BA (produced from mono-combustion of MSW) in the ceramics production (due to significant quantities of SiO_2 and Al_sO_3) [61]. However, the CaO amount found in BA, which is higher than that of several ceramic materials, may contribute to lower the melting temperature of the mix, and possibly lead to energy savings in the ceramics manufacturing process. These findings suggest attractive reuses of BA coarse fractions (1000-1400 µm), investigated in this work, that seems more suitable compared to FA (produced from mono-combustion of MSW) for glass and ceramic manufacturing.

An important application could be investigated, on the basis of the high amount of amorphous contained in this waste. For this purpose, the reactivity of BA was investigated by

mixing with FA derived from the same thermal valorization process FA, with the aim to test their heavy metals immobilization capacity. The capability of BA to stabilize leachable Pb and Zn was recently proved [66]. Because it is based on the use of wastes produced in the same location (BA and FA), it is suitable to be applied with low impact on incinerator plants, allowing to simplify the actual waste strategy management of FA, which generally involves its transport and stabilization treatment before its landfilling. Thanks to the use of BA as a stabilizing agent, the stabilization mechanism is attributed to the formation of amorphous calcium silicate hydrate (C-S-H), with a pozzolanic reaction, able to reduce heavy metals solubility [66].

Table 13 shows that stabilized samples revealed a significant decrease in heavy metals leaching, especially Pb and Zn (almost one orders of magnitude), compared to FA, due to the stabilization effect. Two months after the stabilization, Ba and Pb concentrations result to be lower than the instrument detection limit, and Cu concentration (that was higher than 7±2 mg/L in the BA leaching solutions) always results lower than 0.10±0.07 mg/L. Thanks to the use of BA, the stabilization mechanism is attributed to a pozzolanic reaction, able to reduce heavy metals solubility. In particular, as a result of the BA characterization that shows the high amount of glassy phase in this by-product (containing Si, Al, and Ca), it is supposed that the reaction of silica and/or alumina with calcium hydroxide, mainly derived from FGD residues, promotes the formation of a hydration product (C-S-H calcium silicate hydrate and/or C-A-H calcium aluminate hydrate), which is reported to be able to stabilize hazardous elements present in FA. The proposed stabilization mechanism was recently discussed using the same raw materials (the only difference is that BA (produced from mono-combustion MSW) was used instead of BA [66]. A similar reaction was already proposed in literature [124], but considering BA (produced from mono-combustion MSW) addition to cement, that contains $Ca(OH)_2$.

Data reported in Table 13 revealed that when SF is used, samples are better stabilized (considering results obtained one month after the process). This is probably due to the fact that SF is completely amorphous. Although, BA contains considerably amounts of reactive amorphous phase, it is lower of almost 30-40% (depending on the considered size fraction), compared to SF. Table 13 also shows that better stabilization results (Pb and Zn leachability is reduced) are obtained if samples are aged for two months. This is due to carbonation reactions. Indeed, as already shown in several papers [65,116,125], the use of by-products with high amount of $Ca(OH)_2$ allows to form calcium carbonate, able to reduce pH to a more neutral level, promoting Pb and Zn stabilization [65].

XRD patterns collected on stabilized samples reveal that detected phases correspond to those already reported for samples obtained by using the proposed stabilization technology (see for example [42,66]. In particular, as described and discussed in the literature [65,125] the presence of intense calcite peaks, coupled with the absence of calcium hydroxide, strongly supports that carbonation reactions were occurred. Moreover, as already found [66], C-S-H and C-A-H phase cannot be completely crystallized, making difficult to highlight pozzolanic reactions by XRD.

In summary, data shown in Table 13 allows also to conclude that, despite of the difference on the amorphous content in the tested fractions is not determinant, for this application, the reactive phases present in BA make it suitable for the heavy metals stabilization.

Table 13 Results of the TXRF analysis and pH values of stabilized samples with various BA fractions after the first (1) and second (2) month. Values are expressed as the average ± standard deviation of three TXRF measurements. Relative sensitivities for elements

Samples	Time (Month)	pH	Elemental Concentration (mg/L)											
			P*	S*	Cl	K	Ca	Fe	Cu	Zn	Br	Rb	Sr	Ba	Pb
MIFA	—	12.2	15 ± 1	128 ± 44	3279 ± 373	482 ± 55	2580 ± 244	0.67 ± 0.39	0.44 ± 0.1	13 ± 1	197 ± 16	6.3 ± 0.4	14 ± 1	2.1 ± 0.7	65 ± 4
1	1	11.12	39 ± 18	647 ± 105	2610 ± 383	450 ± 160	1972 ± 776	0.28 ± 0.10	< LOD	0.50 ± 0.37	101 ± 11	4.6 ± 0.7	19 ± 4	< LOD	< LOD
	2	9.26	23 ± 9	329 ± 28	2065 ± 47	267 ± 17	1278 ± 64	0.20 ± 0.10	< LOD	< LOD	96 ± 17	4.1 ± 0.7	12 ± 3	< LOD	< LOD
2	1	12.17	54 ± 2	352 ± 81	3759 ± 398	571 ± 100	2848 ± 233	0.41 ± 0.09	0.05 ± 0.03	1.07 ± 0.10	81 ± 3	2.8 ± 0.2	13 ± 1	1.6 ± 0.4	4.0 ± 0.2
	2	10.05	23 ± 11	282 ± 189	1856 ± 324	244 ± 90	1142 ± 215	0.23 ± 0.18	0.07 ± 0.03	0.05 ± 0.01	92 ± 6	4.4 ± 0.5	15 ± 1	< LOD	< LOD
3	1	12.16	37 ± 17	342 ± 92	3461 ± 481	518 ± 113	2587 ± 299	0.39 ± 0.14	0.08 ± 0.02	0.91 ± 0.27	89 ± 9	3.2 ± 0.3	16 ± 1	1.4 ± 0.2	3.8 ± 1.2
	2	10.26	29 ± 5	382 ± 112	2306 ± 504	336 ± 62	1484 ± 363	0.28 ± 0.11	0.07 ± 0.04	0.08 ± 0.002	75 ± 9	3.7 ± 0.4	13 ± 1	< LOD	< LOD
4	1	12.14	47 ± 8	316 ± 30	3879 ± 242	533 ± 59	2944 ± 147	0.27 ± 0.17	0.13 ± 0.02	1.06 ± 0.19	88 ± 3	3.1 ± 0.2	14 ± 1	1.5 ± 0.7	4.2 ± 0.6
	2	9.38	27 ± 12	502 ± 71	2181 ± 430	351 ± 39	1408 ± 88	0.32 ± 0.21	0.07 ± 0.03	0.05 ± 0.01	84 ± 11	3.9 ± 0.2	14 ± 1	< LOD	< LOD

6 Carbonation tests

Mineral carbonation, involving reactions of alkaline earth oxides with CO_2, has received great attention, as a potential carbon dioxide sequestration technology. Indeed, once converted into mineral carbonate, CO_2 can be permanently stored in an inert phase. Several studies have been focalized to the utilization of industrial waste as a feedstock and the reuse of some by-products as possible materials for the carbonation reactions.

6.1 Description of the experiment

In my studies MSW incineration FA and other ashes, as BA, CFA, flue gas desulphurization residues, and SF, are stabilized by low-cost technologies. In this context, the CO_2 is used as a raw material to favor the chemical stabilization of the wastes, by taking advantage of the pH reduction. Four different stabilization treatments at room temperature are performed and the carbonation reaction evaluated for three months. The crystalline calcium carbonate phase was quantified by the Rietveld analysis of XRD patterns. Results highlight that the proposed stabilization strategy promotes CO_2 sequestration, with the formation of different calcium carbonate phases, depending on the wastes. This new sustainable and promising technology can be an alternative to more onerous mineral carbonation processes for the carbon dioxide sequestration.

In Table 14, a description of sample preparation is reported. Then, about 200 mL of ultrapure de-ionized water was added and the mixture was mixed for 20 min. All the samples were aged at room temperature for 3 months.

Table 14 Samples description

Samples	MSWI FA (g)	CFA (g)	FGD (g)	Silica Fume (g)	MSWI-BA (g)	%MSWI FA (%)	%FGD (%)
A	130	30	40	20	-	59.1	18.2
B	130	30	-	-	20	72.2	-
C	130	30	40	-	20	59.1	18.2
D	130	30	40	-	-	65	20

6.2 Composition analysis

6.2.1 Leaching test, XRD and Rietveld analysis

To verify the heavy metals immobilization, the leaching tests of Zn and Pb were performed. The pH of the filtrates was measured by a pH meter. Leaching solutions were analyzed for the initial ashes and one (1 month) and two months after the stabilization process in order to verify the efficacy of the process.

FA contains high amount of S, K and Ca (>19 g/kg), while Fe is almost one order on magnitude lower than the value found in BA (about 4 g/kg). Indeed, Ca and Fe are the major elements in BA (>40 g/kg). K, S, P, and Cu are also found in relevant amounts (>6 g/kg). CFA mainly contains S, K, Ca, and Fe (>9 g/kg). FGD residues contain large amount of Ca (>160 g/kg) and S (>95 g/kg).

By Rietveld analysis it was found that FA contains calcite (about 10%), CaClOH (about 24%), and soluble salts (NaCl, KCl, with total amount of about 9%). FA contains also a large amount of amorphous phase (about 56%). Calcite was attributed to the natural carbonation process, occurred during the FA storage [78]. Figure 27 shows also the XRD pattern of CFA, FGD residues and BA. In accord with previous reported data [67], the major crystalline calcium (magnesium) silicate and potassium iron silicate phases are also detected. FGD residues contain portlandite, hannebachite, gypsum as the main crystalline phases. As well, CFA contains quartz and mullite as the major crystalline phases.

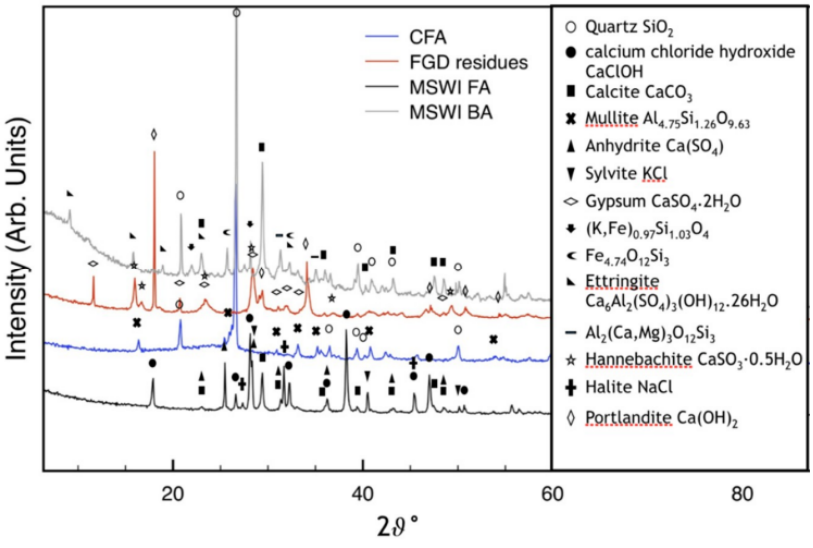

Figure 27 X-ray diffraction (XRD) patterns of FA, CFA, FGD residues, and BA.

Results of the leaching tests, obtained on FA, are shown in Table 15. Pb and Zn are found in high concentration in FA sample (35 and 9 mL, respectively), while concentrations of these elements in the other ashes result to be two order of magnitude lower. The high concentration of Zn and Pb in FA is likely related to the high pH (about 12) with consequent high Zn and Pb solubility.

The stabilization technology used is based on amorphous silica sources for metals immobilization [125]. Amorphous silica can be found in Sample A, due to the SF addition, and in samples B and C, due to the use of BA [67]. Table 15 reports the concentration of heavy metals (Pb and Zn) detected in the leaching solutions of the stabilized materials, one and two months after the treatment.

All the stabilized samples revealed lower concentrations of Pb and Zn in their leaching solutions, in respect to the starting FA and the results are better after two months. Considering the pH of the leaching solutions, it results that it is always lowering with aging. This stabilization effect and the pH reduction were attributed to carbonation reactions, as diffusely discussed in several studies [109,115].

Table 15 Concentration of Zn and Pb in leaching solution of ashes and stabilized samples after one and two months. Results are reported as the average ± standard deviation of three TXRF measurements. Data about FA, BA, CFA, and FGD residues do not change in the two months.

Samples	pH	Months	Elemental Concentration (mg/L)					
			Zn			Pb		
MWSI-FA	12.18	-	8.80	±	4.30	34.60	±	2.40
MWSI-BA	10.69	-	0.05	±	0.04	0.09	±	0.05
CFA	11.81	-	0.24	±	0.02	0.13	±	0.03
FGD	12.68	-	0.1	±	0.04		<LOD	
A	11.73	1	0.15	±	0.09		<LOD	
	8.92	2	0.11	±	0.01		<LOD	
B	12.22	1	1.52	±	0.19	12.20	±	0.70
	10.23	2	0.14	±	0.00		<LOD	
C	12.06	1	0.39	±	0.02	3.20	±	0.50
	10.37	2	0.07	±	0.01		<LOD	
D	12.22	1	0.80	±	0.40	6.40	±	1.60
	11.07	2	0.07	±	0.001		<LOD	

<LOD—Limit Of Detection.

Table 16 Results of Rietveld analysis at different aging times (semi-quantitative analysis)

Samples	Months	Amorphous (%)	Calcite (%)	Hannebachite (%)	Thaumasite (%)	Gypsum (%)	Quartz (%)	Vaterite (%)	Sylvite (%)	Halite (%)	Anhydrite (%)
Sample A	0		6 *								
	1	69	12	5	<1	1	1	3	2	3	4
	1.5	69	17	4	<1	3	<1	2	1	2	2
	2	67	17	5	<1	<1	1	1	2	2	5
	2.5	63	19	5	<1	<1	1	2	1	3	5
	3	63	20	4	<1	3	2	2	1	2	3
Sample B	0		11*								
	1	72	14	2	<1	1	2	2	2	4	<1
	1.5	70	16	<1	3	1	2	3	1	2	<1
	2	67	17	<1	<1	1	3	6	<1	2	3
	2.5	67	17	<1	<1	1	2	4	1	2	4
	3	64	19	3	<1	2	<1	1	1	3	4
Sample C	0		9*								
	1	69	13	6	<1	1	<1	2	2	3	3
	1.5	70	16	5	<1	2	1	2	1	2	2
	2	69	16	4	<1	2	1	2	1	1	3
	2.5	63	19	4	<1	1	2	2	1	2	6
	3	64.	20	3	<1	1	<1	3	1	1	5
Sample D	0		7*								
	1	66	14	7	<1	<1	<1	2	2.	3	4
	1.5	65	21	6	<1	1	1	2	1	2	1
	2	65	18	6	<1	2	1	2	<1	2	3
	2.5	63	22	5	<1	<1	2	3	<1	2	2
	3	61	20	4	<1	2	3	2	1	2	5

* indicates the amount of calcite present in the mixed powders, before reaction (month 0). It represents the natural carbonation contribution.

The main reactive species for carbon dioxide sequestration in FA are generally CaClOH (calcium chloride hydroxide) and $C(OH)_2$ (portlandite).

CaClOH is available for carbonation reactions through the following reaction:

$$2CaOHCl + CO_2 \rightarrow CaCO_3 + CaCl_2 + H_2O \quad (1)$$

The carbonation reaction for $Ca(OH)_2$ is:

$$Ca(OH)_2 + CO_2 \rightarrow CaCO_3 + H_2O \quad (2)$$

Indeed, natural carbonation of FA was generally regarded as an interesting process controlling pH variation and limiting the heavy metals solubility, but it is an extremely slow process, requiring decades [111].

The stabilization mechanism of the proposed technology, involving the mixing of different wastes and by-products. Also involves carbonation reactions, that allow to reduce the pH of the stabilized materials and heavy metals leachability. Indeed, the reduction of heavy metals leaching was explained by two combined reactions, respectively due to the absorption in the amorphous silica and the carbonation. Moreover, the immobilization of residual heavy metals, after the stabilization technology obtained by lowering the pH (for example by forming insoluble phases), was attributed to indirect consequence of carbonation [78].

In present case, $Ca(OH)_2$ cannot be found in the starting FA. However, this phase (portlandite) is available in FGD residues (see Figure 27). The XRD and Rietveld analysis were performed, collecting small portions of samples (about 1 g). at different aging times.

Rietveld refinement was performed because it is useful not only to made qualitative analysis of XRD patterns, since missing mineral phases inevitably involve significant differences between calculated and experimental patterns, but also because it allows to evaluate the amount of all detected phases. This fundamental for our study to follow the evolution of the formed quantities of calcium carbonate crystalline phases, as a function of time and samples compositions. Moreover, the Rietveld method permits the quantification of the amorphous phase, since changes in the amorphous amount must be checked to obtain reliable information about phases evolution.

Figure 28 shows the XRD pattern collected on stabilized sample A, one month after the sample synthesis. It also reports the results of the Rietveld refinement and the difference between experimental and calculated intensity is also plotted. A representative example is reported. The small differences obtained for the two patterns confirm the reliability of the qualitative characterization carried out.

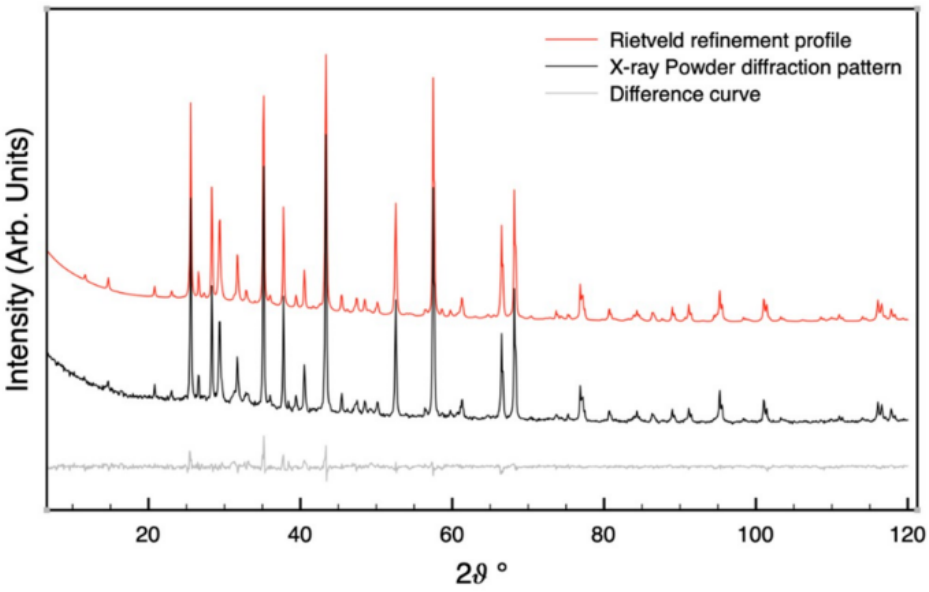

Figure 28 XRD pattern and corresponding Rietveld refined profile made on stabilized sample A, one month after the sample synthesis. Difference curve is also plotted.

Table 16 shows the results of the Rietveld analysis on all the samples, after different aging times. Following carbonation, the $Ca(OH)_2$ and CaClOH peaks disappeared in the XRD patterns, whereas many $CaCO_3$ peaks appeared. In particular, two carbonates were identified, calcite and aragonite, likely due to reactions (1) and (2). Calcite was already present in the FA possibly because of partial natural carbonation. Vaterite, the thermodynamically least stable phase among the three polymorphic forms of calcium carbonate, was detected in FA

sample, as already found in similar experiments [78]. Vaterite is generally formed at a relatively low temperature condition (also at room temperature) [126].

Another interesting result found by Rietveld analysis is the quantification of the amorphous phase and its variation during the investigated period. These data are reported in Figure 29. The amount of amorphous is quite high in all the samples (more than 65%) and decreases during reaction with the carbon dioxide. The reduction of the amorphous content is correlated with the increase of the crystalline phases. All the Rietveld results are reported in Table 16.

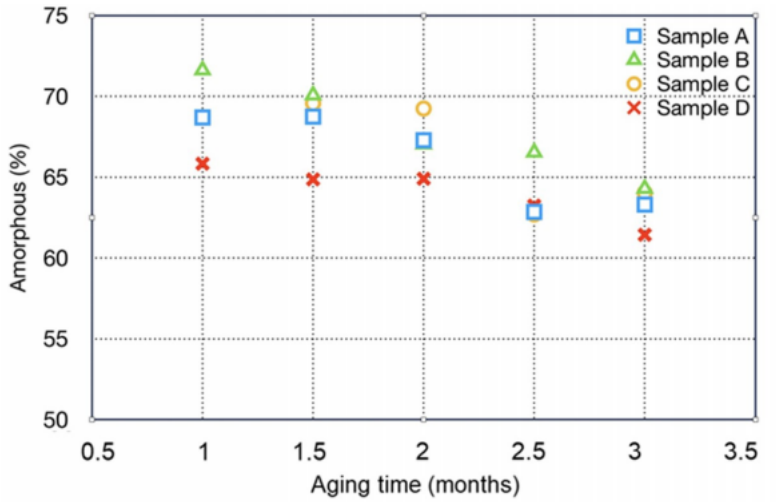

Figure 29 Amount of amorphous, evaluated by Rietveld method, as a function of samples aging time.

Based on the amount of calcite and vaterite present in the original samples, the crystalline calcium carbonate content in the mixture induced by carbonation reactions was calculated. In Figure 30, it is shown that the amount of crystalline calcium carbonate phases (calcite and vaterite) increases when the amorphous phase decreases.

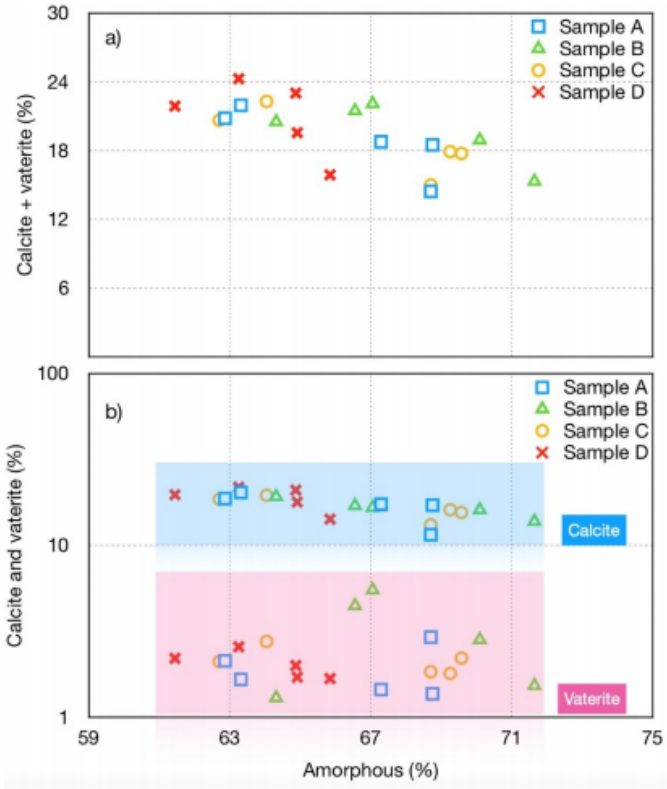

Figure 30 Amount of crystalline calcium carbonate phases (calcite and vaterite), evaluated as a global calcium carbonate crystalline phase (a) and separately (b). These data were calculated by Rietveld method, in respect to corresponding amorphous content.

All the samples, before aging, contain calcite, in the range of 6%–10% (see Table 16) and vaterite was not detected. Considering the original sample, the $CaCO_3$ content increased about 70% in samples A and D, while in sample C the $CaCO_3$ is increased about 40% and in sample B it is about 30%. It is interesting to notice that in sample B, FGD (that contains portlandite) was not added. This may explain the low carbonation. Sample D, where the amount of FGD on total ashes content is the highest, shows the largest global increase of crystalline calcium carbonate, that was more than 70% in 3 months. On this basis, we calculated that the treated material is able to sequestrate more than 90 g CO_2/kg of ash (taking into account also the natural carbonation of FA). This result is great, because the maximum CO_2 sequestration quantity reported for the carbonation of FA was about 58 g CO_2/kg and the carbonation reactions were also supported by thermal annealing [127]. A very recent paper [94] reaches the maximum capacity of carbon dioxide sequestration of 60 g CO_2/kg of FA at atmospheric pressure, but it was achieved at 600 ºC with 20% H_2O (g) addition. The better results obtained in this work can likely be ascribed to the addition of FGD residues. It is also important to highlight that amorphous calcium carbonate cannot be quantified by XRD and therefore, the amount of CO_2 sequestrated is expected to be higher than that evaluated only

considering the crystalline calcium carbonate. Figure 30 shows the calcite + vaterite content to enlighten their behavior in respect to the change of the amorphous content. The data, plotted for the four different samples (in logarithm scale), show a linear inverse correlation between the amount of calcite and vaterite with the amorphous content. Moreover, sample B, which contains the highest amount of FA but not FGD residues, shows the largest amount of vaterite and the lowest amount of calcite. This result supports the hypothesis that the carbonation of FGD residues favors the calcite formation. On the contrary, the vaterite formation can be related to the FA carbonation (FA amount is 72% for sample B). It is expected that vaterite ultimately reverts to calcite [128]. Indeed, vaterite, that is less dense than calcite, can be formed by bio-mineralization, with a stability that can take several months. Some authors suggested that the formation of amorphous calcium carbonate is a transient intermediate, which transforms to the crystalline vaterite [128]. In Figure 29 it is shown that sample B has the highest reduction of the amorphous phase during the aging (more than 10% from month 1 to month 3), in respect to the other samples (that show generally a reduction of 7%). Then it is very likely that in this sample the amorphous calcium carbonate transforms in vaterite. In Figure 29 is also shown that sample B, at the end of the aging, has a lower vaterite percentage (1.3%), in respect to 5.5% found two months after the treatment. This is in accordance with the possible phase transformation of vaterite into calcite, occurred as a stabilization of the metastable vaterite phase formed as a consequence of mineralization. The amount of the other detected crystalline phases (gypsum, quartz, hannebachite, anhydrite, sylvite, and halite) was also evaluated (data are reported in Table 16) and no evident correlations with the change of the amorphous content amount were found. Thus, we can conclude that the increase of the crystalline calcium carbonate phases is due to crystallization of an amorphous phase. Indeed, the D sample, that shows the highest amount of crystalline $CaCO_3$, has the lowest amount of amorphous percentage.

7 Reuse of the stabilized fly ash

The large quantities of ashes deriving from the incineration of waste, the high cost of disposal and the scarce availability of sites to be used as landfills added to the already known problems related to the atmospheric emissions of incinerators, those relating to disposal of the ashes. In this way, "alternative" practices to the landfill were sought, such as those of the so-called "valorisation" of the residues produced by incinerators, which create further concerns for the environmental impact and for the risks to human health. "Man, other organisms and the environment are exposed to a 'cocktail' of chemicals whose effects are not adequately known, due to the absence of experimental data" [4].

7.1 Composites polymeric matrixes

The goal of the experiment is to verify if stabilised ash can be used as a composites polymeric matrixes filler. It has been chosen the 'unwashed' and ground powder variant because one advantage of the material is its physical shape, in order to have more fine particles. The unground material in fact appears visually as small agglomerations similar to stones of varying sizes, while ground, it appears in powder form and therefore can be used as a filler in a composite, made by mixing a matrix with a powder. Consequently, in principle, this material could be used with all matrices that require inorganic filler. The unwashed stabilized material contains soluble salts (especially NaCl and KCl) which are not a problem for the environment, but which they could be if it was used in civil construction.

The filler used in the study was obtained by using BA to stabilize FA and was considered for the production of composite materials. The goal of this study is to characterize and evaluate the real possibility of the new filler reuse. In addition, an evaluation of the advantages, in terms of energies and emissions required for the material synthesis are quantitated in comparison with the use other resources. For this aim, a recently proposed simplified approach is used [42].

This study can be considered a virtuous example of resource use efficiency, with focus on wastes-the circular economy approach assumes that the resources extracted and produced must be always in circulation, avoiding the landfilling. In this specific case, the reuse of stabilized waste is proposed in order to promote the transition to more circulare economy

(CE), by eco-innovation aiming at a “zero waste economy”. And even though the European Union (EU) action plan about CE does not explicity address ashes from waste incineration, using these resources more efficiently may contribute to reach some scopes defined in the CE action plan and helps to close a gap in the CE loop [129].

This study reports and analyzes the mechanical properties of some composites obtained using stabilized waste with two different polymeric matrixes. For comparison, correspondent composite samples were realized using as a filler an industrial grade calcium carbonate ($CaCO_3$) Calcite V40 (Carrara, Italy), with a particle size distribution below 60 μm (99%).

7.1.1 Epoxy resin composites

The composite material matrix consists of Epoxy resin E-227 (produced by Prohima), also known as polyepoxides. This is a class of reactive pre-polymers and polymers characterized by the presence of epoxide groups. The bi-component product is formed by polymer and catalyst that must be mixed according to the ratio indicated by the manufacture equal to ½ in weight to obtain the final product.

7.1.1.1 Composite samples preparation

Calcite and stabilized sample were used as filler. A series of five specimens: 0%, 10%, 30%, 50% and 70% wt were prepared by mixing the epoxy resin with calcite or stabilized sample in a beaker for about 5 min. After that, the mixture was drained in a mold and maintained for 24 h at room temperature to obtain a sufficient hardness. The samples of epoxy composites with different filler were fabricated according to the following steps:

1. Silicone rubber molds have been produced in order to realize the negative shape of the samples;
2. The stabilized sample has been mixed with the epoxy resin before pouring the mix in the molds;
3. Material stand-by for 4 days at room temperature. The same procedure has been applied to prepare the specimens with calcite as a filler.

Figure 31 shows the two different samples prepared with stabilized FA (a) and calcite (b).

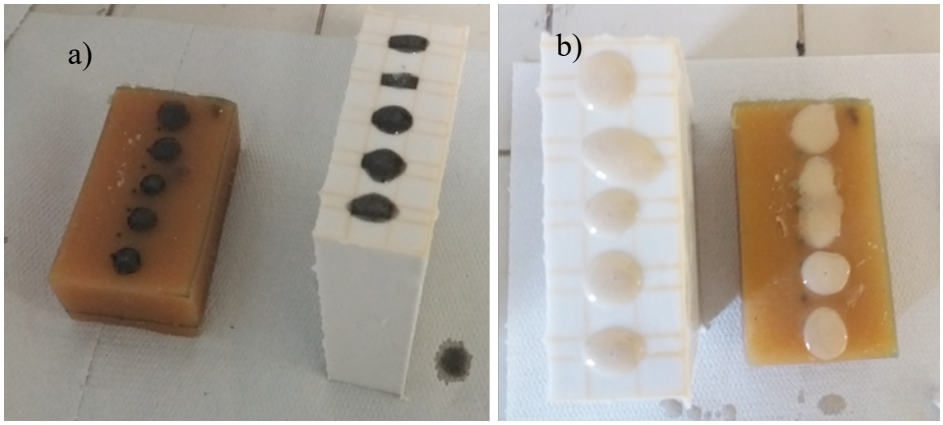

Figure 31 Specimen preparation: (a) stabilized sample-composite material, (b) $CaCO_3$-composite material.

7.1.1.2 Mechanical characterization

A comparison mechanical test has been conducted in order to evaluate the differences between the use of stabilized ash and calcite as a filler of composites materials.

7.1.1.2.1 Three Point Bending Test

Flexural strength and modulus of elasticity were obtained through a three-point bending test. Figure 32 reports a stress-strain curves obtained at different content (50% and 70%) of calcium carbonate and stabilized sample (ash) in comparison with neat polymer. Flexural modulus, evaluated from the slope of the stress versus strain deflection curve determines how much a sample will bend when a given load is applied, while flexural strength is calculated as the maximum bending stress.

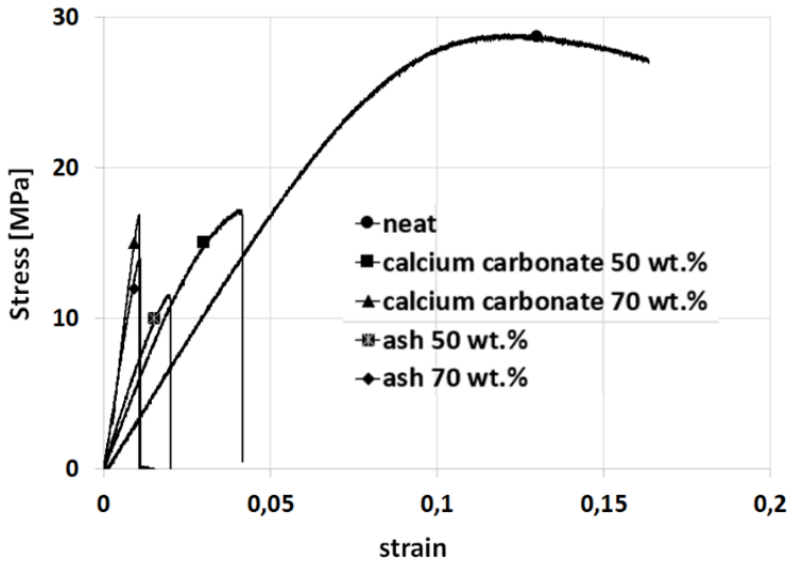

Figure 32 Stress-strain curves obtained from flexural tests for different composites.

In Figure 33, it is possible to notice first that the neat epoxy shows an elongation at break much higher than that both stabilized sample-epoxy and calcium carbonate-epoxy composites. Moreover, the neat epoxy did not break brittle but it yields above the peak. The presence of 50% by weight of filler significantly reduces the elongation at break of the composites and major amount of filler up to 70% by weight further decreases it. The influence of stabilized FA as filler in epoxy resin matrix on the elongation at break is similar to that of calcium carbonate. As expected, increasing the filler amount in the epoxy matrix the elongation and the straight at break decrease, while the flexural modulus increases [130–132]. In general, the same content [% wt] of ash and calcium carbonate affects the composite flexural behavior similarly. The flexural modulus and flexural strength of $CaCO_3$/epoxy and stabilized sample/epoxy composites with different filler amount are shown in Figure 33 and 34, respectively.

Figure 33 shows the trend of flexural modulus of stabilized sample-epoxy and calcium carbonate-epoxy composites at different filler content (from 10% up to 70% by weight). It should be noted that the flexural modulus of stabilized sample (ash) and calcium carbonate composites is similar for each filler content and the curves almost overlap. The flexural modulus remains approximately constant up to a filler amount of 30% wt, then it slightly increases to a filler amount of 50% and it strongly increases for filler amount of 70% wt. In general, the flexural modulus raises increasing the filler content by more than 30% by weight of filler content independently of whether the filler is stabilized sample or calcium carbonate.

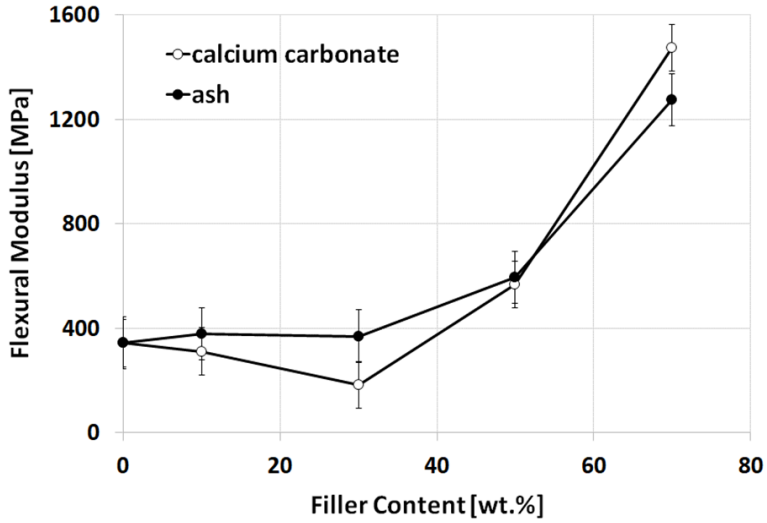

Figure 33 Flexural modulus as a function of filler content.

Figure 34 shows the trend of flexural strength for of stabilized sample-epoxy and calcium carbonate-epoxy composites at different filler content (from 10% up to 70% by weight).

Flexural strength and elongation at brake reduction of composites decreased with increasing of filler loading mainly due to agglomeration process acting as defects in the polymer matrix. It is worthwhile to note that the flexural strength decreases increasing the filler content up to 30% by weight for both ash and calcium carbonate. The composite stabilized sample-epoxy shows a constant decrease in the flexural strength up to a filler content of 50 wt.% and then it shows a slight increase up to 70 wt.%. Due to this trend and its standard deviation, it is possible to consider the flexural strength constant for stabilized sample content above 30 wt.% as well as for calcium carbonate composite. The experimental data show a change in tendency of flexural modulus and strength for stabilized FA and calcium carbonate content greater than 30% by weight.

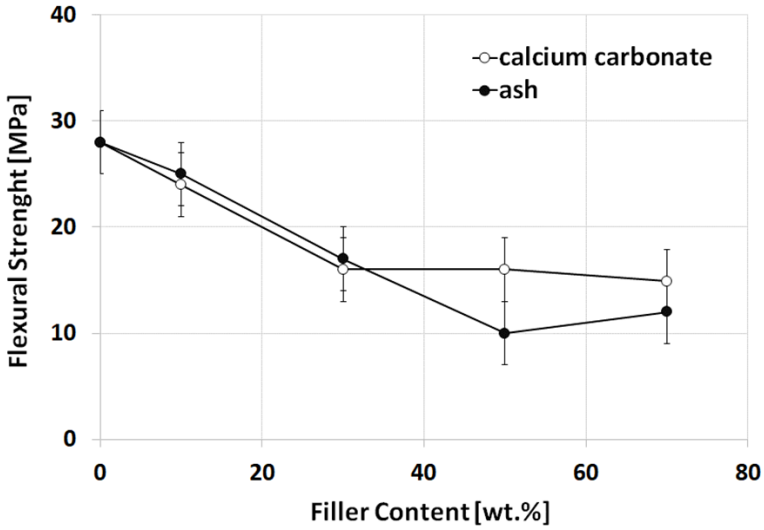

Figure 34 Flexural strength as a function of filler content.

7.1.1.3 Sustainability evaluation of the proposed technology

Embodied energy (EE) and CO_2 footprint (CF) parameters of the synthesis of the proposed new filler were considered to evaluate environmental sustainability.

Data about EE and CF of the recycled stabilized material were obtained by using the CES Selector software [133] taking into account the stabilization procedure, which involves the BA grinding and considering the mixing of different ashes typologies, as described in the experimental section and discussed in literature [67]. For the stabilized material, an EE from 0.061 to 0.062 MJ/kg and a CF of about 0.03 kg/kg resulted.

Table 17 reports the SUB-RAW indices evaluated by comparing the new proposed material in comparison with calcite, which is a natural resource that is often used as a filler, to produce

some composites. As a reference, this index was also calculated in comparison with sandstone, talc and resin used to synthesize the composites for this work.

Table 17 SUB-RAW Indices were calculated comparing the obtained composite using stabilized FA sample with other materials.

Materials	SUB-RAW Index–New Filler
Sandstone	1.24
Calcite	0.83
Talc	2.24
Resin	3.31

From calculated SUB-RAW indices, it is evident that the new proposed inert is more sustainable if compared to some natural resources, as for example calcite, talc and sandstone. Obviously it is also more sustainable in comparison with a resin [115]. Then, it is possible to conclude that it may be used to produce composited materials. In principle, its market applicability is potentially very promising. To evaluate this, also the price of the materials reported in this work have been considered.

Figure 35 shows the EE for several materials (ceramic, glass and composites) as a function of their commercial price. Data were obtained from CES Selector 2019 [133]. Data on the carbon footprint of Appl. Sci. 2020, 10, 754 12 of 16 the same materials, reported as a function of their commercial price, have the same behavior already shown by Bontempi et al. [134]. In correspondence of the EE of the new proposed material, an orange dotted horizontal line is reported.

From the analysis of Figure 35, it can be seen that the new obtained stabilized material can be compared to wollastonite in terms of the EE environmental parameter used to quantify the sustainability of a material. Figure 35 shows that the energy needed to synthesize the new proposed material is lower than that of the almost majority of ceramic and glass materials. It results evident that it is more sustainable that the previous proposed COSMOS filler, obtained by adding an external silica source [42,125] to stabilize MSWI FA. Indeed, EE of COSMOS resulted higher than that of calcite. On the contrary, in the present case, it is demonstrated that the new obtained stabilized material can be used, with environmental advantages, in substitution of calcite. This is due to the fact that BA is a by-product produced on the same incinerator plant where FA is generated. As a consequence, its EE and CF can be assumed to be zero. It is possible to conclude that the new filler is strongly suggested to be used for the synthesis of composites materials, avoiding the natural resources employ. The price, which is

generally used to evaluate the commercial applications of a material, is an important criterion, which must be also taken into account, because it can be related to the new material market. In the present case, this is unknown but the Figure 35 reports the price of several materials, allowing us to verify the market opportunities for the new proposed filler.

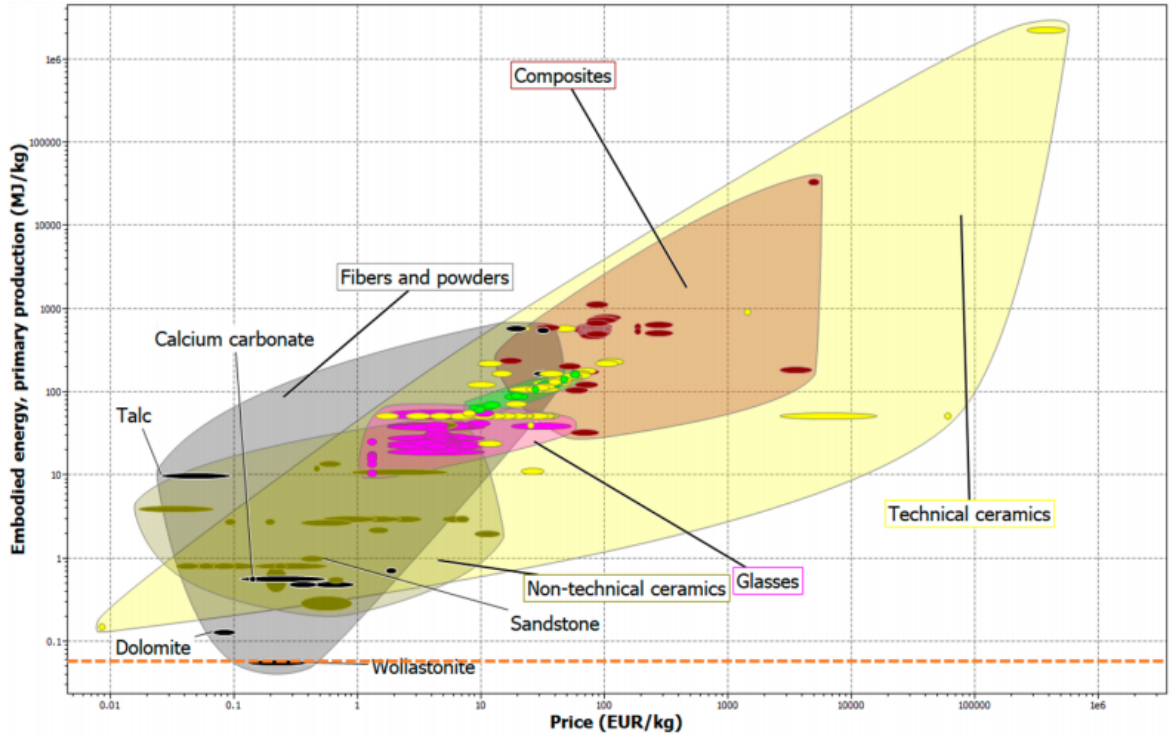

Figure 35 Embodied energy, primary productions (MJ/kg) vs. price (EUR/kg) of various materials and composites [135].

7.1.2 Polypropylene composites

The production of polypropylene (PP) composite materials using the stabilized FA as a filler through the injection molding machine was made. The stabilized ash was obtained by the same process discussed previously.

Figure 36 shows the scheme of the machine used to produce the samples that were fed by granules of PP and stabilized FAes with different percentages by mixing the two components before introducing them into the machine. Figure 36 also shows that using endless screws adopted by the injection molding machine helped not only to melt and push the material outside through the extruder, but also to mix and obtain more homogeneous material. The complete mold filling depended on the viscosity of the composite material, which depended also on the filler charge set and the geometry complex.

Figure 37 shows a set of composite samples obtained by the injection molding process with different filler more percentages. Figure 37c,d shows that some streaks were present on the

surface of the samples with more of filler due to the crushing of stabilized ash grains. This problem can be resolved by adding some colorant product to the mixture.

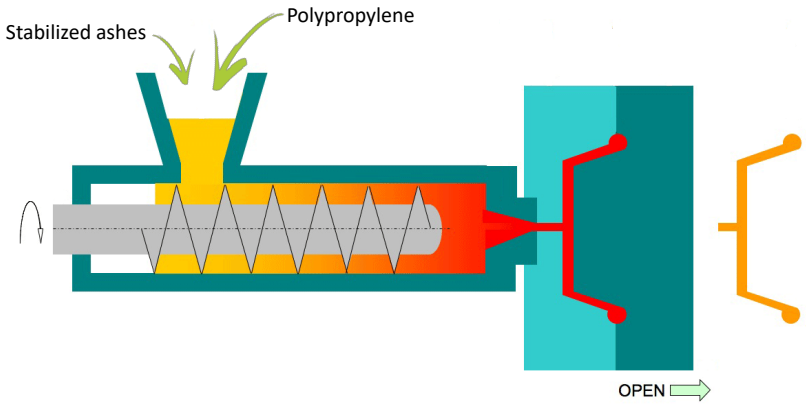

Figure 36 Injection molding machine.

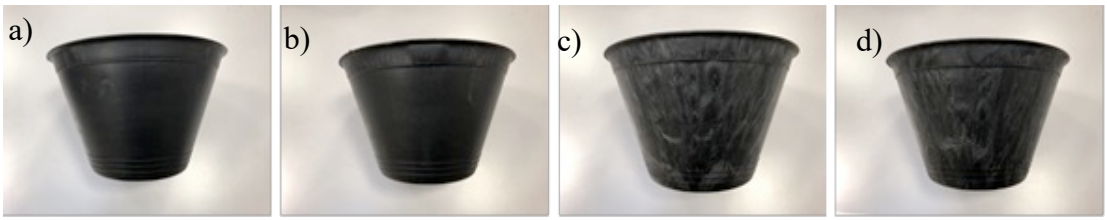

Figure 37 Sample products with different % of ash: (a) PP, (b) 10%, (c) 20%, (d) 30%.

7.1.2.1 Mechanical characterization

In order to evaluate the performance of the stabilize ash as a filler, a series of mechanical tests have been performed and compared to literature data.

7.1.2.1.1 Tensile test

The tensile test was performed according to (UNI ISO 527). The specimen geometries used were the dog-bone specimen. The test was conducted by applying a uni-axial load through the ends of the specimen. The results of the test are reported in Table 1 and show that as the weight fraction of filler increased in the composites up to 20 wt%, the results of the tensile strength decreased up to 26.5 MPa, the elongation percentage decreased from 121.3% as the initial value of PP without filler to 11.4%, and the tensile modulus increased at high fly ash content. This can be attributed to the fillers that occupied the interstitial volume. There might have been less PP matrices that could have contributed to the tensile strength, as reported by Paliwal [136], and to a bad interfacial bonding between the fly ash and the matrix [137]. Furthermore, as reported by Srivastava [138], the inhibition and propagation of the crack

inside the composite material can be attributed to the presence of fly ash particles. The results obtained from the tensile modulus, tensile strength, and breaking elongation were similar to the results reported by Maiti [139] by using CaCO3 as a filler of the PP composite material.

7.1.2.1.2 Three point bending test

The flexural modulus was obtained through a three-point bending test performed by means of an electromechanical dynamometer according to (UNI ISO 178). The flexural modulus determines how much a sample will bend when a given load is applied, calculated from the slope of the stress vs. The strain deflection curve, as reported by Assi [140]. As reported in Table 18 and as expected, increasing the filler amount in the PP matrix increased the flexural modulus [132]. Due to the addition of fly ash in the composite material, the crystalline of composites increased and the flexural modulus increased. This resulted in an agreement with the results obtained by Gummadi [141] for smaller particle sizes of fly ash, due to higher contact surface. As reported by Sengupta [142], due to the strong interfacial bonding between the fly ash and the PP matrix, the flexural property increased. The results obtained using fly ash as a filler were similar to those obtained using CaCO3, as reported by Yang [143].

7.1.2.1.3 Impact strength test

The impact test (Izod test) was performed according to (UNI ISO 180) and the ASTM standard. The results of the impact test of the composite material are reported in Table 18. The values of the impact strength decreased, so the energy absorbed in the process of plastic deformation of the matrix material/reinforcement interface decreased by more than 150% by increasing the percentage of filler. This can be attributed to the high surface occupied by the particles of fly ash, as reported by Gupta [144], and by making the material more brittle due to the limited ability of adopting the deformation [145], and the particles can act as a microcrack initiator [146]. Maiti [139] also reports that increasing the percentage of CaCO3 as a filler of the PP composite decreases the impact strength.

Table 18 Data of mechanical experiments.

Material	Breaking elongation [%]	Tensile strength [%]	Tensile strength [MPa]	Flexural modulus [MPa]	Impact strength [J/m^2]
PP	121,3	27	377,3	1176	5,4
PP + 10% stabilized FA	16,3	27,1	412	1437	3,6
PP + 20% stabilized FA	11,4	26,5	455,3	1627	2,4

Conclusion

During this thesis work, some variables were tested and applied to the inertization process of co-incineration FA. The co-incineration of SS and MSW is a well-established technology. The new technology used to stabilize FA is patented by the University of Brescia. As part of the RENDERING project, a new source of amorphous silica was first tested, in order to reduce the production costs of the final material and make this process more sustainable from both an economic and environmental point of view. BA, a by-product of the co-incineration process, was tested as a new stabilising agent. This waste has very interesting characteristics for the process since it has a high amorphous phase content and has a particle size distribution, which guarantees a considerable areas of application. Since the finest particle size can be used a stabilizing agent and the coarse can be used in the civil field.

The tests made during the thesis work, after optimizing the mixing recipe, made it possible to verify the potential of this material and to confirm that inert material, obtained using this source of silica, is an inert product like that prepared with silica fume (SF), commercial silica and rice husk ash.

BA, unlike the traditional stabilization processes, for its preparation requires only waste materials and can be prepared at room temperature. These two characteristics make it more sustainable than previously used processes. Also, the use of other by-product like FGD and CFA makes this process a zero-waste approach. The use of BA also allows the new technology to be applied even in continental areas where raw materials such as SF, rice husk ash are not available. During the thesis work, the issue of the development of this process for the industrialization and therefore of the criticalities that the small-scale method presented was subsequently addressed. A first problem to be faced was that of the maturation times of the material: the process envisaged maturation times in range of 1-3 months with a variability that depended on the season in which the material was prepared. The transfer on an industrial scale with these premises was tested by using an pilot plant situated at the waste-to-energy plant. Thanks to a campaign of tests conducted by varying the conditions of temperature during the maturation of the material, it was possible to optimize the process by drastically reducing the curing times. It has been verified that a treatment at 120 ° C in ventilated conditions allows to obtain an inert material in just four hours. However, such a rapid

treatment leads to the formation of a material with a lower percentage of calcite than that which is formed in a month of maturation at room temperature. This crystalline phase is formed by the reaction of the calcium hydroxides present in the mixture that react with the carbon dioxide present in the air. The carbonation process was then studied in more detail through a carbonation test in which different specimens were analysed.

The Rendering project not only involves blocking the heavy metals present in the initial waste, but also aims to transform a hazardous waste into an inert product that can then be reused as a filler within certain matrices. Once the process was optimized, inert materials was tested as a second raw material within a polymeric matrix, to create some composite product. The material obtained gave good results: it was possible to add up to 30% by weight of aggregates in the polymeric mixture, obtaining a reduction in the costs of the raw materials used. Excellent results were also achieved from the mechanical tests comparing with the instantaneous commercial filler.

References

1. Chimenos, J.M.; Segarra, M.; Fernández, M.A.; Espiell, F. Characterization of the bottom ash in municipal solid waste incinerator. *J. Hazard. Mater.* **1999**, *64*, 211–222.
2. Statistics Explained Available online: https://ec.europa.eu/eurostat/statistics-explained/index.php?title=Main_Page (accessed on Jan 11, 2021).
3. Directive 2010/75/EU Available online: https://eur-lex.europa.eu/legal-content/EN/TXT/?uri=celex%3A32010L0075 (accessed on Jan 10, 2021).
4. Adella, L.; Aragona, G.; Lupica, I.; Muto, L.; Iaboni, V.; Pasquale De Stefanis *Rapporto sul recupero energetico da rifiuti in Italia*; 2019;
5. Brunner, P.H.; Rechberger, H. Waste to energy - key element for sustainable waste management. *Waste Manag.* **2015**, *37*, 3–12.
6. Mininni, G.; Santori, M. Problems and perspectives of sludge utilization in agriculture. *Agric. Ecosyst. Environ.* **1987**, *18*, 291–311.
7. Jurič, B.; Hanžič, L.; Ilić, R.; Samec, N. Utilization of municipal solid waste bottom ash and recycled aggregate in concrete. *Waste Manag.* **2006**, *26*, 1436–1442.
8. Nikravan, M.; Ramezanianpnour, A.A.; Maknoon, R. Technological and environmental behavior of petrochemical incineration bottom ash (PI-BA) in cement-based using nano-SiO2 and silica fume (SF). *Constr. Build. Mater.* **2018**, *191*, 1042–1052.
9. Chiang, Y.W.; Ghyselbrecht, K.; Santos, R.M.; Meesschaert, B.; Martens, J.A. Synthesis of zeolitic-type adsorbent material from municipal solid waste incinerator bottom ash and its application in heavy metal adsorption. *Catal. Today* **2012**, *190*, 23–30.
10. Alam, Q.; Hendrix, Y.; Thijs, L.; Lazaro, A.; Schollbach, K.; Brouwers, H.J.H. Novel low temperature synthesis of sodium silicate and ordered mesoporous silica from incineration bottom ash. *J. Clean. Prod.* **2019**, *211*, 874–883.
11. Penilla, R.P.; Bustos, A.G.; Elizalde, S.G. Zeolite Synthesized by Alkaline Hydrothermal Treatment of Bottom Ash from Combustion of Municipal Solid Wastes. *J. Am. Ceram. Soc.* **2003**, *86*, 1527–1533.
12. Bourtsalas, A.; Vandeperre, L.J.; Grimes, S.M.; Themelis, N.; Cheeseman, C.R. Production of pyroxene ceramics from the fine fraction of incinerator bottom ash. *Waste Manag.* **2014**, *45*, 217–225.
13. Caprai, V.; Florea, M.V.A.; Brouwers, H.J.H. Evaluation of the influence of mechanical activation on physical and chemical properties of municipal solid waste incineration sludge. *J. Environ. Manage.* **2018**, *216*, 133–144.
14. Quina, M.J.; Bordado, J.C.; Quinta-Ferreira, R.M. Treatment and use of air pollution control residues from MSW incineration: An overview. *Waste Manag.* 2008, *28*, 2097–2121.
15. Nikravan, M.; Ramezanianpour, A.A.; Nikravan, M.; Maknoon, R. *Characterization of Bottom Ash from Petrochemical Waste Incinerator Zero-emission and Green building View project Life cycle assessment for comparing waste management options of BA/FA in civil engineering applications View project Characterization of Bottom Ash from Petrochemical Waste Incinerator*; 2017;
16. Dou, X.; Chen, D.; Hu, Y.; Feng, Y.; Dai, X. Carbonization of heavy metal impregnated sewage sludge oriented towards potential co-disposal. *J. Hazard. Mater.* **2017**, *321*, 132–145.

17. Hjelmar, O.; Holm, J.; Crillesen, K. Utilisation of MSWI bottom ash as sub-base in road construction: First results from a large-scale test site. *J. Hazard. Mater.* **2007**, *139*, 471–480.
18. Husgafvel, R.; Karjalainen, E.; Linkosalmi, L.; Dahl, O. Recycling industrial residue streams into a potential new symbiosis product – The case of soil amelioration granules. *J. Clean. Prod.* **2016**, *135*, 90–96.
19. Zacco, A.; Borgese, L.; Gianoncelli, A.; Struis, R.P.W.J.; Depero, L.E.; Bontempi, E. Review of fly ash inertisation treatments and recycling. *Environ. Chem. Lett.* 2014, *12*, 153–175.
20. Zhu, F.; Xiong, Y.; Wang, Y.; Wei, X.; Zhu, X.; Yan, F. Heavy metal behavior in "Washing-Calcination-Changing with Bottom Ash" system for Recycling of Four Types of Fly Ashes. *Waste Manag.* **2018**, *75*, 215–225.
21. Diliberto, C.; Meux, E.; Diliberto, S.; Garoux, L.; Marcadier, E.; Rizet, L.; Lecomte, A. A zero-waste process for the management of MSWI fly ashes: production of ordinary Portland cement. *Environ. Technol.* **2020**, *41*, 1199–1208.
22. Haugsten, K.E.; Gustavson, B. Environmental properties of vitrified fly ash from hazardous and municipal waste incineration. *Waste Manag.* **2000**, *20*, 167–176.
23. Cheng, T.W.; Chen, Y.S. On formation of CaO-Al2O3-SiO2 glass-ceramics by vitrification of incinerator fly ash. *Chemosphere* **2003**, *51*, 817–824.
24. Dong, Y.; Jow, J.; Su, J.; Lai, S.-Y. *Fly Ash Separation Technology and its Potential Applications*; 2013;
25. Schramke, J.A. Neutralization of alkaline coal fly ash leachates by CO2(g). *Appl. Geochemistry* **1992**, *7*, 481–492.
26. Anthony, E.J.; Jia, L.; Woods, J.; Roque, W.; Burwell, S. Pacification of high calcic residues using carbon dioxide. *Waste Manag.* **2000**, *20*, 1–13.
27. Mangialardi, T. Disposal of MSWI fly ash through a combined washing-immobilisation process. *J. Hazard. Mater.* **2003**, *98*, 225–240.
28. Shi, H.S.; Kan, L.L. Leaching behavior of heavy metals from municipal solid wastes incineration (MSWI) fly ash used in concrete. *J. Hazard. Mater.* **2009**, *164*, 750–754.
29. Qian, G.; Cao, Y.; Chui, P.; Tay, J. Utilization of MSWI fly ash for stabilization/solidification of industrial waste sludge. *J. Hazard. Mater.* **2006**, *129*, 274–281.
30. Saikia, N.; Kato, S.; Kojima, T. Production of cement clinkers from municipal solid waste incineration (MSWI) fly ash. *Waste Manag.* **2007**, *27*, 1178–1189.
31. Youcai, Z.; Lijie, S.; Guojian, L. Chemical stabilization of MSW incinerator fly ashes. *J. Hazard. Mater.* **2002**, *95*, 47–63.
32. Arpae Emilia-Romagna Available online: https://www.arpae.it/ (accessed on Jan 11, 2021).
33. Panepinto, D.; Fiore, S.; Genon, G.; Acri, M. Thermal valorization of sewer sludge: Perspectives for large wastewater treatment plants. *J. Clean. Prod.* **2016**, *137*, 1323–1329.
34. Qin, L.B.; Han, J.; Chen, W.S.; Wang, G.G.; Luo, G.Q.; Yao, H. Simultaneous removal of SO2 and PAHs by adding calcium-based additives during sewage sludge incineration in a fluidized bed incinerator. *J. Mater. Cycles Waste Manag.* **2017**, *19*, 1061–1068.
35. Lin, H.; Ma, X. Simulation of co-incineration of sewage sludge with municipal solid waste in a grate furnace incinerator. *Waste Manag.* **2012**, *32*, 561–567.
36. Magdziarz, A.; Wilk, M.; Gajek, M.; Nowak-Woźny, D.; Kopia, A.; Kalemba-Rec, I.; Koziński, J.A. Properties of ash generated during sewage sludge combustion: A multifaceted analysis. *Energy* **2016**, *113*, 85–94.

37. Batistella, L.; Silva, V.; Suzin, R.C.; Virmond, E.; Althoff, C.A.; Moreira, R.F.P.M.; José, H.J. Gaseous emissions from sewage sludge combustion in a moving bed combustor. *Waste Manag.* **2015**, *46*, 430–439.
38. Biganzoli, L.; Grosso, M.; Giugliano, M.; Campolunghi, M. Chemical and sewage sludge co-incineration in a full-scale MSW incinerator: Toxic trace element mass balance. *Waste Manag. Res.* **2012**, *30*, 1081–1088.
39. Bosio, A.; Rodella, N.; Gianoncelli, A.; Zacco, A.; Borgese, L.; Depero, L.E.; Bingham, P.A.; Bontempi, E. A new method to inertize incinerator toxic fly ash with silica from rice husk ash. *Environ. Chem. Lett.* **2013**, *11*, 329–333.
40. Bosio, A.; Gianoncelli, A.; Zacco, A.; Borgese, L.; Rodella, N.; Zanotti, D.; Depero, L.E.; Siviero, G.; Cinosi, A.; Bingham, P.A.; et al. A new nanotechnology of fly ash inertization based on the use of silica gel extracted from rice husk ash and microwave treatment. *Proc. Inst. Mech. Eng. Part N J. Nanoeng. Nanosyst.* **2014**, *228*, 27–32.
41. Rodella, N.; Pasquali, M.; Zacco, A.; Bilo, F.; Borgese, L.; Bontempi, N.; Tomasoni, G.; Depero, L.E.; Bontempi, E. Beyond waste: new sustainable fillers from fly ashes stabilization, obtained by low cost raw materials. *Heliyon* **2016**, *2*.
42. Rodella, N.; Bosio, A.; Dalipi, R.; Zacco, A.; Borgese, L.; Depero, L.E.; Bontempi, E. Waste silica sources as heavy metal stabilizers for municipal solid waste incineration fly ash. *Arab. J. Chem.* **2017**, *10*, S3676–S3681.
43. Wei, Q.; Jiang, X. Green concrete. In Proceedings of the Civil Engineering and Urban Planning 2012 - Proceedings of the 2012 International Conference on Civil Engineering and Urban Planning; 2012; pp. 291–294.
44. Youcai, Z. *Pollution Control and Resource Recovery: Municipal Solid Wastes Incineration: Bottom Ash and Fly Ash*; Elsevier Inc., 2016; ISBN 9780128124970.
45. Loginova, E.; Volkov, D.S.; van de Wouw, P.M.F.; Florea, M.V.A.; Brouwers, H.J.H. Detailed characterization of particle size fractions of municipal solid waste incineration bottom ash. *J. Clean. Prod.* **2019**, *207*, 866–874.
46. Ouhadi, V.R.; Yong, R.N.; Amiri, M.; Ouhadi, M.H. Pozzolanic consolidation of stabilized soft clays. *Appl. Clay Sci.* **2014**, *95*, 111–118.
47. Mostafa, N.Y.; El-Hemaly, S.A.S.; Al-Wakeel, E.I.; El-Korashy, S.A.; Brown, P.W. Characterization and evaluation of the pozzolanic activity of Egyptian industrial by-products: I: Silica fume and dealuminated kaolin. *Cem. Concr. Res.* **2001**, *31*, 467–474.
48. Bosio, A.; Rodella, N.; Depero, L.E.; Bontempi, E. Rice husk ash based composites, obtained by toxic fly ash inertization, and their applications as adsorbents. *Chem. Eng. Trans.* **2014**, *37*, 631–636.
49. Work Programme 2017 | European Commission Available online: https://ec.europa.eu/commission/work-programme-2017_en (accessed on Jan 11, 2021).
50. Acque reflue: il trattamento dei fanghi di depurazione Available online: https://www.teknoring.com/guide/guide-sicurezza-e-ambiente/acque-reflue-il-trattamento-dei-fanghi-di-depurazione/ (accessed on Jan 11, 2021).
51. De, G.; Sabino, F.; Gisi, D.; Galasso, M.; Flaccovio Editore, D. *Fanghi di Depurazione: Produzione, Caratterizzazione e Trattamento*; Prima edizione.; 2013; Vol. 1; ISBN 9788857902111.
52. Allegrini, E.; Maresca, A.; Olsson, M.E.; Holtze, M.S.; Boldrin, A.; Astrup, T.F. Quantification of the resource recovery potential of municipal solid waste incineration bottom ashes. *Waste Manag.* **2014**, *34*, 1627–1636.
53. Blasenbauer, D.; Huber, F.; Lederer, J.; Quina, M.J.; Blanc-Biscarat, D.; Bogush, A.; Bontempi, E.; Blondeau, J.; Chimenos, J.M.; Dahlbo, H.; et al. Legal situation and

current practice of waste incineration bottom ash utilisation in Europe. *Waste Manag.* **2020**, *102*, 868–883.
54. Huber, F.; Blasenbauer, D.; Aschenbrenner, P.; Fellner, J. Chemical composition and leachability of differently sized material fractions of municipal solid waste incineration bottom ash. *Waste Manag.* **2019**, *95*, 593–603.
55. Stabile, P.; Bello, M.; Petrelli, M.; Paris, E.; Carroll, M.R. Vitrification treatment of municipal solid waste bottom ash. *Waste Manag.* **2019**, *95*, 250–258.
56. Šyc, M.; Simon, F.G.; Hyks, J.; Braga, R.; Biganzoli, L.; Costa, G.; Funari, V.; Grosso, M. *Metal recovery from incineration bottom ash: state-of-the-art and recent 1 developments 2*;
57. Al-Rawas, A.A.; Hago, A.W.; Al-Sarmi, H. Effect of lime, cement and Sarooj (artificial pozzolan) on the swelling potential of an expansive soil from Oman. *Build. Environ.* **2005**, *40*, 681–687.
58. Tang, Y.Y.; Hölzel, B.K.; Posner, M.I. The neuroscience of mindfulness meditation. *Nat. Rev. Neurosci.* 2015, *16*, 213–225.
59. Chimenos, J.M.; Segarra, M.; Fernández, M.A.; Espiell, F. Characterization of the bottom ash in municipal solid waste incinerator. *J. Hazard. Mater.* **1999**, *64*, 211–222.
60. Chen, C.H.; Chiou, I.J. Distribution of chloride ion in MSWI bottom ash and de-chlorination performance. *J. Hazard. Mater.* **2007**, *148*, 346–352.
61. Dhir OBE, R.K.; De Brito, J.; Ciaran J. Lynn; Silva, R. *Sustainable Construction Materials: Municipal Incinerated Bottom Ash*; 1st editio.; Woodhead Publishing, 2017; ISBN 9780081009970.
62. Alam, Q.; Schollbach, K.; van Hoek, C.; van der Laan, S.; de Wolf, T.; Brouwers, H.J.H. In-depth mineralogical quantification of MSWI bottom ash phases and their association with potentially toxic elements. *Waste Manag.* **2019**, *87*, 1–12.
63. Caviglia, C.; Confalonieri, G.; Corazzari, I.; Destefanis, E.; Mandrone, G.; Pastero, L.; Boero, R.; Pavese, A. Effects of particle size on properties and thermal inertization of bottom ashes (MSW of Turin's incinerator). *Waste Manag.* **2019**, *84*, 340–354.
64. Huber, F.; Blasenbauer, D.; Aschenbrenner, P.; Fellner, J. Chemical composition and leachability of differently sized material fractions of municipal solid waste incineration bottom ash. *Waste Manag.* **2019**, *95*, 593–603.
65. Assi, A.; Federici, S.; Bilo, F.; Zacco, A.; Depero, L.E.; Bontempi, E. Increased Sustainability of Carbon Dioxide Mineral Sequestration by a Technology Involving Fly Ash Stabilization. *Materials (Basel).* **2019**, *12*, 2714.
66. Assi, A.; Bilo, F.; Zanoletti, A.; Ponti, J.; Valsesia, A.; La Spina, R.; Depero, L.E.; Bontempi, E. Review of the Reuse Possibilities Concerning Ash Residues from Thermal Process in a Medium-Sized Urban System in Northern Italy. *Sustainability* **2020**, *12*, 4193.
67. Assi, A.; Bilo, F.; Zanoletti, A.; Ponti, J.; Valsesia, A.; La Spina, R.; Zacco, A.; Bontempi, E. Zero-waste approach in municipal solid waste incineration: Reuse of bottom ash to stabilize fly ash. *J. Clean. Prod.* **2020**, *245*, 118779.
68. Liu, R.P.; Guo, B.; Ren, A.; Bian, J.F. The chemical and oxidation characteristics of semi-dry flue gas desulfurization ash from a steel factory. *Waste Manag. Res.* **2010**, *28*, 865–871.
69. Benassi, L.; Pasquali, M.; Zanoletti, A.; Dalipi, R.; Borgese, L.; Depero, L.E.; Vassura, I.; Quina, M.J.; Bontempi, E. Chemical Stabilization of Municipal Solid Waste Incineration Fly Ash without Any Commercial Chemicals: First Pilot-Plant Scaling Up. *ACS Sustain. Chem. Eng.* **2016**, *4*, 5561–5569.
70. Bontempi, E.; Zacco, A.; Borgese, L.; Gianoncelli, A.; Ardesi, R.; Depero, L.E. A new method for municipal solid waste incinerator (MSWI) fly ash inertization, based on

colloidal silica. *J. Environ. Monit.* **2010**, *12*, 2093–2099.
71. Kost, D.A.; Bigham, J.M.; Stehouwer, R.C.; Beeghly, J.H.; Fowler, R.; Traina, S.J.; Wolfe, W.E.; Dick, W.A. Chemical and physical properties of dry flue gas desulfurization products. *J. Environ. Qual.* **2005**, *34*, 676–686.
72. Liu, S.; Yang, H.; Zhang, Z.; Chen, J.; Chen, C.; Guo, T.; Cao, Y.; Jia, W. Emission characteristics of fine particles from wet flue gas desulfurization system using a cascade of double towers. *Aerosol Air Qual. Res.* **2018**, *18*, 1901–1909.
73. Bosio, A.; Gianoncelli, A.; Zacco, A.; Borgese, L.; Rodella, N.; Zanotti, D.; Depero, L.E.; Siviero, G.; Cinosi, A.; Bingham, P.A.; et al. A new nanotechnology of fly ash inertization based on the use of silica gel extracted from rice husk ash and microwave treatment. *Proc. Inst. Mech. Eng. Part N J. Nanoeng. Nanosyst.* **2014**, *228*, 27–32.
74. Shoumkova, A.S. Magnetic separation of coal fly ash from Bulgarian power plants. *Waste Manag. Res.* **2011**, *29*, 1078–1089.
75. Hower, J.C.; Rathbone, R.F.; Robertson, J.D.; Peterson, G.; Trimble, A.S. Petrology, mineralogy, and chemistry of magnetically-separated sized fly ash. *Fuel* **1999**, *78*, 197–203.
76. Alegbe, J.; Ayanda, O.S.; Ndungu, P.; Alexander, N.; Fatoba, O.O.; Petrik, L.F. Chemical, Mineralogical and Morphological Investigation of Coal Fly Ash Obtained from Mpumalanga Province, South Africa. *Res. J. Environ. Sci.* **2018**, *12*, 98–105.
77. Wang, S.; Zhang, C.; Chen, J. Utilization of Coal Fly Ash for the Production of Glass-ceramics With Unique Performances: A Brief Review. *J. Mater. Sci. Technol.* **2014**, *30*, 1208–1212.
78. Benassi, L.; Pasquali, M.; Zanoletti, A.; Dalipi, R.; Borgese, L.; Depero, L.E.; Vassura, I.; Quina, M.J.; Bontempi, E. Chemical Stabilization of Municipal Solid Waste Incineration Fly Ash without Any Commercial Chemicals: First Pilot-Plant Scaling Up. *ACS Sustain. Chem. Eng.* **2016**, *4*, 5561–5569.
79. Ramezanianpour, A.A. *Cement Replacement Materials; Properties, Durability, Sustainability.*; 2014; Vol. 7; ISBN 978-3-642-36720-5.
80. Sambandam, B.; Palanisami, E.; Abbugounder, R.; Prakhya, B.; Thiyagarajan, D. Characterizations of coal fly ash nanoparticles and induced in vitro toxicity in cell lines. *J. Nanoparticle Res.* **2014**, *16*.
81. Xu, G.; Shi, X. Characteristics and applications of fly ash as a sustainable construction material: A state-of-the-art review. *Resour. Conserv. Recycl.* 2018, *136*, 95–109.
82. Zanoletti, A.; Federici, S.; Borgese, L.; Bergese, P.; Ferroni, M.; Depero, L.E.; Bontempi, E. Embodied energy as key parameter for sustainable materials selection: The case of reusing coal fly ash for removing anionic surfactants. *J. Clean. Prod.* **2017**, *141*, 230–236.
83. Rodella, N.; Bosio, A.; Zacco, A.; Borgese, L.; Pasquali, M.; Dalipi, R.; Depero, L.E.; Patel, V.; Bingham, P.A.; Bontempi, E. Arsenic stabilization in coal fly ash through the employment of waste materials. *J. Environ. Chem. Eng.* **2014**, *2*, 1352–1357.
84. Chindaprasirt, P.; Jaturapitakkul, C.; Chalee, W.; Rattanasak, U. Comparative study on the characteristics of fly ash and bottom ash geopolymers. *Waste Manag.* **2009**, *29*, 539–543.
85. Chen, Y.; Shah, N.; Huggins, F.E.; Huffman, G.P. Transmission Electron Microscopy Investigation of Ultrafine Coal Fly Ash Particles. *Environ. Sci. Technol.* **2005**, *39*, 1144–1151.
86. Berra, M.; Tavano, S. *PROPRIETA' DI MISCELE CEMENTIZIE CONTENENTI FUMO DI SILICE CONDENSATO*;
87. Zanoletti, A.; Vassura, I.; Venturini, E.; Monai, M.; Montini, T.; Federici, S.; Zacco, A.; Treccani, L.; Bontempi, E. A New Porous Hybrid Material Derived From Silica

Fume and Alginate for Sustainable Pollutants Reduction. *Front. Chem.* **2018**, *6*.
88. Zhou, C.; Yan, C.; Zhao, J.; Wang, H.; Zhou, Q.; Luo, W. Rapid synthesis of morphology-controlled mesoporous silica nanoparticles from silica fume. *J. Taiwan Inst. Chem. Eng.* **2016**, *62*, 307–312.
89. Chan, Y.W.; Chu, S.H. Effect of silica fume on steel fiber bond characteristics in reactive powder concrete. *Cem. Concr. Res.* **2004**, *34*, 1167–1172.
90. Babu, K.G.; Babu, D.S. Behaviour of lightweight expanded polystyrene concrete containing silica fume. *Cem. Concr. Res.* **2003**, *33*, 755–762.
91. EN 13055-1:2002 - CEN/TC 154 - CEN - CEN Available online: http://store.uni.com/catalogo/index.php/norme/root-categorie-cen/cen/cen-tc-154/en-13055-1-2002 (accessed on Nov 14, 2019).
92. Assi, A.; Bilo, F.; Zanoletti, A.; Ducoli, S.; Ramorino, G.; Gobetti, A.; Zacco, A.; Federici, S.; Depero, L.E.; Bontempi, E. A Circular Economy Virtuous Example—Use of a Stabilized Waste Material Instead of Calcite to Produce Sustainable Composites. *Appl. Sci.* **2020**, *10*, 754.
93. Borgese, L.; Dalipi, R.; Riboldi, A.; Bilo, F.; Zacco, A.; Federici, S.; Bettinelli, M.; Bontempi, E.; Depero, L.E. Comprehensive approach to the validation of the standard method for total reflection X-ray fluorescence analysis of water. *Talanta* **2018**, *181*, 165–171.
94. Liu, Y.; Zeng, F.; Sun, B.; Jia, P.; Graham, I.T. Structural Characterizations of Aluminosilicates in Two Types of Fly Ash Samples from Shanxi Province, North China. *Minerals* **2019**, *9*, 358.
95. Chang, F.Y.; Wey, M.Y. Comparison of the characteristics of bottom and fly ashes generated from various incineration processes. *J. Hazard. Mater.* **2006**, *138*, 594–603.
96. Yu, J.; Sun, L.; Xiang, J.; Jin, L.; Hu, S.; Su, S.; Qiu, J. Physical and chemical characterization of ashes from a municipal solid waste incinerator in China. *Waste Manag. Res.* **2013**, *31*, 663–73.
97. Clavier, K.A.; Watts, B.; Liu, Y.; Ferraro, C.C.; Townsend, T.G. Risk and performance assessment of cement made using municipal solid waste incinerator bottom ash as a cement kiln feed. *Resour. Conserv. Recycl.* **2019**, *146*, 270–279.
98. Guo, F.; Zhong, Z.; Xue, H. Partition of Zn, Cd, and Pb during co-combustion of sedum plumbizincicola and sewage sludge. *Chemosphere* **2018**, *197*, 50–56.
99. Rietveld, H.M. A profile refinement method for nuclear and magnetic structures. *J. Appl. Crystallogr.* **1969**, *2*, 65–71.
100. De La Torre, A.G.; Bruque, S.; Aranda, M.A.G. Rietveld quantitative amorphous content analysis. *J. Appl. Crystallogr.* **2001**, *34*, 196–202.
101. Doebelin, N.; Kleeberg, R. Profex: A graphical user interface for the Rietveld refinement program BGMN. *J. Appl. Crystallogr.* **2015**, *48*, 1573–1580.
102. Carmona, N.; Ortega-Feliu, I.; Gómez-Tubío, B.; Villegas, M.A. x. *Mater. Charact.* **2010**, *61*, 257–267.
103. Dreibrodt, S.; Furholt, M.; Hofmann, R.; Hinz, M.; Cheben, I. P-ed-XRF-geochemical signatures of a 7300 year old Linear Band Pottery house ditch fill at Vráble-Ve'lké Lehemby, Slovakia - House inhabitation and post-depositional processes. *Quat. Int.* **2017**, *438*, 131–143.
104. Rodella, N.; Pasquali, M.; Zacco, A.; Bilo, F.; Borgese, L.; Bontempi, N.; Tomasoni, G.; Depero, L.E.; Bontempi, E. Beyond waste: new sustainable fillers from fly ashes stabilization, obtained by low cost raw materials. *Heliyon* **2016**, *2*, e00163.
105. Chou, J. dong; Wey, M.Y.; Liang, H.H.; Chang, S.H. Biotoxicity evaluation of fly ash and bottom ash from different municipal solid waste incinerators. *J. Hazard. Mater.* **2009**, *168*, 197–202.

106. Seniunaite, J.; Vasarevicius, S. Leaching of Copper, Lead and Zinc from Municipal Solid Waste Incineration Bottom Ash. In Proceedings of the Energy Procedia; Elsevier Ltd, 2017; Vol. 113, pp. 442–449.
107. Youcai, Z. *Pollution Control and Resource Recovery: Municipal Solid Wastes Incineration: Bottom Ash and Fly Ash*; Elsevier Inc., 2016; ISBN 9780128124970.
108. Li, J.; Zheng, L.; Sha, X.; Chen, P. Microstructural and mechanical characteristics of graphene oxide-fly ash cenosphere hybrid reinforced epoxy resin composites. *J. Appl. Polym. Sci.* **2020**, *137*, 47173.
109. Benassi, L.; Pasquali, M.; Zanoletti, A.; Dalipi, R.; Borgese, L.; Depero, L.E.; Vassura, I.; Quina, M.J.; Bontempi, E. Chemical Stabilization of Municipal Solid Waste Incineration Fly Ash without Any Commercial Chemicals: First Pilot-Plant Scaling Up. *ACS Sustain. Chem. Eng.* **2016**, *4*, 5561–5569.
110. *PÔLE ENVIRONNEMENT ET GENIE DES PROCEDES Centre de Tarnos THE INFLUENCE OF PVC ON THE QUANTITY AND HAZARDOUSNESS OF FLUE GAS RESIDUES FROM INCINERATION _____ FINAL REPORT*; 2000;
111. Wei, Y.; Shimaoka, T.; Saffarzadeh, A.; Takahashi, F. Mineralogical characterization of municipal solid waste incineration bottom ash with an emphasis on heavy metal-bearing phases. *J. Hazard. Mater.* **2011**, *187*, 534–543.
112. Introduction to Geochemistry - Konrad Bates Krauskopf - Google Libri Available online: https://books.google.it/books/about/Introduction_to_Geochemistry.html?id=QOAhXGzPuHQC&redir_esc=y (accessed on Jan 13, 2021).
113. GOODARZI, M.; MATAR, M.M.; SHAFA, M.; TOWNSEND, J.E.; GONZALEZ, I. A prospective randomized blinded study of the effect of intravenous fluid therapy on postoperative nausea and vomiting in children undergoing strabismus surgery. *Pediatr. Anesth.* **2006**, *16*, 49–53.
114. Tzanakos, K.; Mimilidou, A.; Anastasiadou, K.; Stratakis, A.; Gidarakos, E. Solidification/stabilization of ash from medical waste incineration into geopolymers. *Waste Manag.* **2014**, *34*, 1823–1828.
115. Benassi, L.; Dalipi, R.; Consigli, V.; Pasquali, M.; Borgese, L.; Depero, L.E.; Clegg, F.; Bingham, P.A.; Bontempi, E. Integrated management of ash from industrial and domestic combustion: a new sustainable approach for reducing greenhouse gas emissions from energy conversion. *Environ. Sci. Pollut. Res.* **2017**, *24*, 14834–14846.
116. Benassi, L.; Zanoletti, A.; Depero, L.E.; Bontempi, E. Sewage sludge ash recovery as valuable raw material for chemical stabilization of leachable heavy metals. *J. Environ. Manage.* **2019**, *245*, 464–470.
117. Bayuseno, A.P.; Schmahl, W.W. Understanding the chemical and mineralogical properties of the inorganic portion of MSWI bottom ash. *Waste Manag.* **2010**, *30*, 1509–1520.
118. Saffarzadeh, A.; Shimaoka, T.; Wei, Y.; Gardner, K.H.; Musselman, C.N. Impacts of natural weathering on the transformation/neoformation processes in landfilled MSWI bottom ash: A geoenvironmental perspective. *Waste Manag.* **2011**, *31*, 2440–2454.
119. Palansooriya, K.N.; Shaheen, S.M.; Chen, S.S.; Tsang, D.C.W.; Hashimoto, Y.; Hou, D.; Bolan, N.S.; Rinklebe, J.; Ok, Y.S. Soil amendments for immobilization of potentially toxic elements in contaminated soils: A critical review. *Environ. Int.* 2020, *134*.
120. Li, X.G.; Lv, Y.; Ma, B.G.; Chen, Q. Bin; Yin, X.B.; Jian, S.W. Utilization of municipal solid waste incineration bottom ash in blended cement. *J. Clean. Prod.* **2012**, *32*, 96–100.
121. Zevenbergen, C.; Vander Wood, T.; Bradley, J.P.; Van der Broeck, P.F.C.W.; Orbons,

A.J.; Van Reeuwijk, L.P. Morphological and chemical properties of MSWI bottom ash with respect to the glassy constituents. *Hazard. Waste Hazard. Mater.* **1994**, *11*, 371–383.
122. Adam, C.; Peplinski, B.; Michaelis, M.; Kley, G.; Simon, F.G. Thermochemical treatment of sewage sludge ashes for phosphorus recovery. *Waste Manag.* **2009**, *29*, 1122–1128.
123. Bernasconi, A.; Dapiaggi, M.; Wright, J.; Ceola, S.; Maurina, S.; Francescon, F.; Pavese, A. High temperature investigation of SiO2-Al2O3-ZnO-Na2O glass for ceramic-glaze: in-situ/ex-situ synchrotron diffraction and conventional approaches. *Ceram. Int.* **2018**, *44*, 6395–6401.
124. Silva, R. V.; de Brito, J.; Lynn, C.J.; Dhir, R.K. Environmental impacts of the use of bottom ashes from municipal solid waste incineration: A review. *Resour. Conserv. Recycl.* 2019, *140*, 23–35.
125. Bosio, A.; Zacco, A.; Borgese, L.; Rodella, N.; Colombi, P.; Benassi, L.; Depero, L.E.; Bontempi, E. A sustainable technology for Pb and Zn stabilization based on the use of only waste materials: A green chemistry approach to avoid chemicals and promote CO2 sequestration. *Chem. Eng. J.* **2014**, *253*, 377–384.
126. Chang, R.; Choi, D.; Kim, M.H.; Park, Y. Tuning crystal polymorphisms and structural investigation of precipitated calcium carbonates for CO2 mineralization. *ACS Sustain. Chem. Eng.* **2017**, *5*, 1659–1667.
127. Tian, S.; Jiang, J. Sequestration of flue gas CO2 by direct gas-solid carbonation of air pollution control system residues. *Environ. Sci. Technol.* **2012**, *46*, 13545–13551.
128. Sarkar, A.; Mahapatra, S. Synthesis of all crystalline phases of anhydrous calcium carbonate. *Cryst. Growth Des.* **2010**, *10*, 2129–2135.
129. Blasenbauer, D.; Huber, F.; Lederer, J.; Quina, M.J.; Blanc-Biscarat, D.; Bogush, A.; Bontempi, E.; Blondeau, J.; Chimenos, J.M.; Dahlbo, H.; et al. Legal situation and current practice of waste incineration bottom ash utilisation in Europe. *Waste Manag.* **2020**, *102*, 868–883.
130. Cornacchia, G.; Agnelli, S.; Gelfi, M.; Ramorino, G.; Roberti, R. Reuse of EAF Slag as Reinforcing Filler for Polypropylene Matrix Composites. *JOM* **2015**, *67*, 1370–1378.
131. Erklig, A.; Alsaadi, M.; Bulut, M. A comparative study on industrial waste fillers affecting mechanical properties of polymer-matrix composites. *Mater. Res. Express* **2016**, *3*.
132. Satheesh Raja, R.; Manisekar, K.; Manikandan, V. Study on mechanical properties of fly ash impregnated glass fiber reinforced polymer composites using mixture design analysis. *Mater. Des.* **2014**, *55*, 499–508.
133. Granta: CES Selector 2019 [WWW Document] Available online: https://www.grantadesign.com/it/products/ces/.
134. Bontempi, E. *Raw Materials Substitution Sustainability*; Springer International Publishing, 2017; ISBN 978-3-319-60830-3.
135. Assi, A.; Bilo, F.; Zanoletti, A.; Ducoli, S.; Ramorino, G.; Gobetti, A.; Zacco, A.; Federici, S.; Depero, L.E.; Bontempi, E. A circular economy virtuous example-use of a stabilized waste material instead of calcite to produce sustainable composites. *Appl. Sci.* **2020**, *10*.
136. Kant, M.; #1, P.; Kumar, S.; #1, C. #2; Al-Falah, #2 An Experimental Investigation of Tensile Strength of Glass Composite Materials With Calcium Carbonate (CaCO 3) Filler. *Int. J. Emerg. trends Eng. Dev. Issue* **2012**, *2*.
137. Reddy, S.P.; Chandra, P. V; Rao, S.; Reddy, A.C.; Parmeswari, G. *TENSILE AND FLEXURAL STRENGTH OF GLASS FIBER EPOXY COMPOSITES*; Advanced

materials, 2014; ISBN 9789382163466.
138. Srivastava, V.K.; Shembekar, P.S. Tensile and fracture properties of epoxy resin filled with flyash particles. *J. Mater. Sci.* **1990**, *25*, 3513–3516.
139. Maiti, S.N.; Mahapatro, P.K. Mechanical properties of i-PP/CaCO3 composites. *J. Appl. Polym. Sci.* **1991**, *42*, 3101–3110.
140. Assi, A.; Bilo, F.; Zanoletti, A.; Ducoli, S.; Ramorino, G.; Gobetti, A.; Zacco, A.; Federici, S.; Depero, L.E.; Bontempi, E. A Circular Economy Virtuous Example—Use of a Stabilized Waste Material Instead of Calcite to Produce Sustainable Composites. *Appl. Sci.* **2020**, *10*, 754.
141. Gummadi, J.; Kumar, G.V.; Rajesh, G. Evaluation of Flexural Properties of Fly Ash Filled Polypropylene Composites. *Int. J. Mod. Eng. Res. www.ijmer.com* **2012**, *2*.
142. Sengupta, S.; Pal, K.; Ray, D.; Mukhopadhyay, A. Furfuryl palmitate coated fly ash used as filler in recycled polypropylene matrix composites. *Compos. Part B Eng.* **2011**, *42*, 1834–1839.
143. Yang, K.; Yang, Q.; Li, G.; Sun, Y.; Feng, D. Mechanical properties and morphologies of polypropylene with different sizes of calcium carbonate particles. *Polym. Compos.* **2006**, *27*, 443–450.
144. Gupta, N.; Brar, B.S.; Woldesenbet, E. Effect of filler addition on the compressive and impact properties of glass fibre reinforced epoxy. *Bull. Mater. Sci.* **2001**, *24*, 219–223.
145. Maiti, S.N.; Sharma, K.K. Studies on polypropylene composites filled with talc particles - Part I Mechanical properties. *J. Mater. Sci.* **1992**, *27*, 4605–4613.
146. Švehlová, V.; Polouček, E. About the influence of filler particle size on toughness of filled polypropylene. *Die Angew. Makromol. Chemie* **1987**, *153*, 197–200.